ON THE OPTIMIZATION OF MASS DISTRIBUTION IN MECHANISMS

by

RICHARD S. BERKOF

A dissertation submitted to the Graduate Faculty in Engineering in partial fulfillment of the requirements for the degree of Doctor of Philosophy, The City University of New York.

1969

This manuscript has been read and accepted for the Graduate Faculty in Engineering in satisfaction of the dissertation requirement for the degree of Doctor of Philosophy.

4/24/69
date

Gerard G. Lowen
Chairman of Examining Committee

30 April 1969
date

Executive Officer

Prof. G. G. Lowen (Chairman)

Prof. S. B. Menkes

Prof. M. L. Pei

Prof. B. Sohmer

Supervisory Committee

The City University of New York

ACKNOWLEDGEMENTS

First and foremost, I wish to express my sincerest thanks to my advisor, Professor Gerard G. Lowen. I am truly indebted to him for his interest, inspiration, and encouragement during our very fruitful relationship.

I would also like to thank the other members of my guidance committee, Professors Sherwood B. Menkes, Ming L. Pei, and Bernard Sohmer, for their interest and counsel. In addition, I appreciate the interest shown by members of my examining committee, namely Professors Antonio F. Baldo, F. R. Erskine Crossley, and Ferdinand Freudenstein.

The financial help of the following is gratefully acknowledged: Regents Fellowships from New York State, Research Assistantships from the City College Fund and the City University of New York, and Grant No. GK-3703 from the National Science Foundation. Appreciation is also due to the City College Computation Center for the extensive use of their facilities, especially the IBM 7040 computer.

I wish to extend special thanks to my employer, the American Can Company, Princeton Laboratory, for their generous support and understanding during the final phases of this research.

Last, but not least, I thank my wife, Madeline, whose great love, patience, and help have made this work possible.

TABLE OF CONTENTS

ABSTRACT

Force and moment balancing of certain plane mechanisms are considered.

A new method, termed the Method of Linearly Independent Vectors, is shown to permit the exact force balance of simple linkages by making the total center of mass of each mechanism stationary. This is accomplished by redistributing the link masses in such a manner that the coefficients of the time-dependent terms of the equation describing the total center of mass trajectory vanish.

Expressions for the shaking moment of unbalanced and force-balanced four-bar linkages with arbitrary link mass distributions are derived. Both translational and rotational mass effects are considered. The above expressions show that no internal mass redistribution can be found which permits perfect moment balance. In addition, it is shown that the shaking moment of a force-balanced four-bar linkage is invariant with respect to reference point.

A novel least-square technique, which minimizes the deviation of the shaking moment from zero, is formulated. This method furnishes the ideal link length relationships for force-balanced crank-and-rocker mechanisms with symmetrical link mass distributions within the Grashof criteria. A design approach is developed which allows the choice of real links according to the above purely geometric optimum criteria.

The concept of the dimensionless moment is introduced. This permits the comparison of the actual magnitudes of the shaking moment of families of force-balanced four-bar linkages.

LIST OF TABLES

LIST OF FIGURES

I. INTRODUCTION

Whenever an unbalanced linkage runs at high speeds, or contains massive links, both a shaking force as well as a shaking moment are transmitted to its surroundings. These disturbances cause vibrations, noise, wear, and fatigue problems, and therefore limit the full potential of many machines.

Although it is clear to the writer that the ultimate questions of the dynamic performance of linkages can only be resolved by taking their elastic properties into account, it is first necessary to expand and formalize the possibilities of the rigid body approach.

This dissertation concerns itself with the problem of balancing rigid body planar mechanisms from the point of view of optimization of mass distribution. To this end, a new and practical approach to the complete elimination of the shaking forces of four-bar and six-bar linkages is presented. Also, a least-square optimization technique is formulated which enables the shaking moment of a force-balanced four-bar linkage to be minimized.

A. Background

Historically speaking, the problem of balancing was first explored and brought to fruition in conjunction with prime movers and pumps utilizing various combinations of slider-crank chains. The presence of large masses and relatively high speeds made it necessary to extend the purely kinematic considerations to dynamic ones.

This need has gained momentum over the years as ingenious linkages were incorporated into machines serving the most varied endeavors. These mechanisms are found not only in the manufacturing, processing, and packaging machines of all industries, but are also highly important components of modern communication and computation equipment.

The ever increasing demands for accuracy and speed necessitate control over the vibrations generated by these machines, as well as the associated noise, wear, and fatigue problems.

While the technical literature abounds in publications concerning balancing of the aggregates of slider-crank mechanisms, there is relatively little to be found which pertains to balancing of other types of planar or spatial linkages. What is available has been presented to a large degree in Russian publications, with additional work done in English and in German. (See literature survey of Part II.)

Most of this work is confined to specific mechanisms, and indicates no practical path towards a general solution of the problem of fully balancing the shaking force. There is much emphasis on partial force balancing by way of the elimination of part or all of the contributions of certain harmonics of the shaking force, and at times these techniques are extended to partial balancing of the shaking moment.

The above indicates that there is a clear need for a more unified approach to the overall problem of linkage balancing.

It is believed that the present work points towards the fulfillment of this need by way of the newly developed Method of Linearly Independent Vectors. This technique of force balancing, as well as a method for optimizing the shaking moment, comprise the main body of this dissertation. The results found in this investigation will now be summarized.

B. Results of Investigation

The results of both the force and moment optimization techniques developed are now summarized.

1. Force Balancing

The new Method of Linearly Independent Vectors assures the stationary location of the total center of mass of certain mechanisms, thus providing complete inertia force balance (shaking force). While there is good indication that this method is applicable to all planar pin-jointed linkages, derivations are confined to the four-bar and a six-bar linkage with arbitrary link mass distributions.

Design equations and relevant examples show the engineering feasibility of this approach.

This technique is especially advantageous since one need not deal with inertia forces on individual links, but only with the displacements of their centers of mass. Due to the stationary nature of the total center of mass, force balance is not affected by variation of input speed and link mass distribution, or kinematic restrictions.

Certain insights concerning the balancing of the shaking force harmonics of a four-bar linkage are also found by means of this method.

2. Moment Optimization

The work concerning moment optimization is confined to the force-balanced four-bar linkage.

The shaking moment, which includes both translational and rotational mass effects, is derived by way of the angular momentum principle for a four-bar linkage with arbitrary link mass distributions.

It is shown that this expression is equivalent to that which describes the combined action of the moments due to the ground bearing forces and the ground reaction to the motor supplied input torque.

When this formulation is applied to a force-balanced four-bar linkage, it is shown mathematically that perfect moment balance is not possible by internal mass redistributions. This shaking moment is a pure couple, independent of reference point.

A least-square technique, which considers the smallest deviation from zero of a function consisting of a linear combination of terms, is derived. This is applied to the moment optimization of force-balanced crank-and-rocker mechanisms. It is assumed that these mechanisms have symmetrical link mass distributions and constant input angular velocity.

This approach furnishes the optimum ratio of coefficients of terms within the moment equation for given linkage dimensions. A design technique is evolved which matches actual coefficient ratios to the above ideal values.

The matching technique not only enables the designer to improve existing mechanisms, but it gives valuable information concerning the favorable link dimensions of a mechanism with given link configurations. The ground link length, as well as the location of the center of mass of the coupler, are of critical importance.

A further new concept which is introduced is that of the dimensionless moment. It permits the comparison of the actual magnitudes of the shaking moment of families of linkages which have been considered.

The bibliographies contain references which are directly employed by means of brackets throughout the present work, as well as source material which is considered relevant to this investigation.

Appendix A contains necessary definitions of terms i addition to mechanics concepts related to this work.

At this juncture, the reader is referred to the table of contents in order to obtain an overall view.

C. Recommendations for Further Study

The following possible areas of study concerning balancing have suggested themselves during the course of this investigation:

(a) The limits of applicability of the Method of Linearly Independent Vectors to planar and spatial linkages.

(b) Extension of moment optimization to the force-balanced four-bar linkage with arbitrary link mass distributions, as well as to other force-balanced mechanisms.

(c) Simultaneous optimization of all relevant dynamic properties.

It is understood that only experimentation can decide which of the theoretical criteria is most valid for optimization.

II. PRESENT STATE OF THE ART OF MECHANISM BALANCING

In an attempt to examine the state of the art of mechanism balancing, the classifications of complete and partial balancing techniques are used.

It is to be noted that almost all past work has been done on simple planar mechanisms. There is a scarcity of applications to complex planar mechanisms, and almost a total absence of applications to spatial mechanisms. Also, a majority of past balancing work has been concentrated on the partial balancing of the shaking force. Complete balancing applications, as well as the balancing of the shaking moment, have just recently been brought under discussion. Also uncommon are applications to mechanisms with unsymmetric link mass distributions.

A. Complete Balancing Techniques

The following references are concerned with the complete balancing of the shaking force and the shaking moment of plane rigid body linkages (the absence of applications to spatial mechanisms is to be noted).

1. Balancing of Shaking Force

In order to cause the shaking force on the frame of a mechanism to vanish, the total center of mass of the mechanism must be made stationary (thus making it unnecessary to find the forces).

Four primary techniques have been employed for this purpose: the method of "static balancing," the method of "principal vectors" and its extensions, the use of cams, and the use of duplicate mechanisms.

The "static balancing" method requires the ability to replace concentrated link masses by statically equivalent systems of masses. By adding counterweights to links, the link centers of mass are progressively brought either to multiple stationary pivots, or to just one ground pivot. The former version was illustrated for the four-bar linkage by F. R. E. Crossley [10], R. L. Maxwell [51], M. R. Smith and L. Maunder [70], and G. J. Talbourdet and P. R. Shepler [71], and for more complex linkages by G. G. Baranov [5], T. H. Davies [13], and L. N. Reshetov [58]. The latter version was illustrated by I. I. Artobolevskii, V. A. Zinov'yev, and B. V. Edel'shtein [4], as well as V. A. Kamenskii [38].

The method of "principal vectors," presented by O. Fischer [21], describes the position of the total center of mass of a mechanism by a series of vectors, each directed along one of the links. Using the magnitudes of these principal vectors, a series of binary structural elements can be added in parallelogram fashion to the original mechanism. The resulting augmented mechanism contains a point which coincides with the total center of mass of the original mechanism. Both Fischer and I. I. Artobolevskii [3] proposed different versions of such a construction. This method is described by many authors such as B. Dizioglu [16], V. P. Goryachkin [30], N. I. Manolescu and D. Maros [50], and V. A. Yudin [78]. The addition of a counterweighted pantograph device to either of these augmented mechanisms enables the combined center of mass to be brought to a stationary point, as shown by H. Hilpert [36].

An alternate construction which enables the center of mass of a given mechanism to be traced out by a point on an attached proportional auxiliary mechanism was proposed by V. A. Shchepetil'nikov [64] in a

method he called a "double contour transformation." By adjusting parameters of the equations relating the auxiliary mechanism to the original mechanism, the total center of mass is made to lie on a rotating point of the proportional auxiliary mechanism. Thus, a redistribution of link masses is required to constrain the center of mass to move in a circle. With the addition of a rotating counterweight, the total center of mass can then be reduced to a stationary point. When the above constructions are applied to the four-bar linkage, it may be shown that the total center of mass trajectory is a curve which is similar to a coupler curve of this mechanism. This was formalized by V. V. Dobrovol'skii [17] and R. Kreutzinger [45,46]. W. Wunderlich [76] came to similar conclusions for a four-bar linkage with a general mass distribution. He extended these findings to the determination of the necessary conditions for redistributing the link masses such that the total center of mass remains stationary.

Other techniques include the use of cam driven masses to keep the total center of mass of a mechanism stationary, as shown by V. A. Kamenskii [38-40]. Also, the addition of an axially symmetric duplicate mechanism to any given mechanism will make the new combined center of mass stationary. This has been illustrated by I. I. Artobolevskii [3], T. H. Davies [13], B. Dizioglu [16], and V. A. Kamenskii [38,39].

By considering the number of equations needed to prescribe full force and/or moment balance, V. A. Kamenskii [40] examined the minimum number of counterweights which were necessary for balancing under given conditions. Depending upon the desired paths of the counterweights, many possibilities exist.

In order to balance mechanisms with variable mass links, A. P. Bessonov [6] considered the theoretical use of counterweights with both constant and variable mass.

2. Balancing of Shaking Moment (with Shaking Force Considerations)

Very few references have been encountered which deal with the exact balancing of the shaking moment.† The use of cams, oscillating counterweights, and duplicate mechanisms are the few devices which enable exact moment balance.

The use of a cam-actuated oscillating counterweight was shown by V. A. Kamenskii [38,39] to provide moment balance for a four-bar linkage. Kamenskii also showed the use of oscillating counterweights which were geared to mechanism rocker links.

It might be interesting to add at this point that W. Meyer zur Capellen [55,56] showed the use of cams in an energy approach to make the input torque vanish. Also, K. Ogawa and H. Funabashi [57] discussed theoretical and experimental methods of reducing this input torque.

By adding a duplicate mechanism such that it has a mirror symmetry with the original mechanism, the shaking moments will be equal and opposite. This has been illustrated by T. H. Davies [13].

---

†Indeed, there is no general agreement as to what constitutes a shaking moment.

B. Partial Balancing Techniques

The following references are concerned with the partial balancing of the shaking force and the shaking moment of rigid body linkages. In all cases but one, the mechanisms under discussion are planar.

The reduction of inertia effects is primarily accomplished by the balancing of harmonics. Another approach lies in the use of added spring elements, which can be used to balance inertia forces.

1. Harmonic or Order Balancing

The balancing of individual shaking force and moment harmonic orders is the most common technique encountered in balancing.

The addition of single or multiple counterweights, which are driven by the input crank at constant angular velocity, is the most common form of harmonic balancing. More complex techniques involve the addition of supplementary masses to other mechanism links, together with the crank driven masses.

Once the counterweight configuration has been chosen, the individual mass placement must be optimized for the desired harmonics by either best average or best uniform techniques. The former includes the Fourier series and Gaussian least squares formulations, and the latter requires a Chebyshev formulation.

a. Force Harmonic Balancing

The force harmonics of the slider-crank mechanisms of various types of engines and other machinery have been balanced with the help of counterweights for over a century. Although means are known by which the slider-crank mechanism can be exactly balanced, the resulting configuration presents impractical construction problems. Partial balancing was therefore turned to for practical design considerations.

Since the present survey concerns itself with mechanisms in general, the large quantity of literature referring to slider-crank dynamics will be disregarded, save for the following comprehensive references: I. I. Artobolevskii [2], C. B. Biezeno and R. Grammel [7], P. Cormac [9], W. E. Dalby [12], V. P. Goryachkin [30], C. W. Ham, E. J. Crane, and W. L. Rogers [32], A. Kobayashi [41], J. Kožesník [44], L. B. Levenson [49], R. E. Root [59], D. L. Thornton [72], S. Timoshenko and D. H. Young [73], and L. Toft and A. T. J. Kersey [74].

For the forces, the alternate harmonic formulations of either the shaking force or the position of the total center of mass may be employed.

For more general mechanisms, N. I. Kolchin [42] finds shaking force harmonics using the position harmonics of the total center of mass, and differentiating these expressions.

The placement of a single mass on the input crank will balance only one directional component of the first harmonic. By having two counterrotating masses driven by the input crank, either one directional component of a shaking force harmonic or any total harmonic may be balanced.

The unidirectional device was conceived by F. W. Lanchester [48] as the "Lanchester balancer." The latter, a "generalized Lanchester balancer," was illustrated by F. E. Crossley [11], Yu. V. Epshtein [18], and M. V. Semenov [63]. The property that any full harmonic resultant describes an elliptic path was extended by Semenov [62,63] to a planetary mechanism balancer.

The addition of supplementary masses to existing mechanism links, together with crank driven masses, provides alternate balancing schemes. M. V. Semenov [60] examined the full balancing of the first harmonic of the shaking force of any complex mechanism. As an alternate to the generalized Lanchester balancer, he added supplementary masses to either a four-bar linkage rocker link or a slider-crank connecting rod.

As another approach to the partial balancing of composite mechanisms, masses are added to existing mechanism links in order to have more parameters available for optimization. P. N. Gartshtein [23] added masses to the coupler and rocker of a four-bar linkage contained in a larger mechanism to have more usable parameters.

In the single reference to spatial mechanisms, the use of three masses set on mutually perpendicular bevel gears was shown by M. V. Semenov [61] to completely balance any three-dimensional shaking force harmonic.

b. Moment Harmonic Balancing

For the balance of any moment harmonic, two identical synchronously rotating masses may be employed, as described by G. G. Baranov [5] and Ya. S. Davydov [14].

The shaking moment contains two components. Most commonly considered is the component due to the moment of the D'Alembert forces. Also present, but included with less frequency, is the D'Alembert moment.

c. Combined Force and Moment Harmonic Balancing

V. A. Shchepetil'nikov [64], by shifting the axis of rotation of a force counterweight, induced a moment which balanced the first shaking moment harmonic. Since two counterrotating masses can generate a moment harmonic as well as a force harmonic, E. Mewes [52] used the combined effect in a balancing scheme. With the use of three masses driven by the input shaft, simultaneous balance of any force and moment harmonic is possible. Ya. L. Geronimus [27] employed this device for total first harmonic balancing.

The optimization of counterweights by best average and best uniform techniques was formulated by Ya. L. Geronimus [24-29]. Best average optimization was performed both graphically (with hodographs) and analytically (with the Fourier series). Best uniform optimization was performed by three methods: graphically (with hodographs), numerically (with a method of successive approximations), and analytically (in which an approximate analytical formula was derived [29]).

Following the optimization methods of Geronimus, V. Ya. Anilovich [1] investigated the optimum magnitudes and location of all masses on a given mechanism. As applied to a shaker screen assembly under the influence of both inertia and external loads, combined force and moment balancing was considered. As another version of the best average technique, Han, Chi-Yeh [33] formulated an analytical least squares approach. This partial first harmonic balancing of inertia forces and their moments was carried out with the help of a single counterweight attached to the input shaft.

d. Quality of Balancing

After surveying methods of balancing, V. A. Kamenskii [38,39] presents criteria by which the quality of balancing may be judged.

Experimental balancing work has been performed by Yu. V. Epshtein and E. P. Rapota [19], V. A. Kamenskii [38], A. I. Komissarov and N. I. Krapivin [43], V. A. Shchepetil'nikov [65,66], and G. J. Talbourdet and P. R. Shepler [71].

2. Addition of Springs to Balance Inertia Forces

The use of springs as energy storage elements attached to mechanism links can partially balance inertia forces. Various configurations and analyses are given by K. Hain [31], H. Hilpert [36], S. A. Cherkudinov and N. V. Speranskii [8], and L. S. Sheino [67], who also presents some experimental verification.

III. FORCE BALANCING BY THE METHOD OF LINEARLY INDEPENDENT VECTORS

The following new method, which has been called the "Method of Linearly Independent Vectors," is shown to make the total center of mass of a mechanism stationary. This is accomplished by redistributing the link masses in such a manner that the coefficients of the time-dependent terms of the equation describing the total center of mass trajectory vanish.

It has been found that this only becomes possible when the foregoing position equation is written in such a form that the time-dependent unit vectors contained within this equation are linearly independent. This method has been applied to a number of planar linkages, and is illustrated for the four-bar and the six-bar linkages next.

A. Application to Four-Bar Linkage

1. Derivation

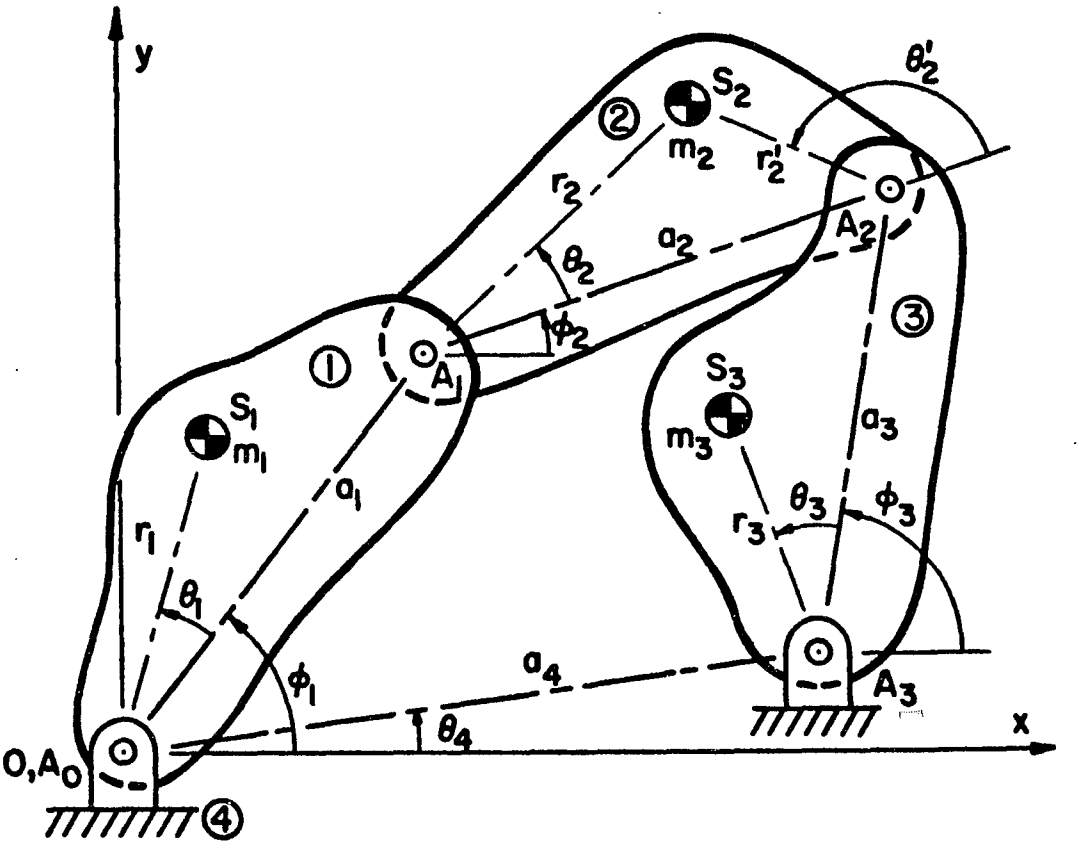

Fig. 1 Four-bar linkage with arbitrary link mass distributions

Fig. 1 shows a four-bar linkage which contains links with arbitrary mass distributions. The total center of mass S of the mechanism may be defined by the position vector $\bar{r}_S$:

$$\bar{r}_S = \frac{1}{\mathcal{M}} \sum_{i=1}^{3} m_i \bar{r}_{S_i} , \qquad (3.1)$$

where the total mass is:

$$\mathcal{M} = \sum_{i=1}^{3} m_i \ . \tag{3.2}$$

(Refer to Appendix A for nomenclature.)

With the reference origin 0 taken as the crank pivot A_o, the position vectors of the individual link centers of mass are given by:

$$\left.\begin{aligned} \bar{r}_{S_1} &= r_1 e^{i(\phi_1+\theta_1)}, \\ \bar{r}_{S_2} &= a_1 e^{i\phi_1} + r_2 e^{i(\phi_2+\theta_2)}, \\ \bar{r}_{S_3} &= a_4 e^{i\theta_4} + r_3 e^{i(\phi_3+\theta_3)}. \end{aligned}\right\} \tag{3.3}$$

Upon substitution, equation (3.1) may be written as:

$$\begin{aligned} \mathcal{M}\bar{r}_S = {} & (m_1 r_1 e^{i\theta_1} + m_2 a_1)\, e^{i\phi_1} + (m_2 r_2 e^{i\theta_2})\, e^{i\phi_2} \\ & + (m_3 r_3 e^{i\theta_3})\, e^{i\phi_3} + m_3 a_4 e^{i\theta_4}. \end{aligned} \tag{3.4}$$

The unit vectors $e^{i\phi_1}$, $e^{i\phi_2}$, and $e^{i\phi_3}$ are related by the loop equation:

$$a_1 e^{i\phi_1} + a_2 e^{i\phi_2} - a_3 e^{i\phi_3} - a_4 e^{i\theta_4} = 0. \tag{3.5}$$

This indicates that the time-dependent terms in equation (3.4) are not linearly independent. However, if one of the unit vectors of equation (3.5) is solved for (such as $e^{i\phi_2}$), and its equivalent is substituted

into equation (3.4), then the desired linearly independent combination of time-dependent terms is obtained:

$$\mathcal{M}\bar{r}_S = (m_1 r_1 e^{i\theta_1} + m_2 a_1 - m_2 \frac{a_1}{a_2} r_2 e^{i\theta_2})\, e^{i\phi_1}$$
$$+ (m_3 r_3 e^{i\theta_3} + m_2 \frac{a_3}{a_2} r_2 e^{i\theta_2})\, e^{i\phi_3} \qquad (3.6)$$
$$+ (m_3 a_4 + m_2 \frac{a_4}{a_2} r_2 e^{i\theta_2})\, e^{i\theta_4}.$$

The above expression shows that the total center of mass S is then stationary at:

$$\bar{r}_S = \frac{1}{\mathcal{M}} (m_3 a_2 + m_2 r_2 e^{i\theta_2}) \frac{a_4}{a_2} e^{i\theta_4}, \qquad (3.7)$$

if the following coefficients of the time-dependent terms vanish:

$$m_1 r_1 e^{i\theta_1} + m_2 a_1 - m_2 \frac{a_1}{a_2} r_2 e^{i\theta_2} = 0, \qquad (3.8)$$

$$m_3 r_3 e^{i\theta_3} + m_2 \frac{a_3}{a_2} r_2 e^{i\theta_2} = 0. \qquad (3.9)$$

Equation (3.8) can be simplified by noting the kinematic identity (see Fig. 1):

$$r_2 e^{i\theta_2} = a_2 + r_2' e^{i\theta_2'}, \qquad (3.10)$$

which leads to:

$$m_1 r_1 e^{i\theta_1} - m_2 \frac{a_1}{a_2} r_2' e^{i\theta_2'} = 0. \qquad (3.11)$$

Finally, the conditions for total force balance of a most general four-bar linkage can be stated with the help of equations (3.11) and (3.9):

$$m_1 r_1 = m_2 r_2' \frac{a_1}{a_2} \qquad \text{and} \qquad \theta_1 = \theta_2', \tag{3.12}$$

$$m_3 r_3 = m_2 r_2 \frac{a_3}{a_2} \qquad \text{and} \qquad \theta_3 = \theta_2 + \pi. \tag{3.13}$$

Equations (3.12) and (3.13) imply that whenever the mass and the location of the center of mass of one of the links of the mechanism are prescribed, then the mass distribution of the remaining two links can be rearranged for full balance. W. Wunderlich [76] obtained a comparable solution starting from a different premise in his investigation of the center of mass trajectory of the four-bar linkage.

Equations (3.12) and (3.13) also imply the existence of a semi-graphical solution. For example, if the properties of link 2 are prescribed, then angles θ_1 and θ_3 may be found. This determines the lines on which the centers of mass of links 1 and 3 must be placed.

For a parallelogram four-bar linkage, only one link mass redistribution is necessary. This represents a degenerate case for which the terms in equation (3.6) are not linearly independent, since $\phi_1 = \phi_3$.

It is also interesting to note that if equation (3.5) was solved for either $e^{i\phi 1}$ or $e^{i\phi 3}$ and substituted into equation (3.4), results equivalent to equations (3.12) and (3.13) would be found.

2. Design Equations

For the case in which the geometry of all the links of a four-bar linkage is prescribed, i.e. the links themselves may not be altered, an equivalent result may be obtained by the addition of counterweights constrained to move with any two links. Generally, it is most advantageous to choose the input and output links.

In order to obtain expressions for the magnitudes and positions of the counterweights of the chosen links i, it is necessary to maintain the following vector equality:

$$m_i r_i \angle \theta_i = m_i^o r_i^o \angle \theta_i^o + m_i^* r_i^* \angle \theta_i^*, \tag{3.14a}$$

where:

$m_i^o r_i^o$, θ_i^o are the parameters of the unbalanced linkage;

$m_i^* r_i^*$, θ_i^* are the parameters of the counterweights; and

$m_i r_i$, θ_i are the parameters resulting from equations (3.12) and (3.13).

In addition, it is generally also necessary to satisfy the second condition of static replacement, i.e.

$$m_i = m_i^o + m_i^*. \tag{3.14b}$$

(See discussion in examples.)

For design purposes, equation (3.14a) is solved for the mass-distance products and the position angles of the counterweights:

$$m_i^* r_i^* = \sqrt{(m_i r_i)^2 + (m_i^o r_i^o)^2 - 2\, m_i m_i^o r_i r_i^o \cos(\theta_i - \theta_i^o)}, \qquad (3.15a)$$

$$\tan \theta_i^* = \frac{m_i r_i \sin \theta_i - m_i^o r_i^o \sin \theta_i^o}{m_i r_i \cos \theta_i - m_i^o r_i^o \cos \theta_i^o}. \qquad (3.15b)$$

3. Example

For this example, it is assumed that the link dimensions and masses of an unbalanced four-bar linkage are given, and that it is required to effect force balance by the addition of counterweights to links 1 and 3, respectively (see Fig. 2). Fig. 3 shows a scale drawing of the resulting balanced linkage. Both the links and the counterweights are assumed to be made of steel.

Table 1 gives the relevant parameters of the original unbalanced linkage. The determination of the magnitudes and the positions of the steel counterweights is described next, and the results are listed in Table 2:

(a) Since the parameters of link 2 are given, equations (3.12) and (3.13) are modified to read:

$$m_1 r_1 = m_2^o r_2'^o \frac{a_1}{a_2} \quad \text{and} \quad \theta_1 = \theta_2'^o, \qquad (3.16)$$

$$m_3 r_3 = m_2^o r_2^o \frac{a_3}{a_2} \quad \text{and} \quad \theta_3 = \theta_2^o + \pi, \qquad (3.17)$$

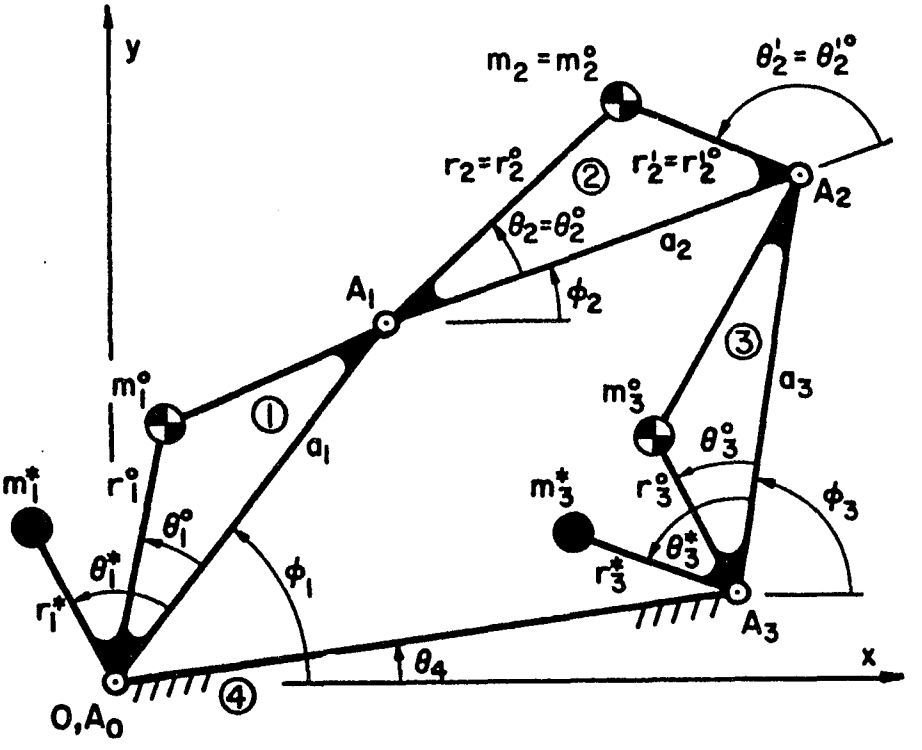

Fig. 2 Balancing of prescribed four-bar linkage by addition of counterweights to links 1 and 3

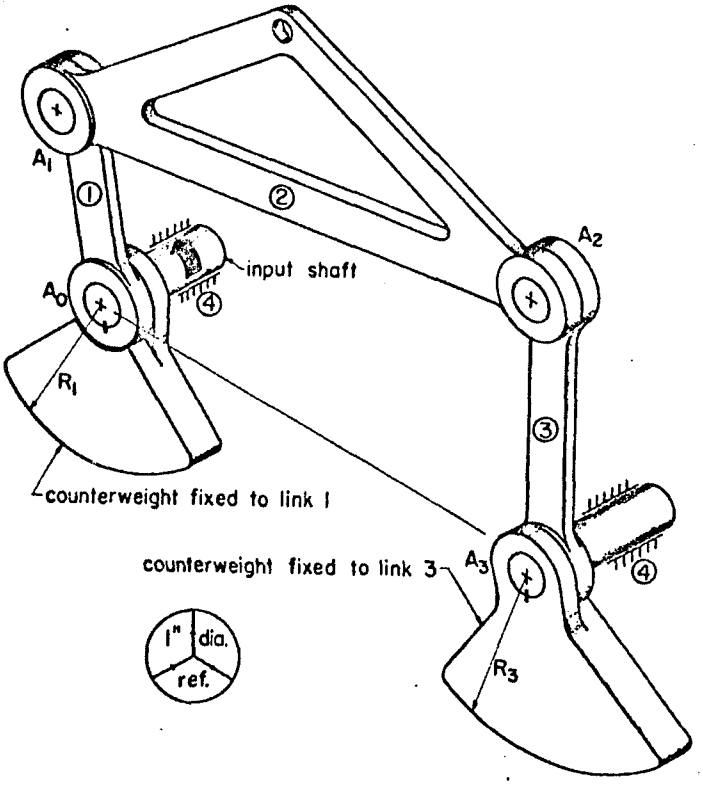

Fig. 3 Counterweight balancing of prescribed four-bar linkage

Table 1 Parameters of unbalanced four-bar linkage

Link i	1	2	3	4
a_i (in)	2.000	6.000	3.000	5.500
r_i^o (in)	1.000	3.190	1.500	...
θ_i^o (deg)	0	16.0	0	0
$r_i'^o$ (in)	...	3.063	...	...
$\theta_i'^o$ (deg)	...	163.3	...	...
m_i^o (lb)	0.102	0.274	0.120	...

Table 2 Parameters calculated for balanced four-bar linkage

Link i	1	3
$m_i r_i$ (lb-in)	0.279	0.437
θ_i (deg)	163.3	196.0
$m_i^* r_i^*$ (lb-in)	0.378	0.612
θ_i^* (deg)	167.9	191.4
m_i^* (lb)	0.311	0.418
R_i (in)	1.97	2.27

and are solved for m_1r_1, θ_1 and m_3r_3, θ_3 .

(b) Equations (3.15a,b) are now used to find $m_1^*r_1^*$, θ_1^* and $m_3^*r_3^*$, θ_3^*.

(c) Finally, suitable counterweights may be computed. For this example, 90° sector-type counterweights were chosen whose radii R_i and masses m_i^* are given in Table 2.

The mass of these counterweights is approximately 1.47 times that of the original unbalanced mechanism. It is to be noted that the designer is left wide latitude in the choice of counterweights, since the balancing requirement is expressed by the mass-distance products $m_i^*r_i^*$, and equation (3.14b) need not be used in this case. This occurs because m_1 and r_1 as well as m_3 and r_3 appear only as their respective mass-distance products, and never separately.

Note: Whenever counterweights are to be attached to the coupler in addition to one of the cranks, the foregoing procedure must be modified. For example, let link 3 be unalterable. Equations (3.13) are first used to obtain m_2r_2 and θ_2. In order to determine r_2' and θ_2', it is necessary to choose one of the parameters m_2 or r_2 arbitrarily, and calculate the other from the known product m_2r_2. With these results, equations (3.12) are used to find m_1r_1 and θ_1. Equations (3.15a,b) are then applied to obtain $m_1^*r_1^*$, θ_1^* and $m_2^*r_2^*$, θ_2^*. The counterweight mass m_2^* must now be found with the help of equation (3.14b), since the magnitude and location of m_2 had to be prescribed in the foregoing. Counterweight m_1^* is not subject to this restriction, since the parameters m_1r_1 have only appeared combined into mass-distance products.

B. Application to Six-Bar Linkage

1. Derivation

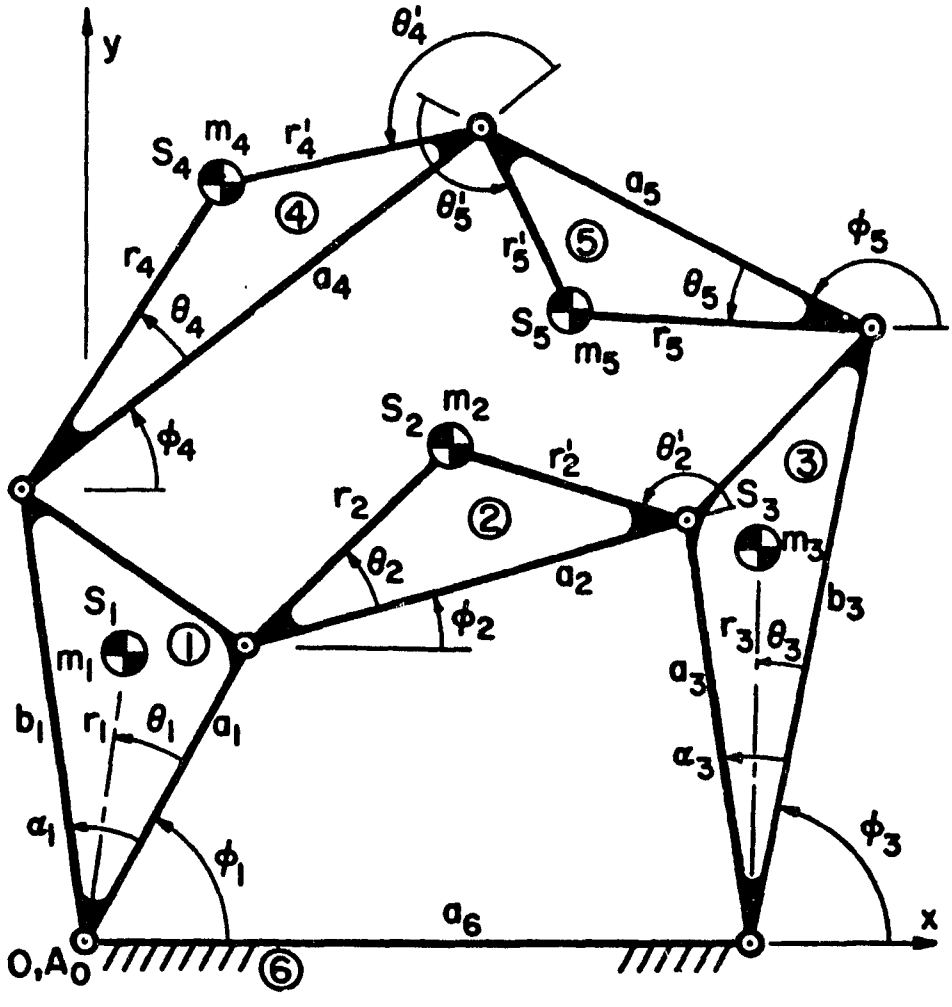

Fig. 4 Six-bar linkage with arbitrary link mass distributions

The configuration in Fig. 4 is used to illustrate the force balancing of a six-bar linkage by the Method of Linearly Independent Vectors. Other types of six-bar linkages may be approached in the identical manner.

The total center of mass of the mechanism is located with the help of:

$$\bar{r}_S = \frac{1}{\mathcal{M}} \sum_{i=1}^{5} m_i \bar{r}_{S_i} \quad , \tag{3.18}$$

where:

$$\mathcal{M} = \sum_{i=1}^{5} m_i \quad . \tag{3.19}$$

With the reference origin 0 taken as point A_o, the position vectors of the individual link centers of mass are given by:

$$\bar{r}_{S_1} = r_1 e^{i(\phi_1+\theta_1)}, \tag{3.20}$$

$$\bar{r}_{S_2} = a_1 e^{i\phi_1} + r_2 e^{i(\phi_2+\theta_2)}, \tag{3.21}$$

$$\bar{r}_{S_3} = a_6 + r_3 e^{i(\phi_3+\theta_3)}, \tag{3.22}$$

$$\bar{r}_{S_4} = b_1 e^{i(\phi_1+\alpha_1)} + r_4 e^{i(\phi_4+\theta_4)}, \tag{3.23}$$

$$\bar{r}_{S_5} = a_6 + b_3 e^{i\phi_3} + r_5 e^{i(\phi_5+\theta_5)}, \tag{3.24}$$

where α_1 and α_3 refer to the angles between pivot lines on ternary links 1 and 3.

The two independent loop equations which may be written for this mechanism are:

$$a_1 e^{i\phi_1} + a_2 e^{i\phi_2} - a_3 e^{i(\phi_3+\alpha_3)} - a_6 = 0, \tag{3.25}$$

and:

$$b_1 e^{i(\phi_1+\alpha_1)} + a_4 e^{i\phi_4} - a_5 e^{i\phi_5} - b_3 e^{i\phi_3} - a_6 = 0. \qquad (3.26)$$

Since there are five moving link angles ϕ_i, two of these can be eliminated, leaving three linearly independent terms (excluding degenerate cases). Choosing to eliminate ϕ_2 and ϕ_4, equations (3.25) and (3.26) are solved for $e^{i\phi_2}$ and $e^{i\phi_4}$ respectively. The results are substituted into equations (3.21) and (3.23), yielding:

$$\bar{r}_{S_2} = -(r_2'\lambda_2 e^{i\theta_2'})\, e^{i\phi_1} + (r_2\mu_2 e^{i(\theta_2+\alpha_3)})\, e^{i\phi_3} + r_2\nu_2 e^{i\theta_2}, \qquad (3.27)$$

$$\bar{r}_{S_4} = -(r_4'\lambda_4 e^{i(\theta_4'+\alpha_1)})\, e^{i\phi_1} + (r_4\mu_4 e^{i\theta_4})\, e^{i\phi_3} + (r_4\kappa_4 e^{i\theta_4})\, e^{i\phi_5} + r_4\nu_4 e^{i\theta_4}, \qquad (3.28)$$

in which:

$$\left.\begin{aligned} \lambda_2 &= \frac{a_1}{a_2},\ \mu_2 = \frac{a_3}{a_2},\ \nu_2 = \frac{a_6}{a_2}, \\ \lambda_4 &= \frac{b_1}{a_4},\ \mu_4 = \frac{b_3}{a_4},\ \nu_4 = \frac{a_6}{a_4},\ \kappa_4 = \frac{a_5}{a_4}, \end{aligned}\right\} \qquad (3.29)$$

and where, according to Fig. 2:

$$\left.\begin{aligned} r_2 e^{i\theta_2} &= a_2 + r_2' e^{i\theta_2'}, \\ r_4 e^{i\theta_4} &= a_4 + r_4' e^{i\theta_4'}, \\ r_5 e^{i\theta_5} &= a_5 + r_5' e^{i\theta_5'}. \end{aligned}\right\} \tag{3.30}$$

Upon the substitution of equations (3.20), (3.22), (3.24), (3.27), (3.28) into (3.18), and the factoring of unit vectors, one obtains:

$$\begin{aligned} \mathcal{M}\bar{r}_S = {} & [m_1 r_1 e^{i\theta_1} - m_2 r_2' \lambda_2 e^{i\theta_2'} - m_4 r_4' \lambda_4 e^{i(\theta_4'+\alpha_1)}]\, e^{i\phi_1} \\ & + [m_2 r_2 \mu_2 e^{i(\theta_2+\alpha_3)} + m_3 r_3 e^{i\theta_3} + m_4 r_4 \mu_4 e^{i\theta_4} + m_5 b_3]\, e^{i\phi_3} \\ & + [m_4 r_4 \kappa_4 e^{i\theta_4} + m_5 r_5 e^{i\theta_5}]\, e^{i\phi_5} \\ & + [m_2 r_2 \nu_2 e^{i\theta_2} + m_4 r_4 \nu_4 e^{i\theta_4} + m_3 a_6 + m_5 a_6]. \end{aligned} \tag{3.31}$$

The total center of mass will therefore be stationary at:

$$\bar{r}_S = \frac{1}{\mathcal{M}}[m_2 r_2 \nu_2 e^{i\theta_2} + m_4 r_4 \nu_4 e^{i\theta_4} + (m_3 + m_5)a_6], \tag{3.32}$$

if the following three coefficients of equation (3.31) vanish:

$$m_1 r_1 e^{i\theta_1} - m_2 r_2' \lambda_2 e^{i\theta_2'} - m_4 r_4' \lambda_4 e^{i(\theta_4' + \alpha_1)} = 0, \tag{3.33}$$

$$m_2 r_2 \mu_2 e^{i(\theta_2+\alpha_3)} + m_3 r_3 e^{i\theta_3} + m_4 r_4 \mu_4 e^{i\theta_4} + m_5 b_3 = 0, \tag{3.34}$$

$$m_4 r_4 \kappa_4 e^{i\theta_4} + m_5 r_5 e^{i\theta_5} = 0. \tag{3.35}$$

If equation (3.35) is substituted into (3.34), and the applicable expressions of (3.29) and (3.30) are used, then equations (3.33) - (3.35) may be rearranged to give the following more useful expressions for the complete force balancing of this six-bar linkage:

$$m_1 \frac{r_1}{a_1} e^{i\theta_1} = m_4 \frac{r_4'}{a_4} \frac{b_1}{a_1} e^{i(\theta_4'+\alpha_1)} + m_2 \frac{r_2'}{a_2} e^{i\theta_2'}, \tag{3.36}$$

$$m_3 \frac{r_3}{a_3} e^{i\theta_3} = m_5 \frac{r_5'}{a_5} \frac{b_3}{a_3} e^{i\theta_5'} - m_2 \frac{r_2}{a_2} e^{i(\theta_2+\alpha_3)}, \tag{3.37}$$

$$m_4 \frac{r_4}{a_4} e^{i\theta_4} = - m_5 \frac{r_5}{a_5} e^{i\theta_5}. \tag{3.38}$$

This set of balancing conditions indicates that:

(a) a certain relationship between links 4 and 5 must be met;

(b) the masses of two links may be prescribed together with the locations of their centers of mass.

2. Design Equations

As in the case of the four-bar linkage, it will generally prove helpful to effect full balance by adding counterweights to selected links of the given linkage. Again, equations (3.15 a,b) may be used.

In order to satisfy equations (3.36) - (3.38), counterweights must be added to three links. One of the chosen links must be either link 4 or 5, while the remaining two may be any pair selected from links 1, 2, and 3. For practical purposes, links 1 and 3 are usually best suited. In the six-bar linkage example, counterweights are added to links 5, 1, and 3.

3. Example

As the example for the six-bar linkage, a typical high-speed transport mechanism, similar to the linkage described by F. E. Crossley [11], is chosen. As before, it is assumed that the link dimensions and masses are prescribed, and that force balancing is to be accomplished by the addition of counterweights. Fig. 5 shows a schematic of this linkage, with counterweights added to links 1, 3, and 5. Fig. 6 gives a scale drawing of the resulting balanced linkage. Both the links and the counterweights are again assumed to be made of steel.

Table 3 gives the relevant parameters of the unbalanced linkage. The manner in which the magnitudes and positions of the steel counterweights are attained is described next, and the results are summarized in Table 4:

(a) Since the parameters of link 4 are given, equation (3.38) is modified to read, in scalar form:

$$m_5 r_5 = m_4^o r_4^o \frac{a_5}{a_4} , \tag{3.39}$$

$$\theta_5 = \theta_4^o + \pi . \tag{3.40}$$

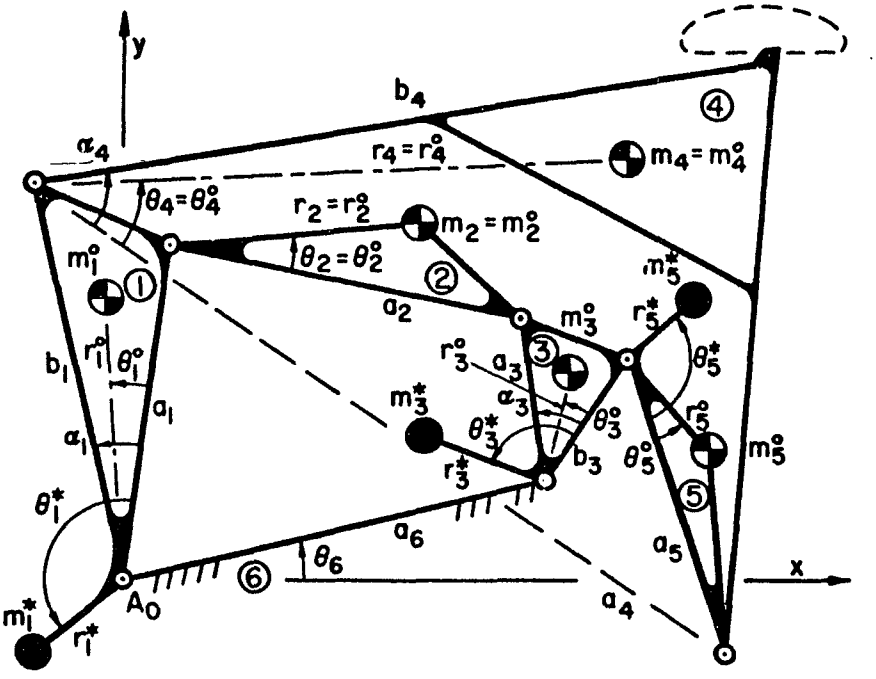

Fig. 5 Balancing of prescribed six-bar linkage by addition of counterweights to links 1, 3, and 5

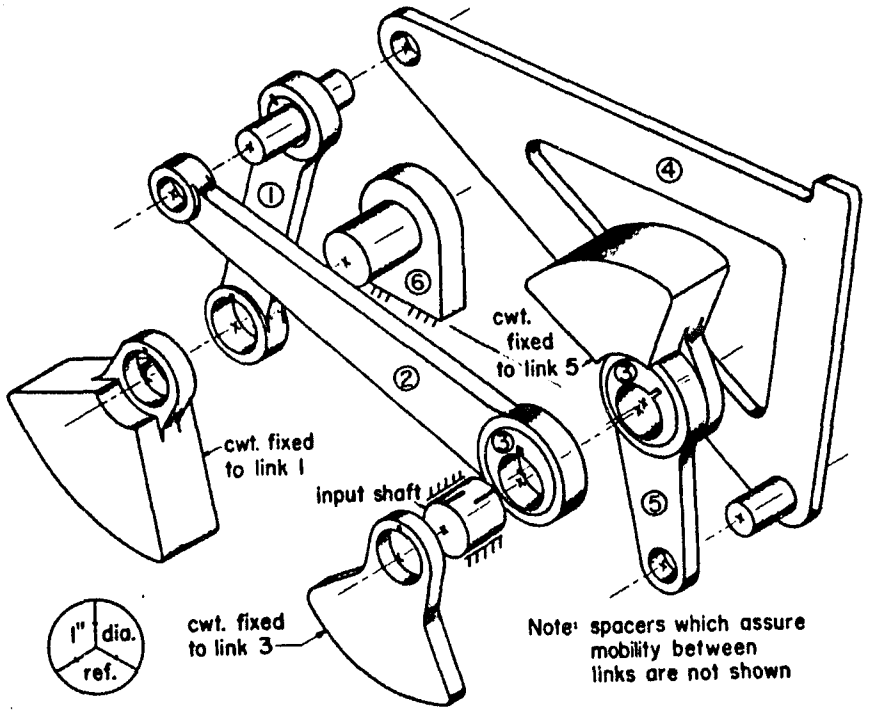

Fig. 6 Counterweight balancing of prescribed six-bar linkage (exploded view)

Table 3 Parameters of unbalanced six-bar linkage

Link i	1	2	3	4	5	6
a_i (in)	2.200	4.750	0.125	5.500	1.750	4.875
b_i (in)	2.300	...	0.120	6.000	...	...
α_i (deg)	6.0	...	16.0	40.4	...	...
r_i^o (in)	1.125	2.480	0.122	3.290	0.776	...
θ_i^o (deg)	3.0	0	5.0	19.0	0	11.0
$r_i'^o$ (in)	...	2.270	...	2.618	...	...
$\theta_i'^o$ (deg)	...	180.0	...	155.9	...	...
m_i^o (lb)	0.134	0.182	0.167	0.382	0.087	...

Table 4 Parameters calculated for balanced six-bar linkage

Link i	1	3	5
$m_i r_i$ (lb-in)	0.603	0.097	0.400†
θ_i (deg)	167.5	187.2	199.0
$m_i^* r_i^*$ (lb-in)	0.749	0.118	0.465
θ_i^* (deg)	170.6	186.8	196.3
m_i^* (lb)	0.607	0.117	0.415
R_i (in)	2.000	1.675	1.750

†r_5 = 0.809 in for design reasons (see part (a) of six-bar linkage example), which leads to m_5 = 0.494 lb, r_5' = 2.529 in, θ_5' = 186.0 deg.

These are solved for $m_5 r_5$ and θ_5.

(b) One of the parameters m_5 or r_5 must now be chosen arbitrarily, while the other one is determined from the result of equation (3.39). The choice of these parameters is subject only to design considerations. Then, r_5' and θ_5' are calculated with the help of equation (3.30).

(c) Equations (3.15a,b) are now used to find $m_5^* r_5^*$ and θ_5^*. Since the product $m_5 r_5$ consists of two known factors, m_5^* must satisfy equation (3.14b).

(d) The quantities $m_1 r_1$, θ_1 and $m_3 r_3$, θ_3 are found from the following modifications of equations (3.36) and (3.37):

$$m_1 r_1 e^{i\theta_1} = m_4^o r_4'^o \frac{b_1}{a_4} e^{i(\theta_4'^o + \alpha_1)} + m_2^o r_2'^o \frac{a_1}{a_2} e^{i\theta_2'^o}, \tag{3.41}$$

$$m_3 r_3 e^{i\theta 3} = m_5 r_5' \frac{b_3}{a_5} e^{i\theta 5'} - m_2^o r_2^o \frac{a_3}{a_2} e^{i(\theta_2^o + \alpha_3)}. \tag{3.42}$$

$m_1 r_1$, θ_1 and $m_3 r_3$, θ_3 may thus be determined.

(e) Equations (3.15a,b) are now used to find $m_1^* r_1^*$, θ_1^* and $m_3^* r_3^*$, θ_3^*.

(f) Finally, from these last results, the counterweights are computed. Since m_1 and r_1 as well as m_3 and r_3 appear only as their respective mass-distance products and never separately (as in the case of link 5), the total masses of links 1 and 3 are not prescribed and equation (3.14b) does not enter into the calculations. Table 4 lists values for R_i and m_i^* for the chosen sector-type counterweights.

For the particular choices made in this design, the mass of the counterweights is 1.20 times that of the original unbalanced mechanism.

C. Conclusions

Certain conclusions concerning the Method of Linearly Independent Vectors may be drawn:

(a) Since the center of mass of the entire mechanism is kept stationary, full force balance is maintained regardless of variation of input speed.

(b) Link masses lying off the joint-to-joint axes may be employed without restriction.

(c) Since the coefficients of all time-dependent terms are made zero permanently, any restrictions on mobility or other purely kinematic limitations on a given linkage do not invalidate the method.

(d) As the examples have shown, the resulting weight increases as well as the physical dimensions of the counterweights can easily conform to the demands of practical applications.

D. Harmonic Considerations for Four-Bar Linkage

Interesting insights into the structure of harmonic balancing of a four-bar linkage become apparent when the expressions describing the total center of mass trajectory obtained by the Method of Linearly Independent Vectors are examined for harmonic content.

While it is clear that a harmonic analysis cannot yield a different total balancing solution than that obtained by the Method of Linearly Independent Vectors, the harmonic form does give additional insights into partial balancing.

The following results are shown in greater detail in Appendix B:

(a) Full first harmonic balance is not possible without the removal of all other harmonics for a four-bar linkage by internal mass redistribution means. As proven in Appendix B, this results from the fact that the parameters which control all harmonics higher than the first also partially contribute to the coefficient of the first harmonic.

(b) All harmonics higher than the first, in addition to part of the first, can be made to vanish if a single mass redistribution condition is satisfied. This condition requires either of links 2 or 3 to be redistributed according to prescribed relations.

(c) Complete balance may be achieved in conjunction with (b) above by externally adding a single counterweight which rotates synchronously with the crank. Recalling that the preceding condition removes all harmonics higher than the first as well as part of the first, one need now only eliminate the effect of the remaining part of the first harmonic. This is simply accomplished by the addition of a counterweight geared to the input link.

IV. DERIVATION OF SHAKING MOMENT EXPRESSIONS

The present section lays the foundation for the shaking moment optimization of a force-balanced four-bar linkage.

The shaking moment is defined as the negative of the time rate of change of angular momentum of the mechanism. This includes both the translational as well as the rotational mass effects (D'Alembert forces and D'Alembert moments), and is equivalent to the combined action of the moments due to the ground bearing forces and the ground reaction to the motor supplied input torque.

The expression for the shaking moment of a force-balanced four-bar linkage is derived, and it is shown that it is generally not possible to make this moment vanish by additional and compatible internal mass redistributions.

Furthermore, the shaking moment of a force-balanced four-bar linkage is a pure couple, and therefore does not depend on the point of reference. This invariance makes it possible to optimize the moment without considering the location of the baseplate center of mass.

A. Formulation

The time rate of change of angular momentum of a system of rigid bodies is equal to the sum of the applied external moments, with respect to an arbitrary inertial origin O. The total angular momentum of a rigid body i, referred to origin O, can be expressed as the sum of two parts: the moment of linear momentum of the center of mass S_i with respect to point O, and the angular momentum of the body about its center of mass. Therefore, for the three moving links of a four-bar linkage, the total angular momentum is given by:

$$\bar{H}_O = \sum_{i=1}^{3} (\bar{r}_{S_i} \times m_i \dot{\bar{r}}_{S_i} + m_i k_i^2 \dot{\bar{\phi}}_i) , \tag{4.1}$$

and then the time rate of change of angular momentum becomes:

$$\dot{\bar{H}}_O = \sum_{i=1}^{3} (\bar{r}_{S_i} \times m_i \ddot{\bar{r}}_{S_i} + m_i k_i^2 \ddot{\bar{\phi}}_i) . \tag{4.2}$$

The shaking moment, which is equivalent to the moment acting on the ground, is given by the negative of eq. (4.2) and may be written as:

$$\bar{M}_{M/G}\Big|_O = - \dot{\bar{H}}_O = \sum_{i=1}^{3} (\bar{r}_{S_i} \times \bar{F}_{D'A_i} + \bar{M}_{D'A_i}) . \tag{4.3}$$

The above expresses the shaking moment as the vector sum of the moments of the D'Alembert forces and the D'Alembert moments. This is also equal to the moments of the ground bearing forces and the ground reaction to the input torque [see Appendix A, eq. (A.13)].

It is to be noted that, from the point of view of vibration analysis, the shaking moment must generally be taken with respect to the moving total mechanism center of mass (which may or may not include the bedplate). If taken with respect to an arbitrary fixed point, the magnitude will vary according to the location of this point. However, it will be shown that, for the force-balanced four-bar linkage under discussion, the value of the shaking moment (and angular momentum) will be invariant when taken with respect to any fixed point, including the total center of mass.

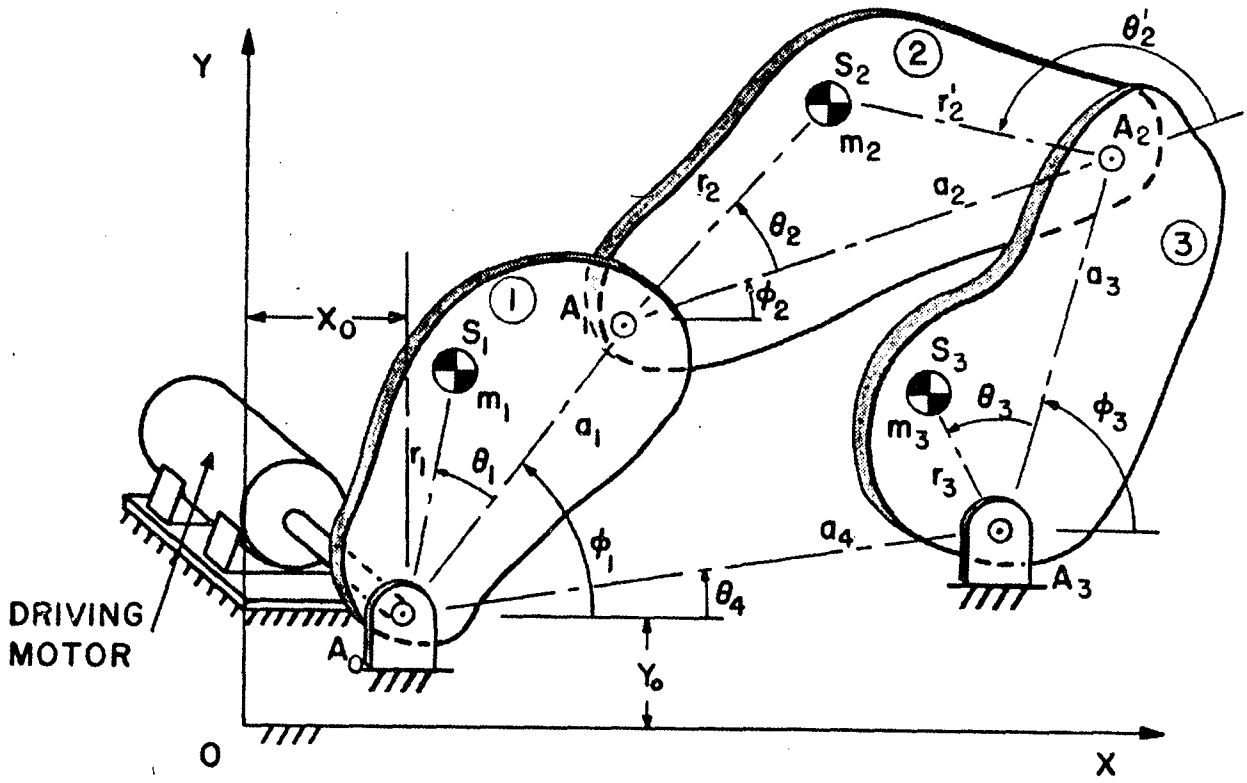

Fig. 7 Four-bar linkage with arbitrary link mass distributions

B. Angular Momentum of Arbitrary Four-Bar Linkage

In order to obtain an expression for the angular momentum of an arbitrary four-bar linkage, as shown in Fig. 7, equation (4.1) is written in scalar form:

$$H_O = \sum_{i=1}^{3} H_i = \sum_{i=1}^{3} m_i(x_i\dot{y}_i - y_i\dot{x}_i + k_i^2\dot{\phi}_i), \tag{4.4}$$

where the x_i and y_i represent the coordinates of the individual link centers of mass S_i with respect to an arbitrary origin O (which does not coincide with a mechanism pivot). Refer to Appendix A for all other nomenclature.

The link center of mass coordinates are given, for $\theta_4 = 0$, by:

$$\left.\begin{aligned} x_1 &= r_1 \cos(\theta_1 + \phi_1) + x_o, \\ y_1 &= r_1 \sin(\theta_1 + \phi_1) + y_o, \\ x_2 &= a_1 \cos\phi_1 + r_2 \cos(\theta_2 + \phi_2) + x_o, \\ y_2 &= a_1 \sin\phi_1 + r_2 \sin(\theta_2 + \phi_2) + y_o, \\ x_3 &= r_3 \cos(\theta_3 + \phi_3) + a_4 + x_o, \\ y_3 &= r_3 \sin(\theta_3 + \phi_3) + y_o. \end{aligned}\right\} \tag{4.5}$$

Upon substitution of equations (4.5) and their derivatives into eq. (4.4), one obtains an expression for the total angular momentum with respect to arbitrary point O:

$$H_O = H_{A_o} + x_o \sum_{i=1}^{3} (m_i\dot{y}_i) - y_o \sum_{i=1}^{3} (m_i\dot{x}_i), \tag{4.6}$$

where the angular momentum with respect to pivot A_o is:

$$\begin{aligned} H_{A_o} &= m_1(k_1^2 + r_1^2)\dot{\phi}_1 + m_2[a_1^2\dot{\phi}_1 + (k_2^2 + r_2^2)\dot{\phi}_2 \\ &\quad + a_1 r_2 \cos(\phi_1 - \phi_2 - \theta_2)(\dot{\phi}_1 + \dot{\phi}_2)] \\ &\quad + m_3[k_3^2 + r_3^2 + r_3 a_4 \cos(\theta_3 + \phi_3)]\dot{\phi}_3. \end{aligned} \tag{4.7}$$

In order to produce an informative expression for the shaking moment, eq. (4.7) is put into a different form. Using the identities:

$$\left.\begin{aligned} \cos(\phi_1 - \phi_2) &= \tau_2 - \lambda, \\ \sin(\phi_1 - \phi_2) &= \tau_1, \end{aligned}\right\} \tag{4.8}$$

and:

$$\left.\begin{aligned} \tau_1 &= \mu \sin(\phi_1 - \phi_3) + \nu \sin \phi_1, \\ \tau_2 &= \mu \cos(\phi_1 - \phi_3) + \nu \cos \phi_1, \end{aligned}\right\} \tag{4.9}$$

in which:

$$\lambda = \frac{a_1}{a_2}, \qquad \mu = \frac{a_3}{a_2}, \qquad \nu = \frac{a_4}{a_2}, \tag{4.10}$$

as well as standard trigonometric identities, eq. (4.7) can be written as:

$$\begin{aligned} H_{A_o} &= \{ m_1(k_1^2 + r_1^2) + m_2 a_1 [a_1 + r_2 (\tau_2 - \lambda) \cos \theta_2 + r_2 \tau_1 \sin \theta_2] \} \dot{\phi}_1 \\ &\quad + m_2 [k_2^2 + r_2^2 + a_1 r_2 (\tau_2 - \lambda) \cos \theta_2 + a_1 r_2 \tau_1 \sin \theta_2] \dot{\phi}_2 \\ &\quad + m_3 [k_3^2 + r_3^2 + r_3 a_4 (\cos \phi_3 \cos \theta_3 - \sin \phi_3 \sin \theta_3)] \dot{\phi}_3. \end{aligned} \tag{4.11}$$

Using the kinematic relationship (see Fig. 7):

$$a_2 - r_2 \cos \theta_2 = - r'_2 \cos \theta'_2 \ , \tag{4.12}$$

and rearranging terms, eq. (4.11) may be written as:

$$\begin{aligned} H_{A_o} = & \left[m_1(k_1^2 + r_1^2) - m_2 a_1 \lambda r'_2 \cos \theta'_2 \right] \dot{\phi}_1 \\ & + m_2 \left[k_2^2 - r_2(a_2 \cos \theta_2 - r_2) \right] \dot{\phi}_2 \\ & + m_3 \left[k_3^2 - r_3(a_3 \cos \theta_3 - r_3) \right] \dot{\phi}_3 + V + W \ , \end{aligned} \tag{4.13}$$

where:

$$\begin{aligned} V = & \left[m_2 a_1 r_2 \tau_2 \dot{\phi}_1 + m_2 a_1 r_2 (\tau_2 - \lambda + \tfrac{1}{\lambda}) \ \dot{\phi}_2 \right. \\ & \left. + m_3 r_3 (a_3 + a_4 \cos \phi_3) \frac{\cos \theta_3}{\cos \theta_2} \dot{\phi}_3 \right] \cos \theta_2 \ , \end{aligned} \tag{4.14}$$

and:

$$W = \left[m_2 a_1 r_2 \tau_1 (\dot{\phi}_1 + \dot{\phi}_2) - m_3 r_3 a_4 \sin \phi_3 \frac{\sin \theta_3}{\sin \theta_2} \dot{\phi}_3 \right] \sin \theta_2 . \tag{4.15}$$

C. Shaking Moment of Arbitrary Four-Bar Linkage

The equation for the shaking moment of an arbitrary four-bar linkage taken with respect to point O is obtained by differentiating eq. (4.6) according to eq. (4.2):

$$M_{M/G}\Big|_O = - \dot{H}_O = - \dot{H}_{A_o} - x_o \sum_{i=1}^{3} (m_i \ddot{y}_i) + y_o \sum_{i=1}^{3} (m_i \ddot{x}_i) \ . \tag{4.16}$$

D. Angular Momentum of Force-Balanced Four-Bar Linkage

It is now of interest to find the extent to which a force-balanced linkage may be moment balanced by means of internal mass rearrangements (see Appendix A, Section 1i).

Under these circumstances eq. (4.6) is reduced to:

$$H_O = H_{A_o} \,. \tag{4.17}$$

The summation terms vanish since, in a force-balanced linkage†, the center of mass is stationary, i.e.

$$\left.\begin{aligned} \sum_{i=1}^{3} (m_i x_i) &= \text{Const.}, \\ \sum_{i=1}^{3} (m_i y_i) &= \text{Const.}, \end{aligned}\right\} \tag{4.18}$$

and the derivatives naturally vanish.

The term H_{A_o} in eq. (4.17) must now be modified to account for the conditions of force balance as given by equations (3.12) and (3.13):

$$\left.\begin{aligned} m_1 r_1 &= m_2 r_2' \lambda \,, \\ \theta_1 &= \theta_2' \,, \end{aligned}\right\} \tag{4.19}$$

$$\left.\begin{aligned} m_3 r_3 &= m_2 r_2 \mu \,, \\ \theta_3 &= \theta_2 + \pi, \end{aligned}\right\} \tag{4.20}$$

in which λ and μ are given by eq. (4.10).

---

†Note that eq. (4.17) shows that, for a force-balanced four-bar linkage, the angular momentum is independent of reference point.

Appropriate substitution of equations (4.19) and (4.20) into eq. (4.13) gives, as explained below:

$$V = 0, \tag{4.21}$$

and:

$$H_{A_o} = \sum_{i=1}^{3} m_i(k_i^2 - r_i t_i)\dot{\phi}_i + W, \tag{4.22}$$

where m_i, r_i, θ_i are the values of a force-balanced mechanism, and where:

$$t_i = a_i \cos \theta_i - r_i , \qquad (i = 1, 2, 3) \tag{4.23}$$

and:

$$W = 2\, m_2 a_2 r_2 \sin \theta_2 \lambda \tau_1 \dot{\phi}_1. \tag{4.24}$$

Eq. (4.21) is arrived at in the following manner. Using eq. (4.20), eq. (4.14) becomes:

$$V = m_2 a_2 r_2 \cos \theta_2 [\lambda \tau_2 \dot{\phi}_1 + (\lambda \tau_2 - \lambda^2 + 1)\dot{\phi}_2 - (\mu + \nu \cos \phi_3)\mu \dot{\phi}_3]. \tag{4.25}$$

Substituting the relationships between angular velocities (derivation not shown):

$$\left.\begin{aligned} \dot{\phi}_2 &= \frac{\lambda}{\tau_3} \sin (\phi_1 - \phi_3)\dot{\phi}_1, \\ \dot{\phi}_3 &= \frac{\lambda \tau_1}{\mu \tau_3} \dot{\phi}_1, \end{aligned}\right\} \tag{4.26}$$

where:

$$\tau_3 = \lambda \sin (\phi_1 - \phi_3) + \nu \sin \phi_3, \tag{4.27}$$

and making use of the Freudenstein equation:

$$\lambda^2 + \mu^2 + \nu^2 - 1 = 2\,\mu\lambda \cos (\phi_1 - \phi_3) + 2\nu(\lambda \cos \phi_1 - \mu \cos \phi_3), \tag{4.28}$$

one obtains the result of eq. (4.21).

In order to arrive at eq. (4.24), one substitutes eq. (4.20) into eq. (4.15) to obtain:

$$W = m_2 a_2 r_2 \sin \theta_2(\lambda\tau_1\dot{\phi}_1 + \lambda\tau_1\dot{\phi}_2 + \mu\nu \sin \phi_3\dot{\phi}_3). \tag{4.29}$$

With the use of eq. (4.26) for $\dot{\phi}_2$ and $\dot{\phi}_3$, the final form of eq. (4.24) is achieved.

E. Shaking Moment of Force-Balanced Four-Bar Linkage

The expression for the shaking moment of a force-balanced four-bar linkage is given by the negative of the derivative of the angular momentum. [See eq. (4.2).] Thus, differentiating eq. (4.22) with respect to time leads to:

$$M_{M/G} = - \dot{H}_{A_o} = - \sum_{i=1}^{3} [m_i(k_i^2 - r_i t_i)\ddot{\phi}_i] - \dot{W}, \tag{4.30}$$

where, with eq. (4.24):

$$\dot{W} = 2\, m_2 a_1 r_2 \sin \theta_2 \, (\tau_1 \ddot{\phi}_1 + \dot{\tau}_1 \dot{\phi}_1) \, . \tag{4.31}$$

As shown in the preceding section, the angular momentum of a force-balanced linkage is the same when taken with respect to any arbitrary point. Therefore, the shaking moment of a force-balanced linkage will also be independent of reference origin, so that this point need no longer be specified.

Eq. (4.30) may also be written as:

$$M_{M/G} = \sum_{i=1}^{3} K_i \, \ddot{\phi}_i + K_4(\tau_1 \ddot{\phi}_1 + \dot{\tau}_1 \dot{\phi}_1), \tag{4.32}$$

where the kinematic constants K_i are given by:

$$\left.\begin{aligned} K_i &= - m_i(k_i^2 + r_i^2 - a_i r_i \cos \theta i), \quad (i = 1, 2, 3) \\ K_4 &= - 2\, m_2 a_1 r_2 \sin \theta_2 \, . \end{aligned}\right\} \tag{4.33}$$

In order to make the shaking moment vanish, it is necessary to make each of the terms in eq. (4.32) vanish individually. Since it is only possible to cause the vanishing of some of the coefficients of the time-dependent terms, it is believed that this expression shows the general impossibility[†] of the full moment balance of a force-balanced four-bar linkage by internal mass rearrangement.

Thus, either some means of external moment balancing, or an optimization approach suggests itself as a possible solution.

[†]Reduced moment characteristics are evident for the following special cases: Parallelogram ($a_1 = a_3$, $a_2 = a_4$) and rhomboid ($a_1 = a_2 = a_3 = a_4$) linkages have the properties that $\ddot{\phi}_1 = \ddot{\phi}_3$ and $\ddot{\phi}_2 = 0$. The deltoid linkage ($a_1 = a_4$, $a_2 = a_3$) has the property that $\ddot{\phi}_2 = -\ddot{\phi}_3$. Thus, in all three cases, the shaking moment vanishes if: (1) the input angular velocity is constant, (2) the coupler link has a symmetrical mass distribution ($\theta_2 = 0$), and (3) for the deltoid linkage only, $K_2 = K_3$.

F. Application of Shaking Moment Equation to Force-Balanced Four-Bar Linkage with Symmetrical Link Mass Distributions and Independent Check

The shaking moment equation (4.30) will now be applied to the inline four-bar linkage illustrated in Fig. 8a, and its validity will be shown by means of an independent check.

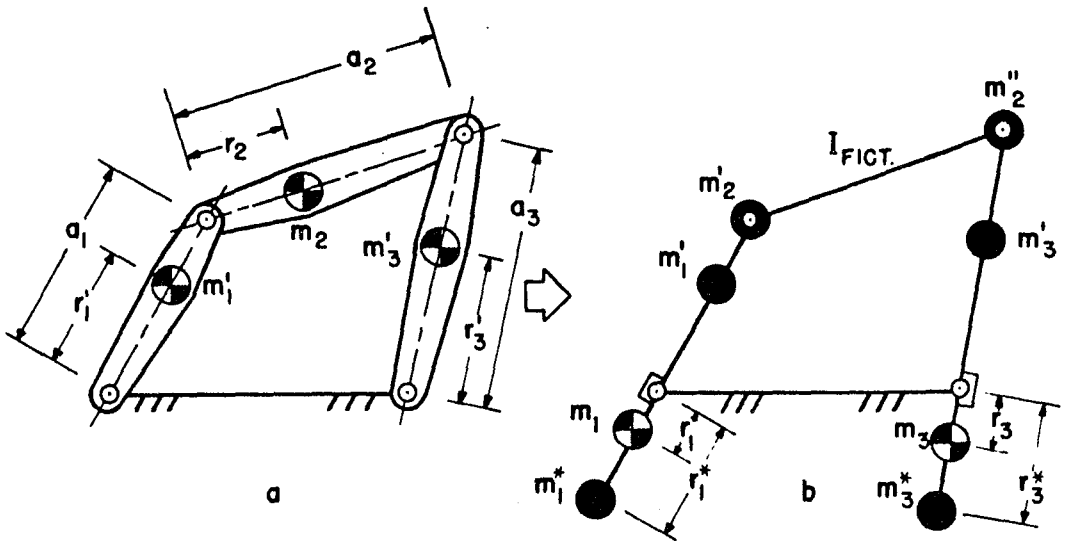

Fig. 8 Dynamic replacement of link masses

The unbalanced mechanism consists of the link masses m_1', m_2, and m_3' at the positions r_1', r_2, and r_3' respectively. Assuming that the values of m_2 and r_2 are given, the values of m_1, r_1, m_3, r_3 which cause the mechanism to be force balanced may be determined by means of equations (4.19) and (4.20).

In this case, $\theta_2 = 0$ and $\theta_2' = \pi$, so that $\theta_1 = \theta_3 = \pi$. Substituting these values into eq. (4.32) leads to:

$$M_{M/G}\Big|_{\substack{\theta_2 = 0 \\ \theta_2' = \pi}} = - m_1(k_1^2 + r_1^2 + a_1 r_1)\ddot{\phi}_1 - m_2(k_2^2 + r_2^2 - a_2 r_2)\ddot{\phi}_2 - m_3(k_3^2 + r_3^2 + a_3 r_3)\ddot{\phi}_3. \tag{4.34}$$

The identical answer may be obtained when one bases the derivation on a combination of static balancing and a dynamic replacement of link masses (see Fig. 8b) as described in Appendix A, Section 1j. This independent check is shown in detail in Appendix C.

Additional forms, first for $\theta_2 = \theta_2' = 0$, and then for $\theta_2 = \pi$, are also shown:

$$M_{M/G}\Big|_{\theta_2 = \theta_2' = 0} = - m_1(k_1^2 + r_1^2 - a_1 r_1)\ddot{\phi}_1 - m_2(k_2^2 + r_2^2 - a_2 r_2)\ddot{\phi}_2 - m_3(k_3^2 + r_3^2 + a_3 r_3)\ddot{\phi}_3 , \tag{4.35}$$

$$M_{M/G}\Big|_{\theta_2 = \pi} = - m_1(k_1^2 + r_1^2 + a_1 r_1)\ddot{\phi}_1 - m_2(k_2^2 + r_2^2 + a_2 r_2)\ddot{\phi}_2 - m_3(k_3^2 + r_3^2 - a_3 r_3)\ddot{\phi}_3 . \tag{4.36}$$

G. Effect of Driving Motor Location

The time rate of change of angular momentum can only be used to find the moment on the ground whenever the driving motor is bolted to the same mounting as represents the frame of the mechanism (it is assumed that this common frame makes contact with the ground).

Whenever motor and mechanism are attached to the ground separately (as may occur with individual spring mountings), while the total moment experienced by the ground is obviously identical, the moment transmitted to the mechanism frame alone is only equal to the moment due to the ground forces (as defined in Appendix A, Section 1g).

Note the alternate formulation for the shaking moment as given in Appendix A, eq. (A.13):

$$\overline{M}_{M/G} = \overline{M}_G + \overline{M}_{14} \ , \qquad (4.37)$$

in which $\overline{M}_{14}$ is the ground reaction to the input torque, and $\overline{M}_G$ is the moment due to the ground forces (see Fig. A1, Appendix A).

For the case of separate mounting, the effect of the input torque (whether additive or subtractive) will not be felt in the shaking moment acting on the mechanism frame.

This concept is also important when designing springs for the mechanism mounting.

V. MOMENT OPTIMIZATION OF FORCE-BALANCED FOUR-BAR LINKAGE WITH SYMMETRICAL LINK MASS DISTRIBUTIONS AND CONSTANT INPUT ANGULAR VELOCITY

This part considers the shaking moment optimization of the reduced case of a force-balanced four-bar linkage with symmetrical link mass distributions and constant input angular velocity.

Where applicable, this optimization is accomplished by means of a least-square formulation. Moment optimization curves are constructed, and their use in selecting the optimum link lengths for a linkage is shown. The influence of the choice of radius for circular counterweights is discussed.

A. Form of Shaking Moment Equation

The force-balanced four-bar linkage under consideration has symmetrical link mass distributions as well as a constant input angular velocity. The coupler link, which is assumed to be specified, will have its center of mass located within the limits $0 \leq r_2 \leq a_2$ for $\theta_2 = 0$. From eq. (4.32), the shaking moment is given by:

$$M_{M/G} = K_2\ddot{\phi}_2 + K_3\ddot{\phi}_3, \tag{5.1}$$

where, according to eq. (4.33):

$$K_2 = - m_2(k_2^2 + r_2^2 - a_2r_2), \tag{5.2}$$

$$K_3 = - m_3(k_3^2 + r_3^2 + a_3r_3). \tag{5.3}$$

[See also equations (4.34)-(4.36).]

In order to optimize the above shaking moment equation, it will be generally necessary to rearrange the mass distribution of the mechanism such that the resulting coefficients K_2 and K_3 will allow $M_{M/G}$ to deviate least from zero over the full cycle. This task will be accomplished in the following sections by means of a least square formulation.

A special case arises when the coupler link has the shape of a "physical pendulum," i.e.

$$k_2^2 = r_2(a_2 - r_2).$$

Since K_2 vanishes, the only feasible optimization consists of making K_3 as small as possible.

B. Formulation of Least-Square Optimization

The general theory concerning the least-square optimization of a function of the type of eq. (5.1) for the shaking moment is derived in Appendix D. This technique allows certain coefficients to be adjusted in such a way that the function deviates least from zero in the least-square sense. The following represents application of this theory to the problem at hand.

In order to make the root-mean-square error of the shaking moment a minimum, the following integral is made a minimum:

$$E = \int_0^{2\pi} (M_{M/G})^2 \, d\phi_1 = \text{minimum.} \tag{5.4}$$

The optimum values of the coefficients K_2 and K_3[†] in eq. (5.1) are required in order to minimize the shaking moment. Thus, the partial derivative of eq. (5.4) is taken, alternately with respect to both coefficients, and then equated to zero:

$$\frac{\partial E}{\partial K_2} = 2\int_0^{2\pi} M_{M/G} \frac{\partial M_{M/G}}{\partial K_2} \, d\phi_1 = 0, \tag{5.5}$$

$$\frac{\partial E}{\partial K_3} = 2\int_0^{2\pi} M_{M/G} \frac{\partial M_{M/G}}{\partial K_3} \, d\phi_1 = 0. \tag{5.6}$$

[†] Appendix D shows a comparable procedure for the four-bar linkage in which the coupler link has a nonsymmetrical mass distribution, and therefore the shaking moment equation has three terms, each with a coefficient K_i.

Upon substitution of eq. (5.1), equations (5.5) and (5.6) become:

$$K_2 \mathcal{I}_{22} + K_3 \mathcal{I}_{23} = 0, \tag{5.7}$$

$$K_2 \mathcal{I}_{23} + K_3 \mathcal{I}_{33} = 0, \tag{5.8}$$

in which the following integrals are shown:

$$\left.\begin{aligned} \mathcal{I}_{22} &= \int_0^{2\pi} \ddot{\phi}_2^{\,2}\, d\phi_1, \\ \mathcal{I}_{33} &= \int_0^{2\pi} \ddot{\phi}_3^{\,2}\, d\phi_1, \\ \mathcal{I}_{23} &= \int_0^{2\pi} \ddot{\phi}_2 \ddot{\phi}_3\, d\phi_1. \end{aligned}\right\} \tag{5.9}$$

The homogeneous system of two equations (5.7) and (5.8) in two unknowns K_2 and K_3 has a nontrivial solution only if the following determinant of the integrals vanishes:

$$\mathcal{D} = \begin{vmatrix} \mathcal{I}_{22} & \mathcal{I}_{23} \\ \mathcal{I}_{23} & \mathcal{I}_{33} \end{vmatrix} = \mathcal{I}_{22}\mathcal{I}_{33} - \mathcal{I}_{23}^2 \tag{5.10}$$

The integral version of Cauchy's Inequality [see eq. (D.14) of Appendix D], as applied to these functions, states that:

$$\int_0^{2\pi} \ddot{\phi}_2^{\,2} d\phi_1 \int_0^{2\pi} \ddot{\phi}_3^{\,2} d\phi_1 > \left(\int_0^{2\pi} \ddot{\phi}_2 \ddot{\phi}_3 d\phi_1 \right)^2, \tag{5.11}$$

unless $A\ddot{\phi}_2 \equiv B\ddot{\phi}_3$, where A and B are constants, not both zero.

It is shown in eq. (I.12) of Appendix I that, except for the parallelogram, rhomboid, and deltoid mechanisms, $\ddot{\phi}_2$ and $\ddot{\phi}_3$ are always linearly independent for four-bar linkages. Therefore, with the noted exceptions:

$$\mathcal{D} > 0, \tag{5.12}$$

and a nontrivial solution does not exist.

Disregarding the trivial solution of equations (5.7) and (5.8), for which $K_2 = K_3 = 0$, and which cannot be translated into physical reality, it becomes necessary to find local optima in the manner described in Section 4 of Appendix D.

A local optimum is defined as the ratio:

$$\xi_{ij} = \frac{K_i \big|_{\text{optimum}}}{K_j \big|_{\text{given}}}, \tag{5.13}$$

where the optimum K_2 is found if K_3 is assumed to be given or, conversely, the optimum K_3 is solved for if K_2 is specified. These optimum ratios are obtained in the following manner.

By specifying K_3 in eq. (5.1), eq. (5.5) reduces to the nonhomogeneous form:

$$K_2 \mathcal{I}_{22} = - K_3 \mathcal{I}_{23} \quad (K_3 \text{ given}), \tag{5.14}$$

which yields:

$$\frac{K_2 \big|_{\text{optimum}}}{K_3 \big|_{\text{given}}} = - \frac{\mathcal{I}_{23}}{\mathcal{I}_{22}}. \tag{5.15}$$

Similarly, by assuming K_2 to be given, eq. (5.6) leads to:

$$\frac{K_3|_{\text{optimum}}}{K_2|_{\text{given}}} = -\frac{\mathcal{I}_{23}}{\mathcal{I}_{33}} \tag{5.16}$$

Referring to the definition of eq. (5.13), equations (5.15) and (5.16) become:

$$\xi_{23} = -\frac{\mathcal{I}_{23}}{\mathcal{I}_{22}}, \tag{5.17}$$

$$\xi_{32} = -\frac{\mathcal{I}_{23}}{\mathcal{I}_{33}}, \tag{5.18}$$

in which the link dimensions a_1, a_2, a_3, a_4 are needed to calculate the integrals $\mathcal{I}_{ij}$.

Graphs of the values of ξ_{23} and ξ_{32}, calculated according to equations (5.15) and (5.16) for various Grashof crank-and-rocker linkages, are found in Appendix E. These calculated values are independent of magnification, as proven in Appendix G. That is, any four-bar linkages whose dimensions are proportional to a_1, a_2, a_3, a_4, i.e. ka_1, ka_2, ka_3, ka_4, have the same values of ξ_{23} and ξ_{32}.

Consequently, ξ_{23} and ξ_{32} for these similar linkages are plotted as functions of the ratios $\frac{a_2}{a_1}$, $\frac{a_3}{a_1}$, $\frac{a_4}{a_1}$ in Appendix E. Each graph deals with a given link length ratio $\frac{a_2}{a_1}$, whereas each curve of a certain graph represents the values of ξ_{ij} plotted against the ratio $\frac{a_4}{a_1}$ for a specified value of $\frac{a_3}{a_1}$.

The ranges of crank-and-rocker linkages within which ξ_{ij} is plotted are:

$$\left.\begin{array}{ll} (1) & 2.0 \leq \dfrac{a_2}{a_1} \leq 5.0, \\ (2) & 1.5 \leq \dfrac{a_3}{a_1} \leq 6.0, \\ (3) & 1.0 \leq \dfrac{a_4}{a_1} \leq 7.0. \end{array}\right\} \qquad (5.19)$$

A sample set of curves for ξ_{32} is illustrated in Fig. 9. This graph shows curves for $\dfrac{a_2}{a_1} = 4$, and includes the values of $\dfrac{a_3}{a_1}$ and $\dfrac{a_4}{a_1}$ as indicated in ranges (2) and (3) above.

It now remains to show the extent to which the optimum ratio ξ_{ij} may be realized in actual linkages.

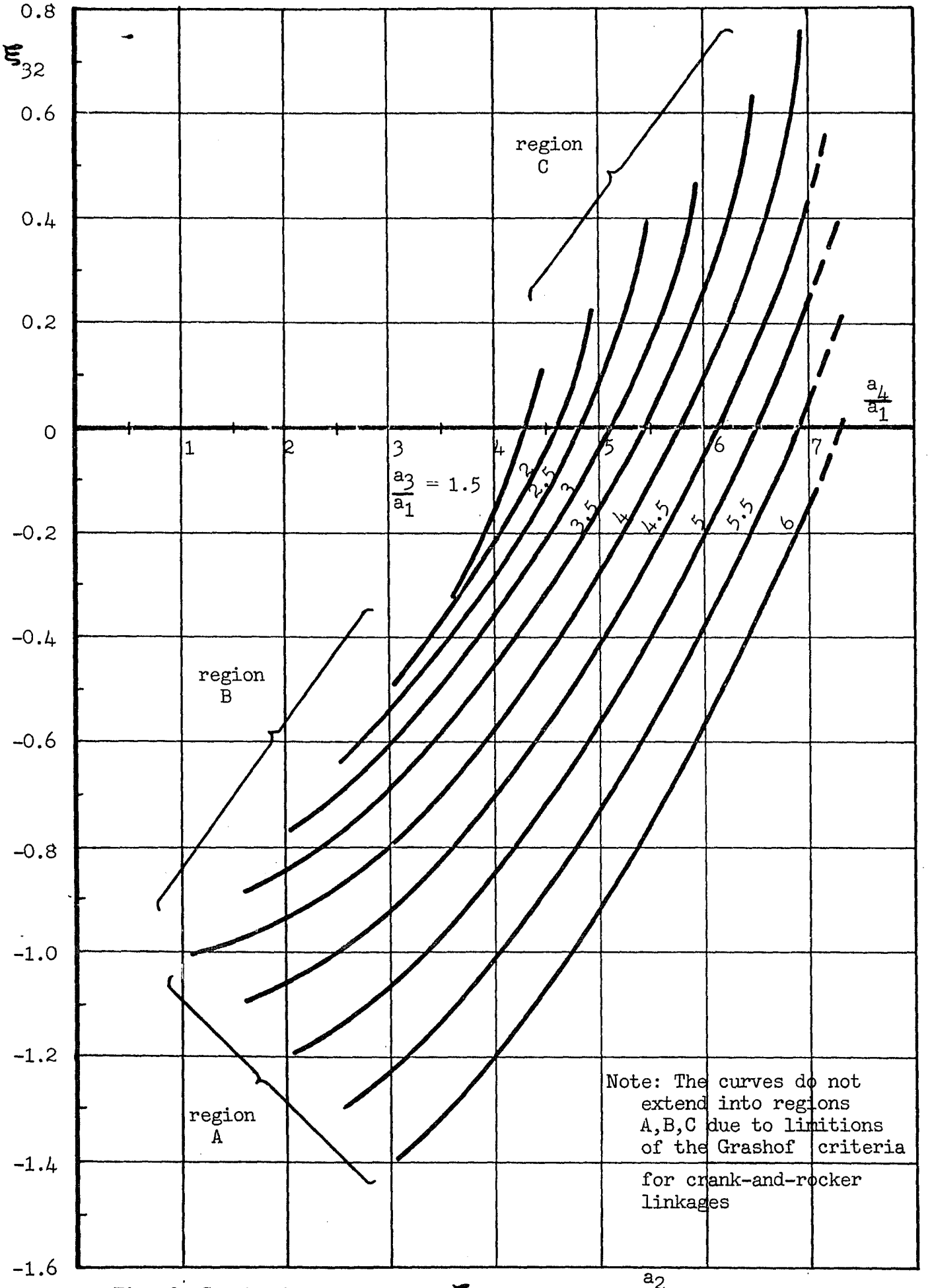

Fig. 9 Graph of optimum ratio ξ_{32} for families $\frac{a_2}{a_1} = 4$

C. Application of Least-Square Optimization

In order to achieve the optimum moment design of a certain force-balanced four-bar linkage with dimensions a_1, a_2, a_3, a_4, it is necessary to arrange the link masses, positions of link centers of mass, and link radii of gyration in such a way that the optimum ratios ξ_{ij} can be satisfied. From the definitions of K_2 and K_3, as given by equations (5.2) and (5.3), the actual ratios η_{ij} are defined as:

$$\eta_{32} = \frac{1}{\eta_{23}} = \frac{K_3}{K_2} = + \frac{m_3(k_3^2 + r_3^2 + a_3 r_3)}{m_2(k_2^2 + r_2^2 - a_2 r_2)} . \qquad (5.20)$$

The indicated optimum design is reached when it is possible to adjust one of the η_{ij} to coincide numerically with the applicable ξ_{ij}. Investigation has shown that it is never possible to match ξ_{23} and ξ_{32} with η_{23} and η_{32} simultaneously. However, it is frequently possible to match one pair of ratios with identical subscripts.

The process of matching η_{32} for a given case with ξ_{32} will now be briefly outlined by means of an example. The background material, proofs, and conclusions are given later on in greater detail. Note that for the given example, η_{23} and ξ_{23} cannot be matched because the values are out of range (see Section 3 following).

(a) For a given linkage configuration (i.e. shapes of links) as well as the position of the coupler center of mass, η_{32} may be found for various ratios of $\frac{a_2}{a_1}$ and $\frac{a_3}{a_1}$. Eq. (5.20) indicates that η_{32} (or η_{23}) is independent of the ground link ratio $\frac{a_4}{a_1}$. Fig. 10 shows η_{32} plotted

against the output link ratio $\frac{a_3}{a_1}$ for the coupler link ratio $\frac{a_2}{a_1} = 4$. (This particular mechanism has its coupler center of mass at $r_2 = 0$, and has the nominal linkage configuration of Section 1 below.)

Point 2 on the curve of Fig. 10 represents a certain length of rocker link for a given coupler link length: $\frac{a_2}{a_1} = 4$, $\frac{a_3}{a_1} = 3$, $\eta_{32} = 0.356$.

(b) This value of η_{32} must now be matched with the identical value of ξ_{32} in Fig. 11 for the given ratios $\frac{a_3}{a_1}$ and $\frac{a_2}{a_1}$. (Fig. 11 is a simplified version of Fig. 9, and considers the same families of linkages as those shown in Fig. 10.) It is seen that matching is only possible for a single value of $\frac{a_4}{a_1}$. For example, this match occurs for point 2 at $\frac{a_4}{a_1} = 5.82$.

All other points of Fig. 10 may be similarly matched, as exemplified by points 1 and 3. The resulting curve represents all optimum mechanisms of the indicated families.

(c) The foregoing shows that for each coupler link and rocker link ratio combination, there will be one ground link ratio which allows the optimum moment to be realized. This means that this procedure is generally better suited to selecting an optimum linkage, rather than improving the moment characteristics of a given linkage, although the latter improvement is possible to a certain extent.

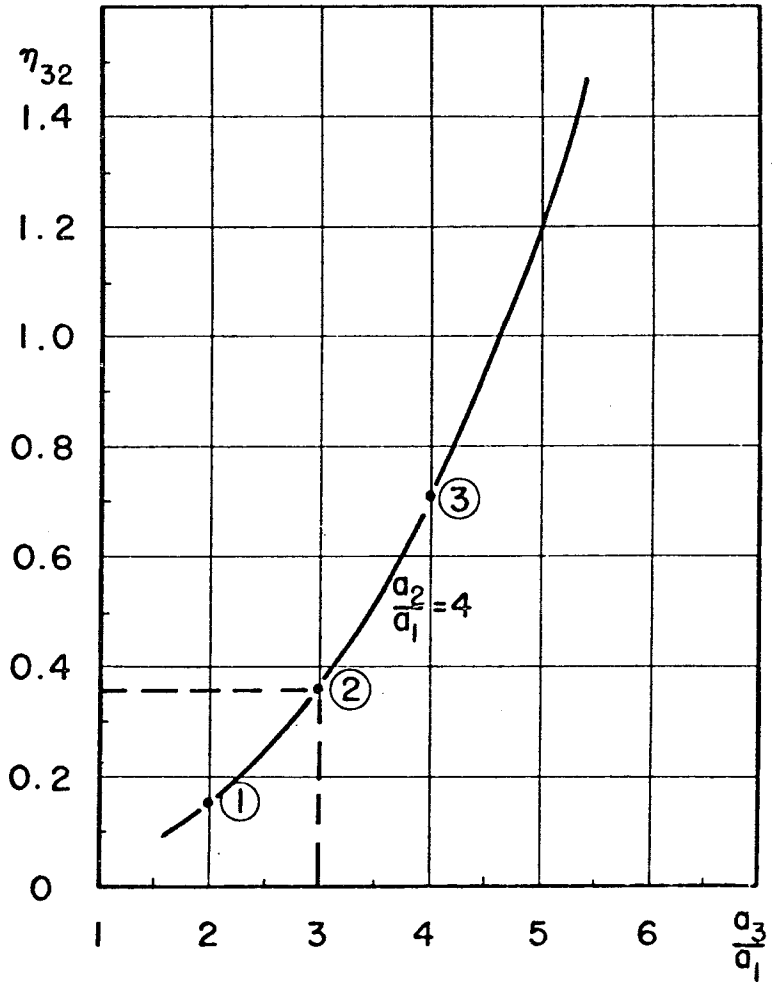

Fig. 10 Graph of actual ratio η_{32} for nominal linkage configuration and $r_2 = 0$

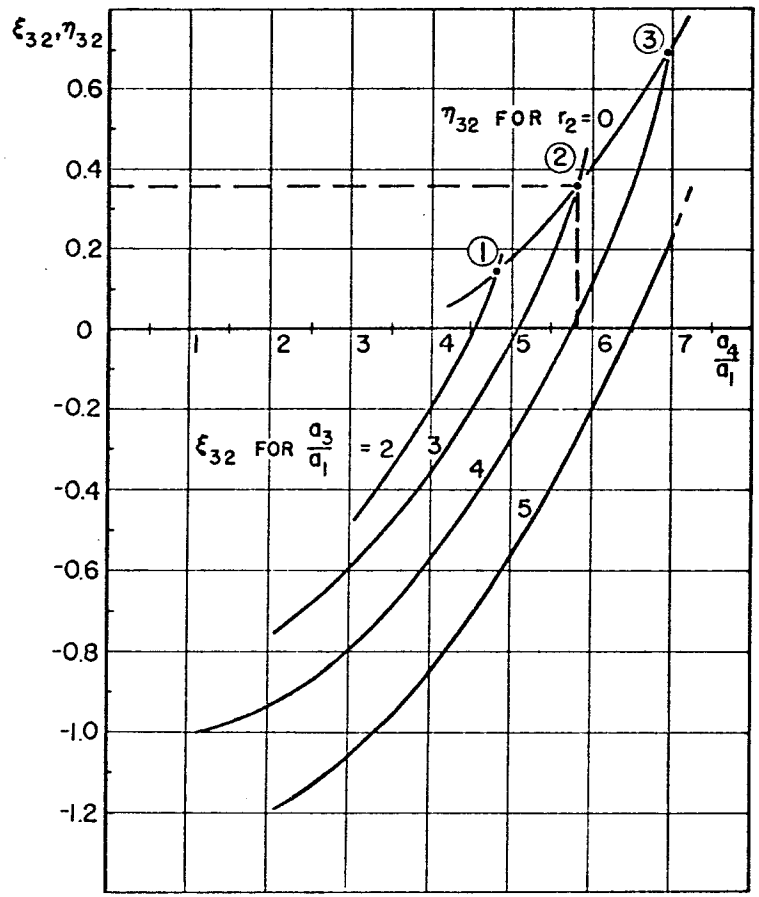

Fig. 11 Moment optimization curve for families $\frac{a_2}{a_1} = 4$

Appendix E gives moment optimization curves, similar to the type of Fig. 11, for all force-balanced crank-and-rocker linkages with symmetrical link mass distributions which correspond to a chosen nominal linkage configuration.

It is now necessary to discuss the conditions which must be fulfilled for the construction of the above moment optimization curves: (1) choice of nominal linkage configuration for determination of η_{ij}, (2) proof of independence of magnification, (3) theoretical restrictions to matching actual and optimum ratios, (4) determination of η_{ij} for moment optimization curves, and (5) effect of parameter variation on moment optimization curves.

1. Choice of Nominal Linkage Configuration

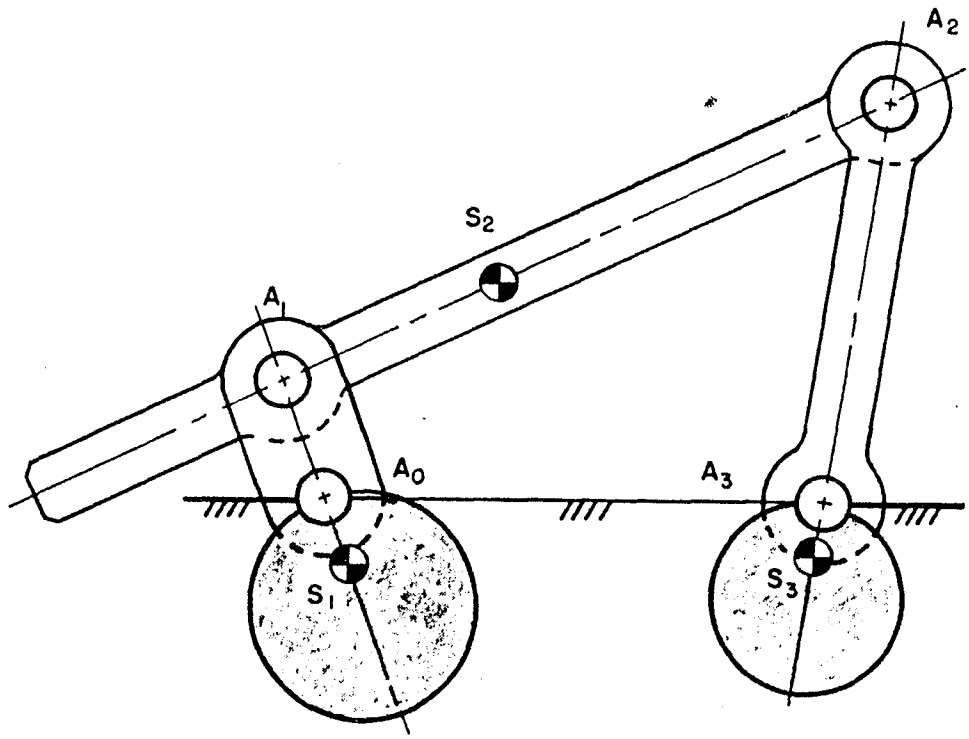

Fig. 12 Four-bar linkage with nominal linkage configuration

The actual ratio η_{ij} depends entirely upon the shapes of the individual links. For present purposes, the linkage configuration illustrated in Figures 12 and 13 is chosen. These figures represent a force-balanced four-bar linkage with symmetrical link mass distributions.

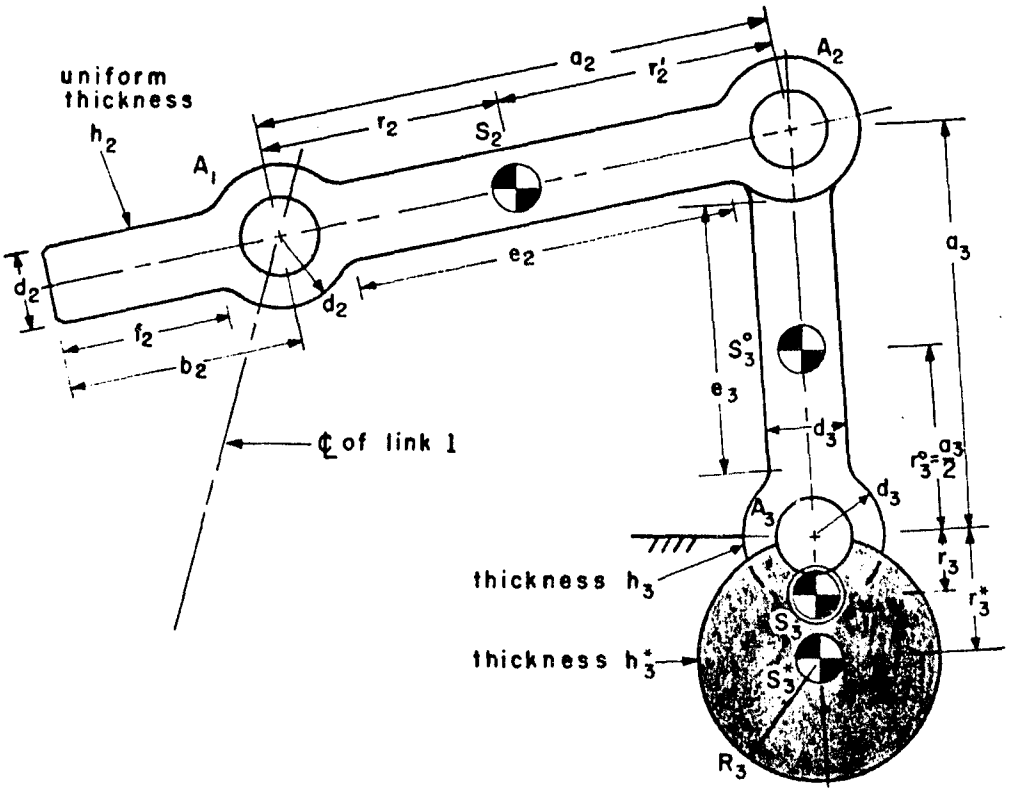

Fig. 13 Parameters of coupler and output links for chosen four-bar linkage configuration

In this nominal linkage, both links 1 and 3 consist of an original link and a counterweight. With the exception of the input link 1, each original link i has a constant width d_i between the bearings, and a circular shape of radius d_i at the bearings (see Fig. 13). The input link differs in that its width is not reduced between bearings.

The coupler link 2 can extend beyond either the bearing at A_1 or the bearing at A_2, such that the position of its center of mass can be located (for $\theta_2 = 0$) between:

$$0 \leq r_2 \leq a_2.$$

(See also Figures 1 and 2.) Also, for each original link, a uniform thickness h_i as well as a uniform mass density ρ are chosen.

The counterweights are circular, and tangent to the centers of rotation (see Appendix H for minimum moment of inertia considerations). They have radii $R_i = r_i^*$, thicknesses h_i^*, and mass density ρ^*.

For generality, the following dimensionless ratios are introduced to describe all link dimensions

$$\left.\begin{aligned} \alpha_i &= \frac{a_i}{a_1}, \quad \beta_i = \frac{d_i}{a_1}, \quad \gamma_i = \frac{h_i}{d_i}, \\ \delta_i &= \frac{h_i^*}{h_i}, \quad \sigma_i = \frac{r_i}{a_i}. \end{aligned}\right\} \tag{5.21}$$

These parameters become especially useful when examining the independence of magnification of the actual ratio η_{ij}.

2. Proof of Independence of Magnification

In order to compare the η_{ij} to the ξ_{ij}, it is necessary that the η_{ij} are also independent of magnification (see explanation in connection with ξ_{ij} in Part VB above). This independence of magnification of η_{ij} may be shown by expanding the coefficients K_2 and K_3 in the following manner:

$$\left.\begin{aligned} K_2 &= \rho a_1^5 P_2, \\ K_3 &= -\rho a_1^5 P_3, \end{aligned}\right\} \qquad (5.22)$$

where P_2 and P_3 are functions only of the dimensionless ratios α_i, β_i, γ_i, δ_i, σ_i as defined in eq. (5.21).

Substitution of eq. (5.22) into eq. (5.20) gives:

$$\eta_{32} = \frac{1}{\eta_{23}} = -\frac{P_3}{P_2}, \qquad (5.23)$$

and η_{ij} is proven to be independent of magnification. Appendix G, Section 2, shows the derivation of equations (5.22) and (5.23) in detail.

3. Theoretical Restrictions to Matching Actual and Optimum Ratios

The sign of the ratio η_{32}, which is the same as the sign of η_{23}, determines the region of possible matching of ξ_{ij} and η_{ij}. Table 5 delineates certain subcases of the four-bar linkage under consideration, showing the corresponding signs of η_{ij}. It is noted that the sign of η_{ij} can be dependent upon the mass distribution of the coupler link, i.e. the relative magnitudes of k_2^2 and $r_2(a_2 - r_2)$.

Table 5 Subcases of four-bar linkage for $\theta_2 = 0$

Case	Location of Link Center of Mass	Mass Distribution	Sign of $\eta_{32} = \frac{1}{\eta_{23}} = \frac{K_3}{K_2}$
I	$r_2 = 0$	All	+
II	$0 < r_2 < a_2$	$k_2^2 < r_2(a_2 - r_2)$	-
III		$k_2^2 = r_2(a_2 - r_2)$	None ($K_2 = 0$)
IV		$k_2^2 > r_2(a_2 - r_2)$	+
V	$r_2 = a_2$	All	+

Thus, cases I, IV, and V can only be made optimum in those cases where ξ_{ij} is positive. Case II is the only case for which ξ_{ij} must be negative in order to be optimizable.

Case III represents the special case of the physical pendulum coupler link in which K_2 vanishes. Here, since no matching is possible, a simple minimization of coefficient K_3 is performed.

One additional limitation exists, which restricts the matching for case II. In Appendix F, it is shown that η_{32} is always out of the range of matching with ξ_{32}, so that optimization can only occur on the basis of matching η_{23} with ξ_{23}.

4. Determination of η_{ij} for Moment Optimization Curves

Appendix E gives a collection of moment optimization curves which are of the same form as Fig. 11. Based upon the linkage configuration of Figures 12 and 13, η_{23} and η_{32} [calculated from eq. (G.49) of Appendix G] are shown for link length ratios $\alpha_i = \frac{a_i}{a_1}$ which satisfy the Grashof criteria [see eq. (5.19)] .

The link dimensions used are expressed by the following parameters [defined in eq. (5.21)] :

$$\beta_i = 0.5 \ , \qquad \gamma_i = 0.4 \ , \qquad \delta_i = 2.5 \ , \tag{5.24}$$

with the coupler center of mass varying between:

$$\sigma_2 = 0, \ 0.25, \ 0.50, \ 0.75, \ 1.00 \ . \tag{5.25}$$

The curves of Appendix E allow the following observations concerning the ability to match η_{ij} and ξ_{ij}:

(a) Whenever matching is possible, i.e. the optimum moment condition is reached, it will occur in the range of the highest values of $\frac{a_4}{a_1}$ for all families of linkages. (See also Part VI.)

(b) The value of $\frac{a_4}{a_1}$ is a function of the parameter $\sigma_2 = \frac{r_2}{a_2}$. As σ_2 approaches 0.5, the optimum ratio $\frac{a_4}{a_1}$ reaches its minimum value for a given family $\frac{a_3}{a_1}$. Conversely, as σ_2 diverges from 0.5 (towards 0 or 1), the optimum ratio $\frac{a_4}{a_1}$ approaches its upper limit for mechanisms within the Grashof criteria. The above described influence of σ_2 becomes more perceptible with increasing ratio $\frac{a_2}{a_1}$.

(c) The sign of the matching η_{ij} is determined by the magnitude of σ_2:

(1) for $\sigma_2 = 0, 0.25, 0.75, 1.00$, η_{ij} is positive;

(2) for $\sigma_2 = 0.50$, η_{ij} is negative.

This is borne out by the theoretical discussion associated with Table 5 in the preceding section.

(d) The match $\eta_{23} = \xi_{23}$ is possible for:

(1) $\sigma_2 = 0.25, 0.50, 0.75, 1.00$, for all families $\frac{a_2}{a_1}$;

(2) $\sigma_2 = 0$, for families $\frac{a_2}{a_1} = 2, 3$;

whereas the match $\eta_{32} = \xi_{32}$ is only possible for families $\frac{a_2}{a_1} = 4, 5$ for $\sigma_2 = 0$. As noted previously, only one of the ξ_{ij} can be matched for a given case.

5. Effect of Parameter Variation on Moment Optimization Curves

The effect of varying the link cross-section as well as the counterweight density for the nominal linkage configuration was investigated. It has been found that these changes, which maintain either a constant link cross-section area or moment of inertia, do not influence the moment optimization curves to any large extent.†

Fig. 14 illustrates a typical moment optimization curve which results from the parameter variations listed in Table 6. Fig. 14 represents the same linkage families as those of Fig. 11. For this case, $\frac{a_2}{a_1} = 4$ and $\sigma_2 = 0$.

Figures E9-E12 of Appendix E show that this type of parameter variation has little influence on the moment optimization curves, for the full range of linkages examined. Bands of variation, which contain the cases of Table 6, are given for the typical cases of $\frac{a_2}{a_1} = 2, 3, 5$ and $\sigma_2 = 0, 0.5, 1.0$.

Thus, it appears that this insensitivity to parameter change permits the use of these original curves for any cross-section configuration in order to obtain an idea of the range of linkages that are optimizable.

---

†Of course, any changes which produce identical ratios $\beta_i = \frac{d_i}{a_1}$ will have identical results for a given linkage configuration. Recall that, according to eq. (5.20):

$$\eta_{32} = \frac{m_3(k_3^2 + r_3^2 + a_3 r_3)}{m_2(k_2^2 + r_2^2 - a_2 r_2)} .$$

The thickness h_i influences m_2 and m_3 proportionally, and has no influence on the terms within the parentheses.

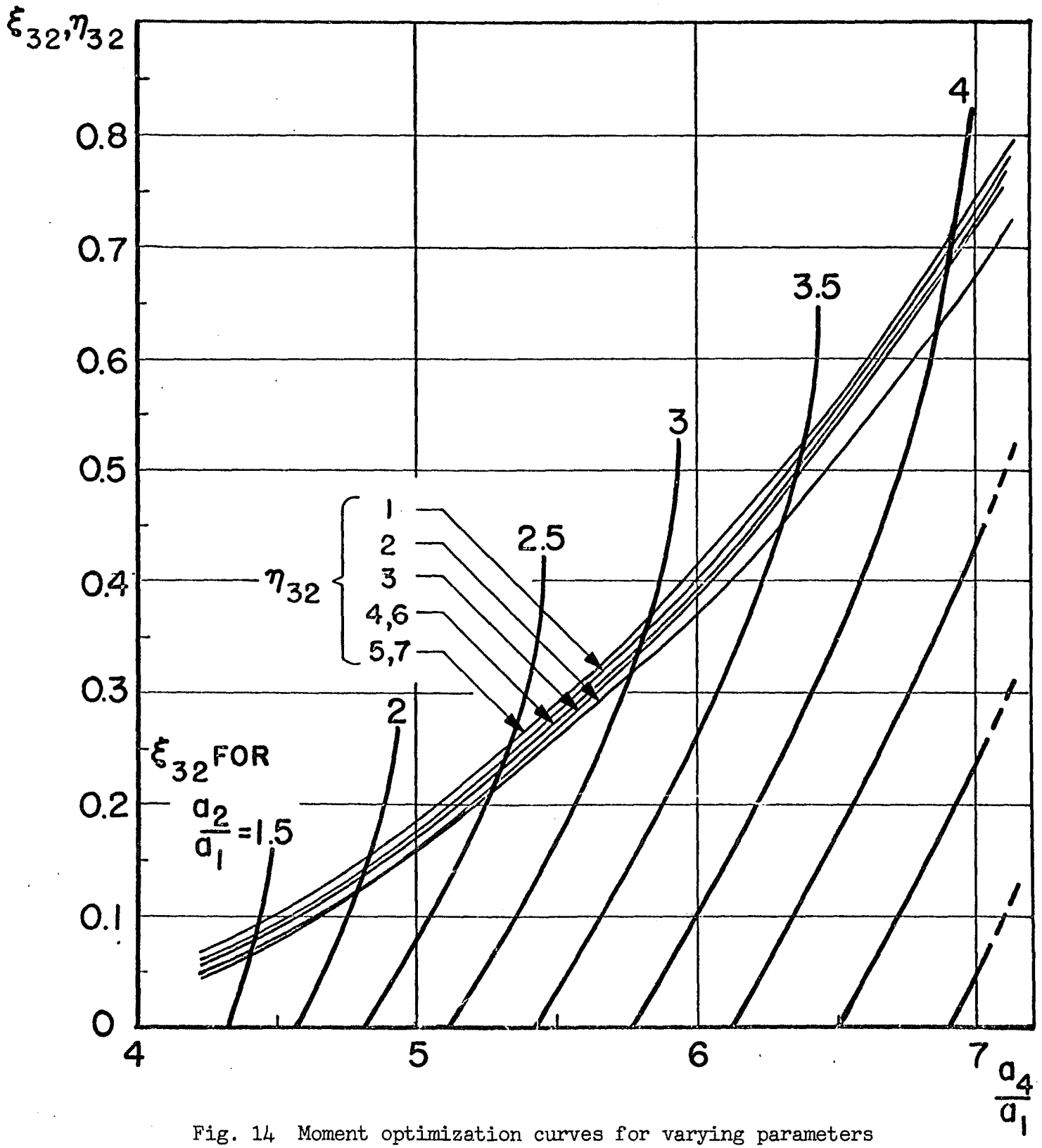

Fig. 14 Moment optimization curves for varying parameters for families. $a_2/a_1 = 4$

Table 6 Variation of nominal cross-section and density parameters

No.	Case	$\beta_i = \frac{d_i}{a_1}$	$\gamma_i = \frac{h_i}{d_i}$	$\delta_i = \frac{h_i^*}{h_i}$	ρ	ρ_3^*
1	nominal case	0.500	0.400	2.5	1	1
2	cwt. density change (link 3)	0.500	0.400	2.5	1	4
3	constant area	0.333	0.900	2.5	1	1
4	constant area	0.400	0.625	2.5	1	1
5	constant area	0.600	0.278	2.5	1	1
6	constant moment of inertia	0.400	0.978	2.5	1	1
7	constant moment of inertia	0.600	0.193	2.5	1	1

D. Example: Selection of Optimum Ground Link Ratio

For this example, it is assumed that the coupler and output link length ratios of the four-bar linkage are given, in addition to parameters describing the actual link shapes, and that it is required to select the ground link ratio such that the shaking moment is optimized.

Thus, assume the following link length ratios:

$$\alpha_2 = \frac{a_2}{a_1} = 4 \ , \qquad \alpha_3 = \frac{a_3}{a_1} = 3.$$

With the linkage configuration chosen as that shown in Figures 12 and 13, let the parameters describing the cross-section and shape for the links be given by:

$$\beta_2 = \frac{d_2}{a_1} = \beta_3 = 0.5 \ , \qquad \gamma_2 = \frac{h_2}{d_2} = \gamma_3 = 0.4 \ ,$$

$$\delta_3 = \frac{h^*_3}{h_3} = 2.5 \ , \qquad \sigma_2 = \frac{r_2}{a_2} = \sigma_3 = 0 \ .$$

Upon substitution of these parameters into eq. (G.49) of Appendix G, the actual ratios become:

$$\eta_{32} = 0.356,$$

$$\eta_{23} = 2.81 \ .$$

The technique for entering values of η_{ij} into the ξ_{ij} curves was illustrated in Section C above. The value of η_{23} in this example is out of range of the ξ_{23} curves, but the η_{32} may be matched to ξ_{32}. Point 2 of Fig. 11 illustrates the matching of just this point, with the resulting ratio $\alpha_4 = \frac{a_4}{a_1} = 5.82$.

Thus, the crank-and-rocker linkage for which $\frac{a_2}{a_1} = 4$, $\frac{a_3}{a_1} = 3$, and $\frac{a_4}{a_1} = 5.82$ has the optimum dimensions, such that the shaking moment is minimum (for the given linkage configuration).

E. Conclusions

The following conclusions may be drawn concerning the optimization of the shaking moment of a force-balanced four-bar linkage by means of the given least-square method:

(a) The technique is most useful for finding the optimum ground link ratio $\frac{a_4}{a_1}$ for a given coupler-rocker family (i.e. ratios $\frac{a_2}{a_1}$ and $\frac{a_3}{a_1}$). The optimum ratio $\frac{a_4}{a_1}$ for any family is a function of the parameter σ_2, which represents the location of the coupler center of mass.

(b) A change of link and counterweight parameters within a given linkage configuration does not influence the resulting optimum ratio $\frac{a_4}{a_1}$ for given coupler-rocker families to any radical extent. This shows that the ratio $\frac{a_4}{a_1}$ represents the most critical parameter in moment optimization for given coupler-rocker families.

(c) The ability to effect these relatively small changes of the moment optimization curves enables the link masses for a given mechanism to be redistributed in such a way that the exact optimum may be obtained if the linkage already lies near this condition. Section F below describes the technique for calculating the counterweight dimensions of the output link such that the optimum moment requirements are exactly satisfied [recall that the input link does not have to be considered] .

(d) While the least-square method indicates the optimum ground link ratio for a given coupler-rocker family, it gives no information concerning the relative magnitudes of these optimum moments. In order to clarify this, Part VI examines the relative magnitudes of moments within the chosen range of linkages.

F. Determination of Optimum Counterweight Radius

Whenever an unbalanced linkage of prescribed dimensions exhibits an optimum ratio ξ_{ij}, which lies near the region of matching in the moment optimization curves (as in Fig. 14), it is possible to design the counterweight of the output link such that it will effect simultaneous force balance and moment optimization. The counterweight of the input link has no influence on the shaking moment in this case, and may be chosen within reasonable limits as described in Part III.

1. Derivation

The sequence of calculations necessary in order to obtain the optimum counterweight radius is now described. The given parameters are (refer to Figures 7 and 13):

(a) link lengths a_1, a_2, a_3, a_4,

(b) optimum ratios ξ_{23} and ξ_{32},

(c) coupler link parameters m_2, r_2, k_2, ($\theta_2 = 0$, $0 \leq r_2 \leq a_2$),

(d) original output link parameters m_3^o, r_3^o, k_3^o.

From eq. (5.2), coefficient K_2 is first calculated:

$$K_2 = - m_2(k_2^2 + r_2^2 - a_2 r_2). \tag{5.26}$$

Depending upon which ratio ξ_{ij} is applicable, the required magnitude of coefficient K_3 is then obtained from either:

$$K_3 = \frac{K_2}{\xi_{23}} , \tag{5.27}$$

or:

$$K_3 = K_2 \xi_{32} . \tag{5.28}$$

The force-balancing condition of eq. (3.13) gives the required mass-distance product of link 3:

$$m_3 r_3 = m_2 r_2 \frac{a_3}{a_2} , \tag{5.29}$$

and the following relationship between the counterweight and the original link must be observed [see eq. (3.15a)].

$$m_3^* r_3^* = m_3 r_3 + m_3^o r_3^o \ . \tag{5.30}$$

The moment of inertia of link 3 is equal to the sum of moments of inertia of the original link and the counterweight, all taken with respect to pivot A_3 (see Fig. 13):

$$I_{3/A_3} = m_3(k_3^2 + r_3^2) = m_3^o(k_3^{o2} + r_3^{o2}) + m_3^*(k_3^{*2} + r_3^{*2}) \ . \tag{5.31}$$

In order to obtain an expression for R_3, the coefficient K_3 must be expanded. From eq. (5.3):

$$K_3 = - m_3(k_3^2 + r_3^2 + a_3 r_3). \tag{5.32}$$

Substituting eq. (5.31) into (5.32), and solving for the counterweight moment of inertia (about pivot A_3) gives:

$$m_3^*(k_3^{*2} + r_3^{*2}) = - K_3 - m_3^o(k_3^{o2} + r_3^{o2}) - m_3 r_3 a_3 \ . \tag{5.33}$$

For the counterweight, which is circular and tangent to its center of rotation (see also Appendix H), the following equations hold:

$$r_3^* = R_3 \ , \tag{5.34}$$

$$k_3^{*2} = \frac{1}{2} R_3^2 \ . \tag{5.35}$$

Substituting these expressions into the left side of eq. (5.33) gives:

$$m_3^*(k_3^{*2} + r_3^{*2}) = \frac{3}{2} (m_3^* r_3^*) R_3 \ . \tag{5.36}$$

If eq. (5.36) is substituted back into eq. (5.33) and solved for R_3 with the help of eq. (5.30), then the final expression for the optimum counterweight radius is obtained:

$$R_3 = \frac{2}{3}\left[\frac{-K_3 - m_3^o(k_3^{o2} + r_3^{o2}) - (m_3 r_3)a_3}{m_3^o r_3^o + m_3 r_3}\right] , \qquad (5.37)$$

in which all terms are either given or may be computed from equations (5.26) - (5.29).

In order to maintain a positive value for R_3, eq. (5.37) indicates that K_3 must satisfy the following inequality:

$$K_3 < \left[-m_3^o(k_3^{o2} + r_3^{o2}) - (m_3 r_3)a_3\right] < 0 . \qquad (5.38)$$

As mentioned above, it is desirable to check whether the ξ_{ij} values are close to the moment optimization curves. This is important only in that the resulting radius R_3 must be a reasonable value. Eq. (5.37) is always applicable, but the solution is not necessarily attainable on the basis of the permissible radius and thickness of counterweight. Note that, from eq. (G.34) of Appendix G, the counterweight thickness h_3^* is given by:

$$h_3^* = \frac{m_3^o r_3^o + m_3 r_3}{\rho^* \pi R_3^3} . \qquad (5.39)$$

2. Example

For this example, it is assumed that all link lengths as well as the parameters describing the original link shapes are given, and that it is required to calculate the counterweight radius such that the shaking moment is optimum.

Table 7 gives the relevant dimensions of the original unbalanced linkage, as illustrated in Fig. 13.

Table 7 Dimensions of unbalanced four-bar linkage

Link i	1	2	3	4
a_i (in)	2.0	8.0	6.0	11.6
r_i^o (in)	N.R.†	0	3.0	...
θ_i^o (deg)	N.R.	0	0	...
d_i (in)	N.R.	1.0	1.0	...
h_i (in)	N.R.	0.4	0.4	...

†N.R. = not required for this example.

For the given link lengths, Figures E5 and E6 of Appendix E show that:

$$\xi_{32} = 0.346 , \qquad \xi_{23} = 0.592.$$

The masses and radii of gyration of links 2 and 3 are calculated according to the equations of Appendix G, Section 2,

as:

$$m_2 = 6.229 \times 10^{-3} \text{ lb-sec}^2/\text{in}, \quad k_2 = 5.526 \text{ in},$$

$$m_3^o = 3.015 \times 10^{-3} \text{ lb-sec}^2/\text{in}, \quad k_3^o = 2.521 \text{ in},$$

in which the mass density is assumed to be that of steel, $\rho = 7.33 \times 10^{-4}$ lb-sec^2/in^4.

From these values, the coefficient K_2 and the mass-distance product $m_3 r_3$ are computed as [see equations (5.26) and (5.29)]:

$$K_2 = - 0.19022 \text{ in-lb-sec}^2,$$

$$m_3 r_3 = 0 .$$

The moment optimization curves E5 and E6 of Appendix E indicate that the ratio ξ_{32} lies near the optimum curve, but that the ratio ξ_{23} cannot be satisfied for this case. Thus, with eq. (5.28) coefficient K_3 becomes:

$$K_3 = - 0.06589 \text{ in-lb-sec}^2.$$

Finally, upon substitution of all values into eq. (5.37), the optimum counterweight radius is found as:

$$R_3 = 1.444 \text{ in.}$$

If the counterweight is constructed of steel, its corresponding thickness is [see eq. (5.39)]:

$$h_3^* = 1.304 \text{ in.}$$

Thus, the unbalanced linkage was close enough to the matching region such that a reasonable optimum counterweight could be designed.

If, instead of $a_4 = 11.6$, the ground link length had been 11.4, then the calculated counterweight dimensions would be:

$$R_3 = 0.477 \text{ in} , \qquad h_3^* = 36.3 \text{ in} ,$$

which are clearly unreasonable.

VI. QUALITY CONSIDERATIONS FOR SHAKING MOMENT OF FORCE-BALANCED FOUR-BAR LINKAGE WITH SYMMETRICAL LINK MASS DISTRIBUTIONS AND CONSTANT INPUT ANGULAR VELOCITY

While the optimization procedure given in Part V establishes the best dimensions for the various families of linkages, it gives no information concerning the actual magnitudes of the moments for these optima. Furthermore, it is not possible to judge the shaking moment near the optima of the various linkages.

The present part introduces the concept of the dimensionless moment, which enables the determination of actual magnitudes. It is thus possible to compare the shaking moments of all families of linkages. This design information is presented in the form of graphs.

A. Introduction of Dimensionless Moment Concept

Consider the reduced shaking moment equation for the force-balanced four-bar linkage as given by eq. (5.1):

$$M_{M/G} = K_2\ddot{\phi}_2 + K_3\ddot{\phi}_3 \ . \tag{6.1}$$

This may be written, with the help of eq. (5.22), as:

$$M_{M/G} = \rho a_1^5 \ (P_2\ddot{\phi}_2 - P_3\ddot{\phi}_3) \ , \tag{6.2}$$

where P_2 and P_3 contain only the dimensionless ratios of eq. (5.21) [see also equations (G.23), (G.24), (G.47), and (G.48) of Appendix G]. Note that eq. (6.2) is applicable to the specific linkage configuration of Fig. 12.

Further, consider that Appendix G, Section 1, shows that $\ddot{\phi}_2$ and $\ddot{\phi}_3$ are independent of magnification and therefore, for a constant input angular velocity $\dot{\phi}_1$, eq. (6.2) can be written as:

$$M_{M/G} = \rho a_1^5 \ \dot{\phi}_1^2 \left[P_2 \left(\frac{\ddot{\phi}_2}{\dot{\phi}_1^2} \right) - P_3 \left(\frac{\ddot{\phi}_3}{\dot{\phi}_1^2} \right) \right] . \tag{6.3}$$

Let the term within the brackets of eq. (6.3) be defined as the dimensionless moment $\bar{\mu}$:

$$\bar{\mu} = P_2 \left(\frac{\ddot{\phi}_2}{\dot{\phi}_1^2} \right) - P_3 \left(\frac{\ddot{\phi}_3}{\dot{\phi}_1^2} \right) . \tag{6.4}$$

This dimensionless moment, which is independent of magnification, is a useful measure of the shaking moment of four-bar linkages.

Thus, once the value of $\bar{\mu}$ is known, multiplication by the applicable values of the density, input link length, and input angular velocity will give the actual shaking moment:

$$M_{M/G} = \rho a_1^{5.2} \phi_1^{2} \bar{\mu} \ . \tag{6.5}$$

Even though the dimensionless moment of eq. (6.4) yields a single curve for the shaking moment of a particular linkage, regardless of its size, it becomes too cumbersome to compare the dynamic effects of linkages of different dimensions on this basis. For the purpose of such comparisons, the root-mean-square dimensionless moment[†] is introduced as a quality index:

$$\bar{\mu}_{RMS} = \sqrt{\frac{1}{2\pi}\int_0^{2\pi} \bar{\mu}^2 \, d\phi_1} \ . \tag{6.6}$$

[†]Note that the total root-mean-square value of the shaking moment can then be found, from eq. (6.5), as:

$$M_{RMS} = \rho a_1^{5.2} \phi_1^{2} \bar{\mu}_{RMS} \ .$$

B. Use of RMS Dimensionless Moment Curves for the Evaluation of Force-Balanced Four-Bar Linkages

Figures 15 - 19 give graphs of the RMS dimensionless moments for the various families of force-balanced four-bar linkages. Thus, values of $\bar{\mu}_{RMS}$ are plotted against ground link length ratios $\frac{a_4}{a_1}$, for various coupler and rocker link length ratios $\frac{a_2}{a_1}$, $\frac{a_3}{a_1}$. The label 53 on a curve means that $\frac{a_2}{a_1} = 5$ and $\frac{a_3}{a_1} = 3$. Separate graphs are given for each of the following values of σ_2, which locates the center of mass of the coupler link:

$$\sigma_2 = \frac{r_2}{a_2} = 0,\ 0.25,\ 0.50,\ 0.75,\ 1.00.$$

The computations† for these graphs are based upon equations (6.6), (6.4), and (G.24), (G.48) of Appendix G. The nominal crank-and-rocker configuration described in Part V is used, with the parameters β_i, γ_i, δ_i given by:

$$\beta_i = \frac{d_i}{a_1} = 0.5, \qquad \gamma_i = \frac{h_i}{d_i} = 0.4, \qquad \delta_i = \frac{h_i^*}{h_i} = 2.5\ .$$

---

†All computations described in this part were performed on the City College IBM 7040 Computer, with programs written in MAD (Michigan Algorithm Decoder).

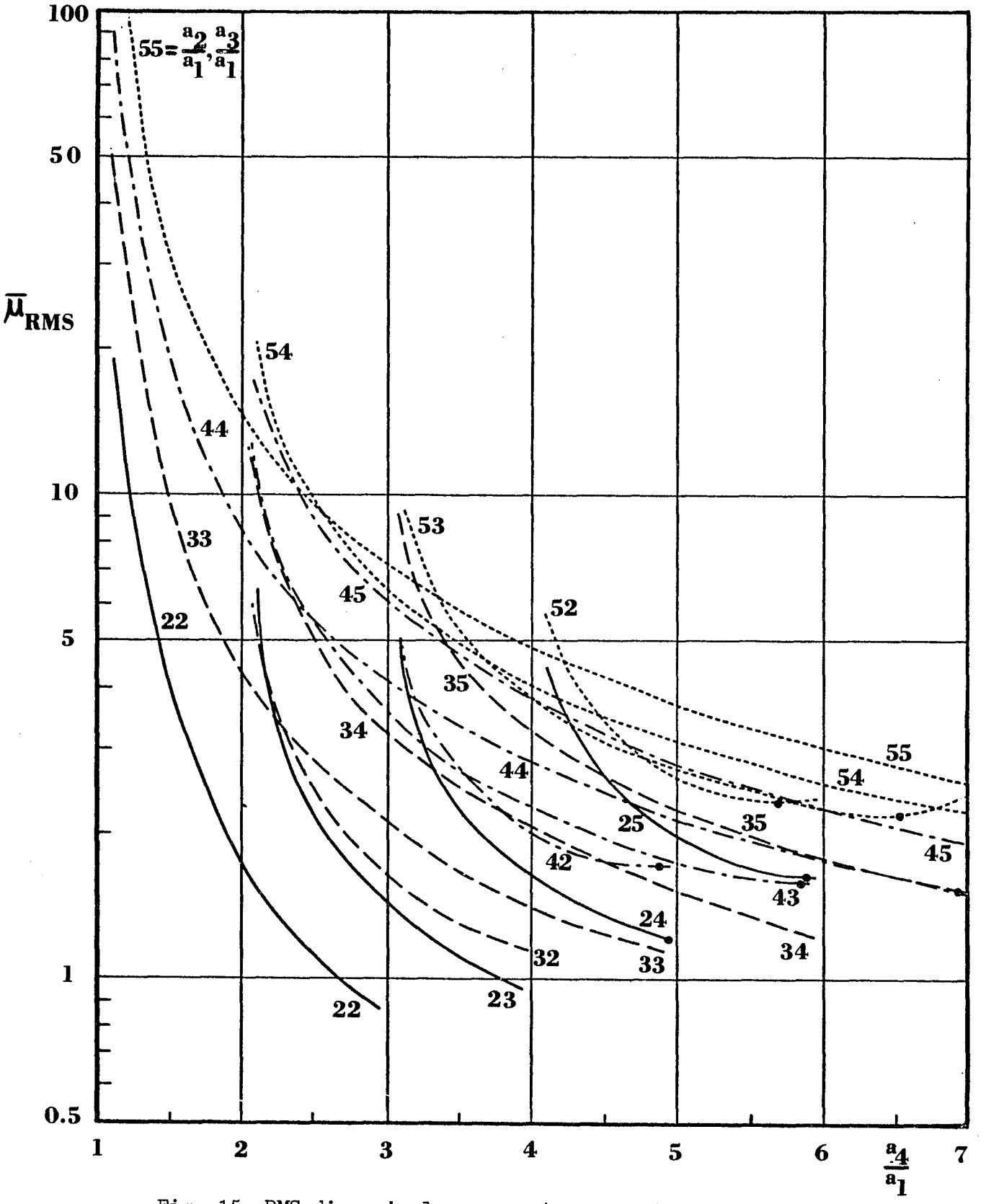

Fig. 15 RMS dimensionless moment curves for $\sigma_2 = 0$

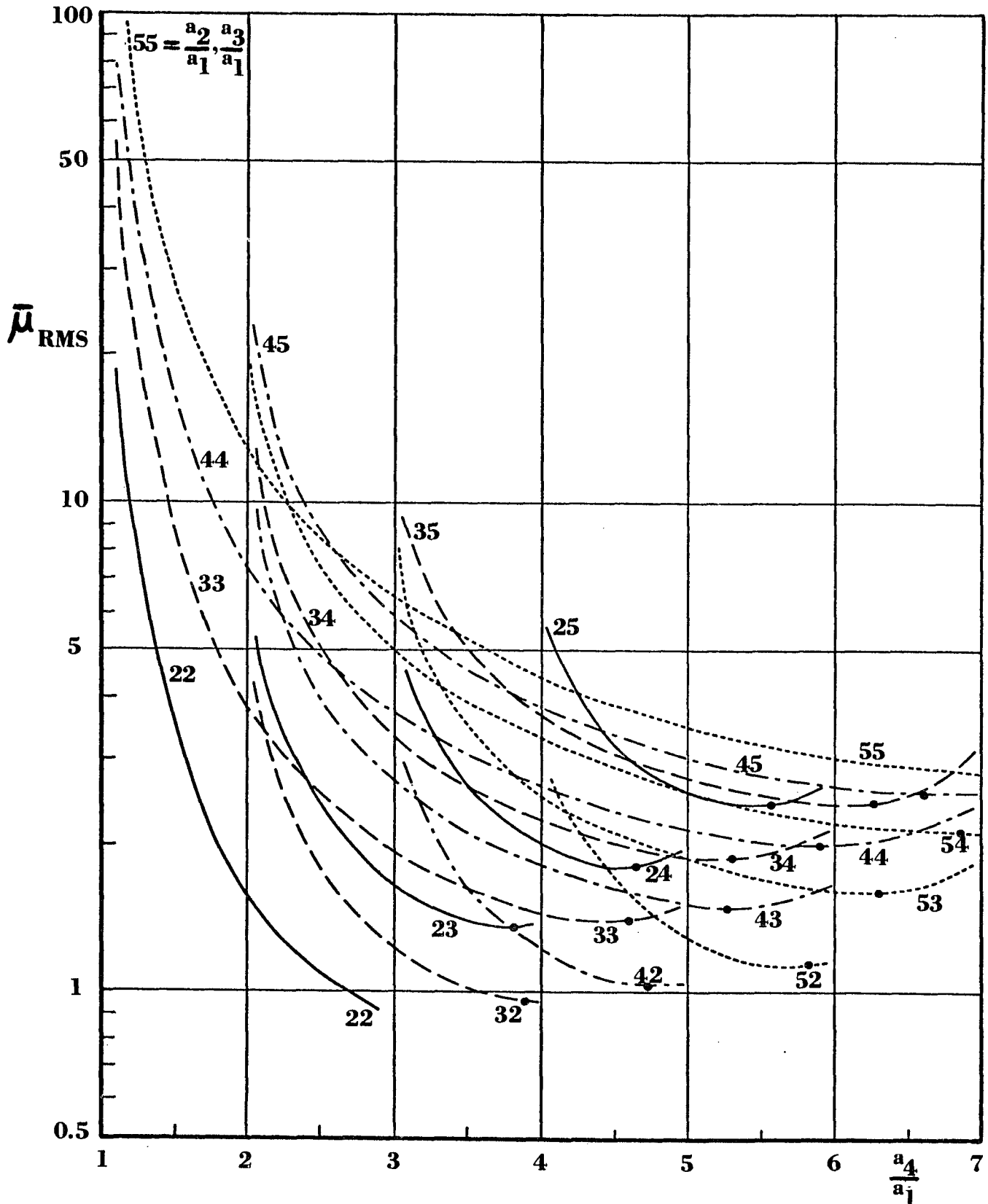

Fig. 16 RMS dimensionless moment curves for $\sigma_2 = 0.25$

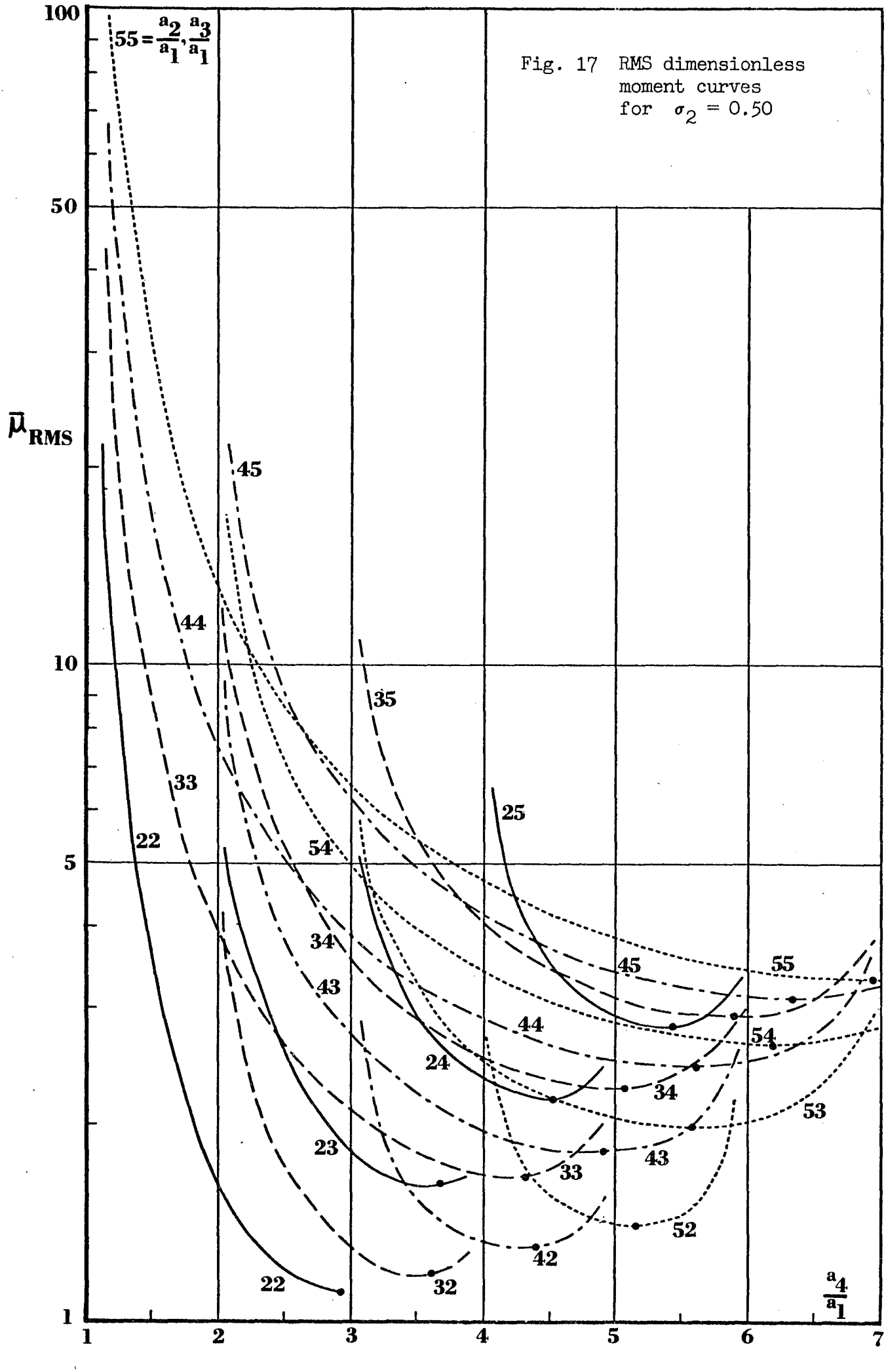

Fig. 17 RMS dimensionless moment curves for $\sigma_2 = 0.50$

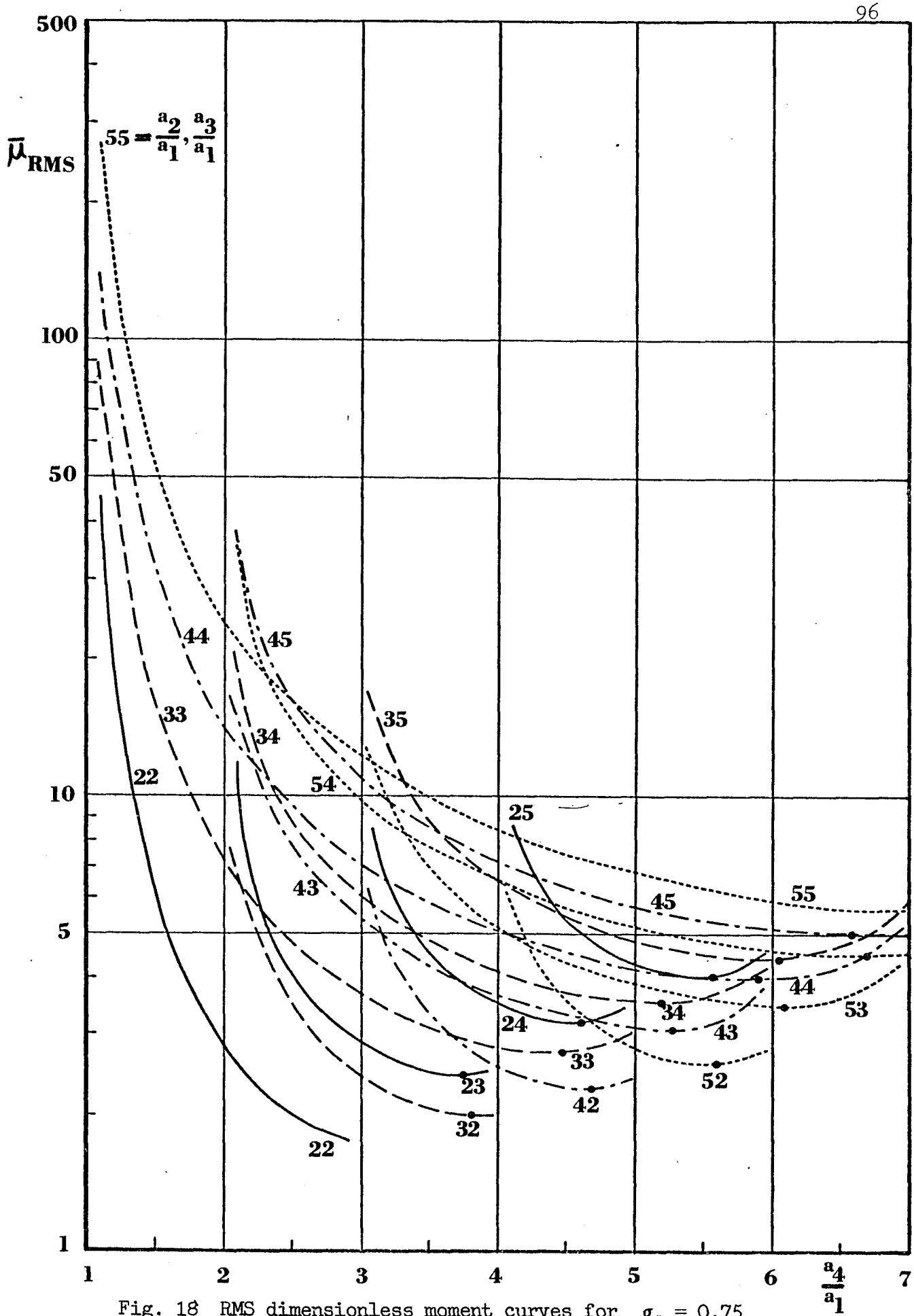

Fig. 18 RMS dimensionless moment curves for $\sigma_2 = 0.75$

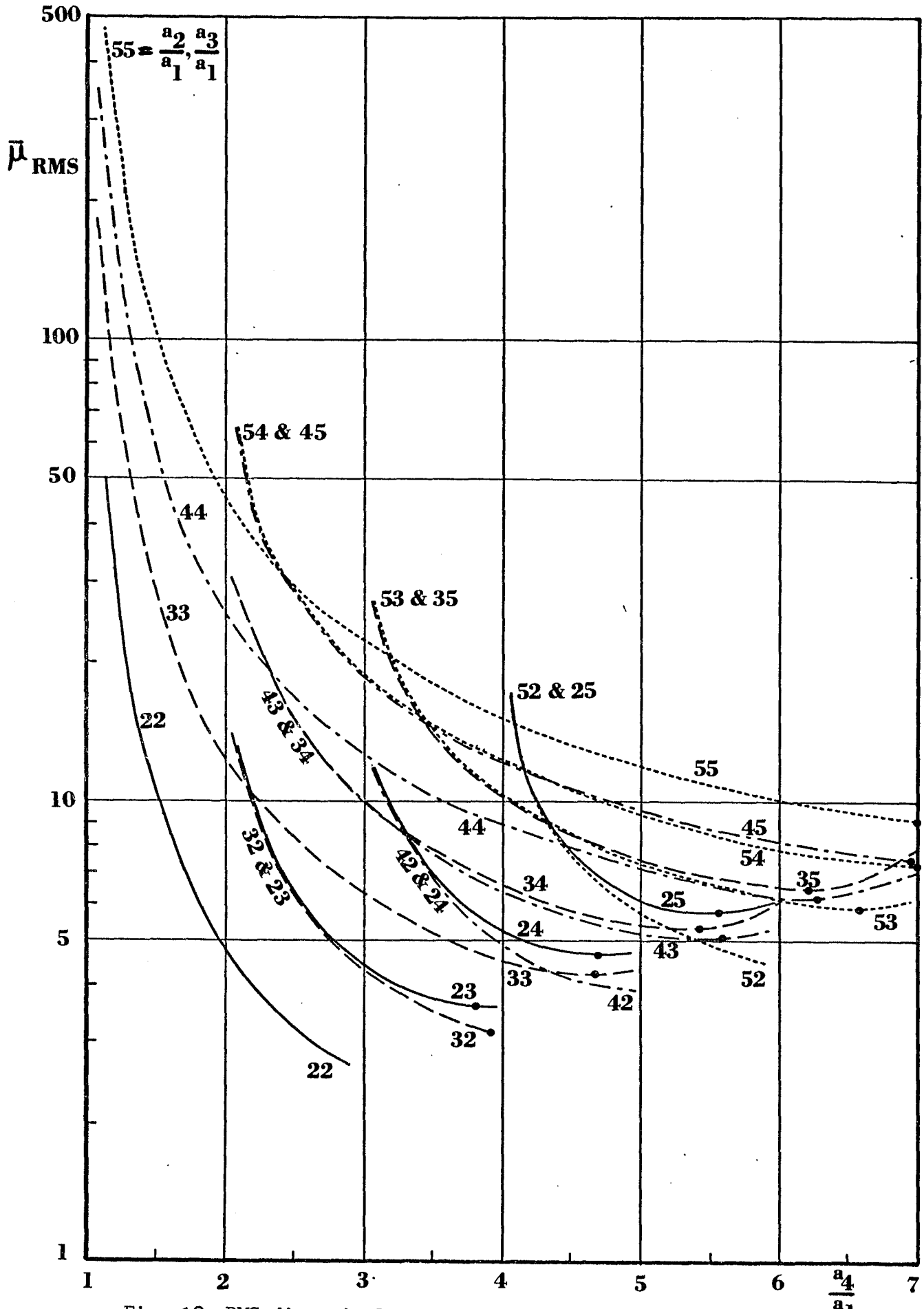

Fig. 19 RMS dimensionless moment curves for $\sigma_2 = 1.00$

C. Conclusions

In addition to the following conclusions which can be drawn from the graphs, the extreme importance of the crank link length must be realized. As shown by eq. (6.5), the shaking moment is a function of the fifth power of the crank length a_1, meaning that a small increase in linkage size can lead to a great increase in moment.

The root-mean-square value of the dimensionless moment for a force-balanced four-bar linkage is a function of the link lengths and the position of the coupler center of mass. It has been found to vary according to the following general patterns:

(a) An increase of the ground link length tends to decrease the dimensionless moment. In addition, each linkage family curve has or approaches a clearly defined minimum† (as in Part V, only cases within the Grashof criteria are treated). Also, the sensitivity of the dimensionless moment to the ground link length varies greatly, i.e. small changes of the latter parameter may or may not influence the dimensionless moment to any extent. Consequently, the exact location of the relative minimum can be important for curves with large slopes.

(b) A decrease of the coupler link length tends to decrease the dimensionless moment.

(c) The closer the coupler center of mass is to the crank pivot (i.e. the smaller σ_2 is), the smaller the dimensionless moment becomes.

---

†The minimum points of these graphs correspond to the optima of Part V.

Finally, it may be stated that the force-balanced four-bar linkage with the best moment characteristics will generally be one in which $\frac{a_2}{a_1}$ and σ_2 tend to be as small as possible, and $\frac{a_4}{a_1}$ is as large as possible.

VII. APPENDICES

APPENDIX A

DEFINITIONS OF TERMS AND RELATED MECHANICS CONCEPTS

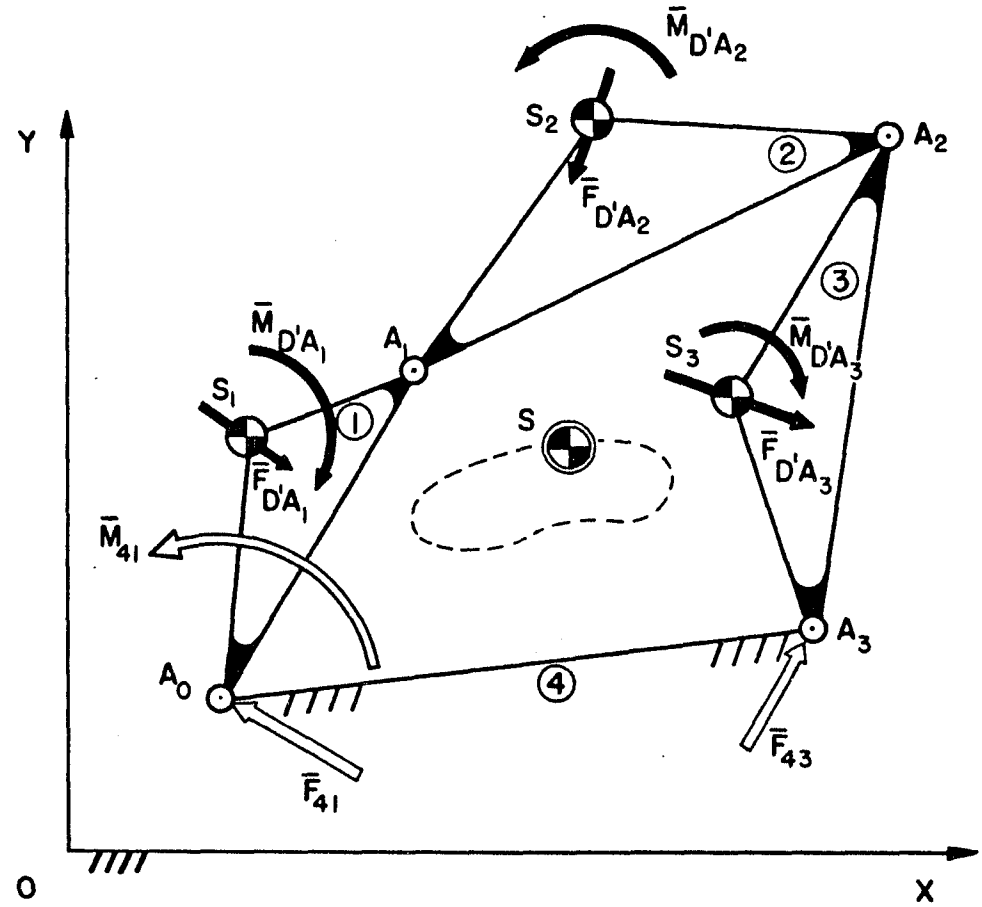

Fig. A1 Four-bar linkage with inertia loading

The following is terminology which is generally applicable to planar mechanisms. A four-bar linkage is shown in Fig. A1, which is referred to for illustrative purposes. It is to be noted that the following material is limited to inertia supplied loading. Modifications must be introduced if other external loads are imposed on the mechanism.

1. Definitions

a. Nomenclature

m_i = mass of link i;

k_i = radius of gyration of link i with respect to center of mass S_i;

$\bar{r}_{S_i}$, $\dot{\bar{r}}_{S_i}$, $\ddot{\bar{r}}_{S_i}$ = position, velocity, and acceleration vectors of the center of mass S_i of link i with respect to reference origin O ($\bar{r}_{S_i} = \overline{OS_i}$);

$\bar{r}_S$, $\dot{\bar{r}}_S$, $\ddot{\bar{r}}_S$ = position, velocity, and acceleration vectors of the total mechanism center of mass S with respect to reference origin O ($\bar{r}_S = \overline{OS}$);

ϕ_i; $\dot{\bar{\phi}}_i$, $\ddot{\bar{\phi}}_i$ = angular position; angular velocity, and angular acceleration vectors of link i;

$\mathcal{M} = \sum_{i=1}^{3} m_i$ = total mass of the moving links of the mechanism.

b. Center of Mass

The position vector of the center of mass of the moving links of the mechanism is given by (with respect to the reference origin O):

$$\bar{r}_S = \frac{1}{\mathcal{M}} \sum_{i=1}^{3} (m_i \bar{r}_{S_i}). \qquad (A.1)$$

c. D'Alembert Force and D'Alembert Moment

The D'Alembert force and the D'Alembert moment are the inertia loads acting on each link i of the mechanism:

$$\bar{F}_{D'A_i} = - m_i \ddot{\bar{r}}_{S_i} , \qquad (A.2)$$

$$\bar{M}_{D'A_i} = - m_i k_i^2 \ddot{\bar{\phi}}_i . \qquad (A.3)$$

d. Ground Forces

$\bar{F}_{14}$ and $\bar{F}_{34}$ are the forces exerted by the mechanism on the ground. Their vector sum represents the net force exerted on the ground by the linkage, i.e. the shaking force [see eq. (A.6)]. Individually, however, these forces contain equal and opposite components, respectively,which are due to the effects of the D'Alembert moments acting on the links.

e. Shaking Force

The net force, or shaking force, transmitted to the ground by the mechanism is equal to the negative of the time rate of change of the total linear momentum:

$$\bar{F}_{M/G} = -\dot{\bar{L}} = -\frac{d}{dt}\sum_{i=1}^{3} m_i \dot{\bar{r}}_{S_i} \quad . \tag{A.4}$$

In terms of the D'Alembert forces [see eq. (A.2)], the shaking force may be written as:

$$\bar{F}_{M/G} = \sum_{i=1}^{3} \bar{F}_{D'A_i} \quad , \tag{A.5}$$

and, in terms of the ground bearing forces, it becomes:

$$\bar{F}_{M/G} = \bar{F}_{14} + \bar{F}_{34} \quad . \tag{A.6}$$

f. Input Torque

The input torque is the torque, usually motor supplied, which is necessary to drive the mechanism. It is denoted by $\bar{M}_{41}$ for the

four-bar linkage of Fig. A1. Aside from traditional force analysis techniques, an analytic expression for the input torque can be found from the principle of virtual work:

$$\bar{M}_{41} \cdot \dot{\bar{\phi}}_1 + \sum_{i=1}^{3} (\bar{F}_{D'A_i} \cdot \dot{\bar{r}}_{S_i} + \bar{M}_{D'A_i} \cdot \dot{\bar{\phi}}_i) = 0 \ . \qquad (A.7)$$

g. Moment Due to Ground Forces

The moment $\bar{M}_{G|O}$ is defined as the moment on the ground due to the ground forces only. It reflects the effects of both the D'Alembert forces and the D'Alembert moments. With respect to arbitrary point O in Fig. A1:

$$\bar{M}_{G|O} = \overline{OA}_o \times \bar{F}_{14} + \overline{OA}_3 \times \bar{F}_{34} \ . \qquad (A.8)$$

Since:

$$\overline{OA}_3 = \overline{OA}_o + \overline{A_oA_3} \ , \qquad (A.9)$$

then, with the help of eq. (A.6):

$$\bar{M}_{G|O} = \overline{OA}_o \times \bar{F}_{M/G} + \overline{A_oA_3} \times \bar{F}_{34} \ . \qquad (A.10)$$

This shows that whenever the mechanism is force balanced, i.e. $\bar{F}_{M/G} = 0$, then $\bar{M}_{G|O}$ is reduced to a pure couple which does not depend on the reference point. (See discussion concerning reference point location in Part IV A).

h. Shaking Moment

The net moment, or shaking moment, transmitted to the ground by the mechanism with respect to arbitrary origin O is equal to the negative of the time rate of change of the total angular momentum (see also Part IV A):

$$\bar{M}_{M/G|O} = -\dot{\bar{H}}_O = -\frac{d}{dt}\sum_{i=1}^{3}(\bar{r}_{S_i} \times m_i \dot{\bar{r}}_{S_i} + m_i k_i^2 \dot{\bar{\phi}}_i) \ . \qquad (A.11)$$

In terms of the D'Alembert forces and the D'Alembert moments, the shaking moment can then be expressed as:

$$\bar{M}_{M/G|O} = \sum_{i=1}^{3}(\bar{r}_{S_i} \times \bar{F}_{D'A_i} + \bar{M}_{D'A_i}) \ . \qquad (A.12)$$

Alternately:

$$\bar{M}_{M/G|O} = \bar{M}_{G|O} + \bar{M}_{14} \ , \qquad (A.13)$$

where $\bar{M}_{G|O}$ is the moment due to the ground forces [see eq. (A.8)], and $\bar{M}_{14}$ represents the ground reaction of the motor which furnishes the input torque $\bar{M}_{41}$.

i. Internal and External Balancing

Internal balancing implies that only masses of existing links have been redistributed, possibly by the attachment of additional masses to these links.

External balancing implies that additional links have been added to the existing configuration. These additional links may be in the

form, for example, of geared counterweights, link dyads, or duplicate mechanisms.

j. Static and Dynamic Replacement of Link Masses

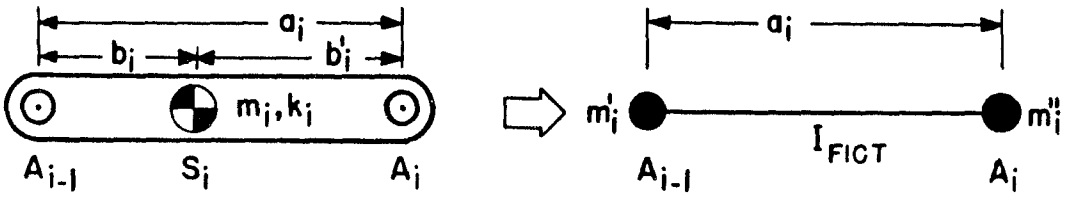

Fig. A2 Equivalent link replacement

For the replacement of a link with distributed mass by a massless link with concentrated masses, as shown in Fig. A2, the following conditions must be fulfilled:

(1) The total mass must remain the same:

$$m_i = m'_i + m''_i \; ; \tag{A.14}$$

(2) The position of the center of mass must remain the same:

$$m'_i b_i = m''_i b'_i \; ; \tag{A.15}$$

(3) The total moment of inertia of the link must remain the same. For this, a fictitious equivalent moment of inertia I_{fict} must be introduced:

$$m_i k_i^2 = I_{fict} + m'_i b_i^2 + m''_i b'^2_i \; . \tag{A.16}$$

Only the first two conditions need be fulfilled for a "static" replacement, whereas all three are required for a "dynamic" replacement.

The magnitudes of the parameters in the replaced system will be:

$$m_i' = m_i \frac{b_i'}{a_i} , \tag{A.17}$$

$$m_i'' = m_i \frac{b_i}{a_i} , \tag{A.18}$$

$$I_{fict} = m_i(k_i^2 - b_i b_i') . \tag{A.19}$$

2. Relationship Between Position of Total Center of Mass and Shaking Force

Equation (A.4) for the shaking force can be rewritten in terms of the total mechanism center of mass and its motion, for any linkage, as:

$$\bar{F}_{M/G} = - \sum_{i=1}^{n} m_i \ddot{\bar{r}}_{S_i} = -\mathcal{M} \ddot{\bar{r}}_S \ . \qquad (A.20)$$

Therefore, in order to cause the net shaking force to vanish, the acceleration of the total center of mass S must vanish. This requires that the total center of mass should either be stationary, or move with a constant velocity. The latter case may only occur if the frame of the mechanism itself moves with a constant velocity (e.g., a linkage in a vehicle).

Thus, if the center of mass of any mechanism is stationary, i.e.

$$\sum_{i=1}^{n} (m_i \bar{r}_{S_i}) = \text{Const.}, \qquad (A.21)$$

then the shaking force vanishes, and the mechanism is completely force balanced.

3. Relationship Between Total Angular Momentum and Shaking Moment

The shaking moment is the negative of the time rate of change of angular momentum. From eq. (A.11), this can be expressed for any linkage as:

$$\bar{M}_{M/G|O} = -\frac{d}{dt}\sum_{i=1}^{n}(\bar{r}_{S_i} \times m_i\dot{\bar{r}}_{S_i} + m_i k_i^2 \dot{\bar{\phi}}_i) \ . \qquad (A.22)$$

Therefore, the shaking moment will vanish if the total angular momentum is constant (or zero), i.e. if:

$$\sum_{i=1}^{n}(\bar{r}_{S_i} \times m_i\dot{\bar{r}}_{S_i} + m_i k_i^2 \dot{\bar{\phi}}_i) = \text{Const.} \qquad (A.23)$$

For the case of a four-bar linkage, eq. (A.23) can never come about by means of an internal mass rearrangement (see Part IV E). However, external techniques, such as the addition of a duplicate mechanism with mirror symmetry, can lead to a case in which eq. (A.23) holds.

APPENDIX B

HARMONIC CONSIDERATIONS OF FORCE BALANCING FOR FOUR-BAR LINKAGE

The following conclusions concerning the harmonic balancing of a four-bar linkage are found when the position equation† of the total center of mass resulting from the Method of Linearly Independent Vectors is examined for harmonic content.

It is found that a first order harmonic balance by an internal rearrangement of masses leads automatically to complete force balance. It is also shown that all harmonics higher than the first may be fully balanced, the first may be partially balanced, and an external counterweight may be added to effect complete balance.

---

† It is permissible to draw certain conclusions concerning the shaking force harmonics from the position equation of the total center of mass. This is possible since the second derivative of the position equation is proportional to the shaking force, and the coefficients of these acceleration terms differ from those of the displacement equations only by the factor $-n^2\dot{\phi}_1^2$ [see eq. (B.4), (B.5)].

1. Position of Total Center of Mass

The equation describing the position of the total center of mass of a four-bar linkage was derived by the Method of Linearly Independent Vectors in Part III. Rewriting eq. (3.6) in component form gives, for $\theta_4 = 0$ (see Fig. 1):

$$\left.\begin{aligned} \mathcal{M} x_S &= \sigma_1 \cos \phi_1 - \sigma_2 \sin \phi_1 + \sigma_3 \cos \phi_3 - \sigma_4 \sin \phi_3 + \sigma_5 , \\ \mathcal{M} y_S &= \sigma_2 \cos \phi_1 + \sigma_1 \sin \phi_1 + \sigma_4 \cos \phi_3 + \sigma_3 \sin \phi_3 + \sigma_6 , \end{aligned}\right\} \qquad (B.1)$$

where the kinematic constants σ_i are defined as:

$$\left.\begin{aligned} \sigma_1 &= m_1 r_1 \cos \theta_1 - m_2 r_2' \lambda \cos \theta_2' , \\ \sigma_2 &= m_1 r_1 \sin \theta_1 - m_2 r_2' \lambda \sin \theta_2' , \\ \sigma_3 &= m_3 r_3 \cos \theta_3 + m_2 r_2 \mu \cos \theta_2 , \\ \sigma_4 &= m_3 r_3 \sin \theta_3 + m_2 r_2 \mu \sin \theta_2 , \\ \sigma_5 &= (m_3 a_2 + m_2 r_2 \cos \theta_2) \nu , \\ \sigma_6 &= m_2 r_2 \nu \sin \theta_2 , \end{aligned}\right\} \qquad (B.2)$$

in which:

$$\left.\begin{aligned} \lambda &= \frac{a_1}{a_2} , \\ \mu &= \frac{a_3}{a_2} , \\ \nu &= \frac{a_4}{a_2} . \end{aligned}\right\} \qquad (B.3)$$

In order to express eq. (B.1) in harmonic form, the sine and cosine of ϕ_3 must be obtained as harmonic functions of ϕ_1.

2. Position of Total Center of Mass in Harmonic Form

F. Freudenstein [22] derived expressions for the output angle ϕ_3 in terms of Fourier harmonics of the input angle ϕ_1 (see Fig. B1). Therefore, the cosine and the sine of the output angle can also be expressed as Fourier series of the form:

$$\left.\begin{aligned} \cos\phi_3 &= \sum_{n=0}^{\infty} (e_n \cos n\phi_1 + f_n \sin n\phi_1), \\ \sin\phi_3 &= \sum_{n=0}^{\infty} (g_n \cos n\phi_1 + h_n \sin n\phi_1). \end{aligned}\right\} \qquad (B.4)$$

Substituting eq. (B.4) into eq. (B.1) and combining terms yields the following equations for the position components of the mechanism center of mass:

$$\mathcal{M}x_S = (\sigma_5 + \sigma_3 e_o - \sigma_4 g_o) \qquad (B.5)$$

$$+ (\sigma_1 + \sigma_3 e_1 - \sigma_4 g_1)\cos\phi_1 - (\sigma_2 - \sigma_3 f_1 + \sigma_4 h_1)\sin\phi_1$$

$$+ \sigma_3 \sum_{n=2}^{\infty} (e_n \cos n\phi_1 + f_n \sin n\phi_1) - \sigma_4 \sum_{n=2}^{\infty} (g_n \cos n\phi_1 + h_n \sin n\phi_1),$$

$$\mathcal{M}y_S = (\sigma_6 + \sigma_3 g_o + \sigma_4 e_o) \qquad (B.6)$$

$$+ (\sigma_2 + \sigma_3 g_1 + \sigma_4 e_1)\cos\phi_1 + (\sigma_1 + \sigma_3 h_1 + \sigma_4 f_1)\sin\phi_1$$

$$+ \sigma_4 \sum_{n=2}^{\infty} (e_n \cos n\phi_1 + f_n \sin n\phi_1) + \sigma_3 \sum_{n=2}^{\infty} (g_n \cos n\phi_1 + h_n \sin n\phi_1).$$

3. Conclusions

a. Complete Force Balance

It is not necessary to perform a harmonic analysis to show that all harmonics will disappear if the coefficients of eq. (B.1) all vanish, i.e.

$$\sigma_1 = \sigma_2 = \sigma_3 = \sigma_4 = 0. \tag{B.7}$$

This has already been shown in unexpanded vectorial form in equations (3.11) and (3.9) of Part III.

It is of interest, however, that an attempt to obtain a first order harmonic balance by an internal rearrangement of masses leads automatically to complete balance.

To obtain complete first harmonic balance, the coefficients of all first harmonic terms must vanish. According to equations (B.5) and (B.6), the following four expressions must be satisfied:

$$\left.\begin{aligned} \sigma_1 + 0 + \sigma_3 e_1 - \sigma_4 g_1 &= 0, \\ 0 + \sigma_2 - \sigma_3 f_1 + \sigma_4 h_1 &= 0, \\ 0 + \sigma_2 + \sigma_3 g_1 + \sigma_4 e_1 &= 0, \\ \sigma_1 + 0 + \sigma_3 h_1 + \sigma_4 f_1 &= 0. \end{aligned}\right\} \tag{B.8}$$

In general, this is a homogeneous system with nonvanishing determinant, allowing only the trivial solution:

$$\sigma_1 = \sigma_2 = \sigma_3 = \sigma_4 = 0. \tag{B.9}$$

As seen in eq. (B.7), this is the complete balancing solution. Therefore, one may conclude that full first harmonic balance is not possible without the removal of all other harmonics for a four-bar linkage by internal redistribution means. [Of course, the first harmonic of any mechanism may be removed by the addition of external counterweights (see Part IIB).]

The above conclusion concerning the impossibility of exclusively balancing the first harmonic hinges on the fact that the parameters which control the coefficients of all harmonics higher than the first also partially contribute to the coefficient of the first harmonic [see equations (B.5) and (B.6)] . These considerations suggest the following new formulation of a partial balancing method for the four-bar linkage.

b. Complete Balancing of All Harmonics Higher than the First, Partial Balance of the First, and Additional External Modification Resulting in Complete Balance

As seen from equations (B.5) and (B.6), or even eq. (B.1), all harmonic orders from 2 to ∞, as well as part of the first, will vanish if:

$$\sigma_3 = \sigma_4 = 0. \tag{B.10}$$

This requires the mass redistribution of a single link, which is accomplished with the help of eq. (B.2). If this is done, the remainders of equations (B.5) and (B.6) will be:

$$\left.\begin{aligned} \mathcal{M}x_S &= \sigma_1 \cos \phi_1 - \sigma_2 \sin \phi_1 + \sigma_5, \\ \mathcal{M}y_S &= \sigma_2 \cos \phi_1 + \sigma_1 \sin \phi_1 + \sigma_6, \end{aligned}\right\} \tag{B.11}$$

which may be rewritten as:

$$\left.\begin{aligned} \mathcal{M}x_S &= A \cos (\phi_1 + \alpha) + \sigma_5, \\ \mathcal{M}y_S &= A \sin (\phi_1 + \alpha) + \sigma_6, \end{aligned}\right\} \tag{B.12}$$

in which:

$$\left.\begin{aligned} A &= \sqrt{\sigma_1^2 + \sigma_2^2}, \\ \alpha &= \tan^{-1}\left(\frac{\sigma_2}{\sigma_1}\right). \end{aligned}\right\} \tag{B.13}$$

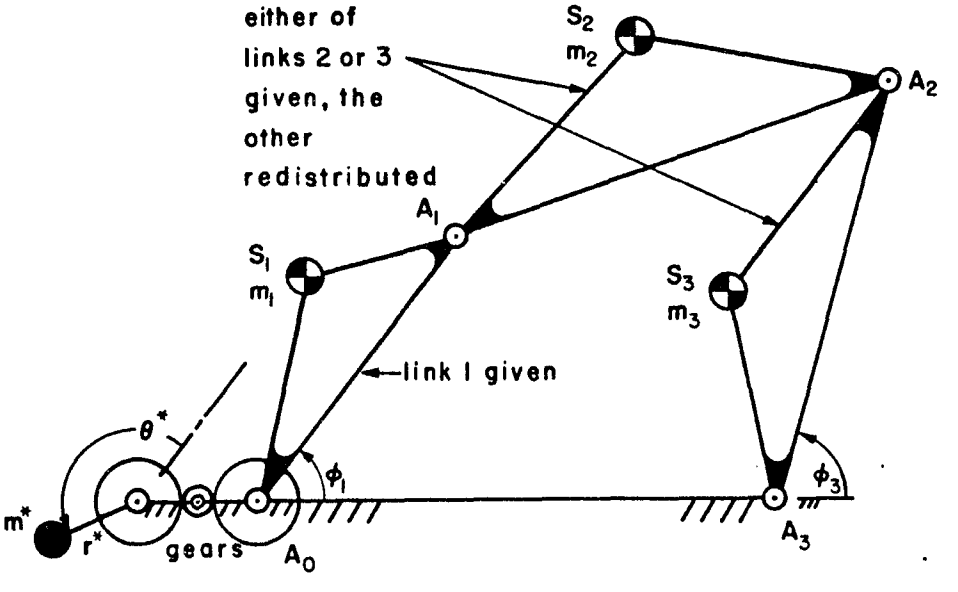

Fig. B1 Four-bar linkage with external counterweight

While the complete internal balancing methods discussed in Section 4a of this appendix necessitated the redistribution of two link masses, another method becomes apparent from the above. Complete balance may be gotten by externally adding a single counterweight which rotates synchronously with the crank (see Fig. B1).

The mass m*, radius r*, and phase angle θ* of this counterweight would therefore be given by:

$$\left.\begin{aligned} m^*r^* &= A = \sqrt{\sigma_1^2 + \sigma_2^2}\ , \\ \theta^* &= \alpha + \pi = \tan^{-1}\left(\frac{\sigma_2}{\sigma_1}\right) + \pi\ . \end{aligned}\right\} \qquad \text{(B.14)}$$

The existence of this particular total balancing solution was found, in a completely different manner, for symmetrical link mass distributions by V. A. Shchepetil'nikov [64] .

APPENDIX C

INDEPENDENT CHECK OF MOMENT EQUATION FOR FORCE-BALANCED FOUR-BAR LINKAGE WITH SYMMETRICAL LINK MASS DISTRIBUTIONS

The equation for the shaking moment of a force-balanced four-bar linkage with symmetrical link mass distributions is shown in eq. (4.34). The identical result may be obtained by basing the derivation on a combination of static and dynamic replacement of link masses (see Appendix A, Section 1j).

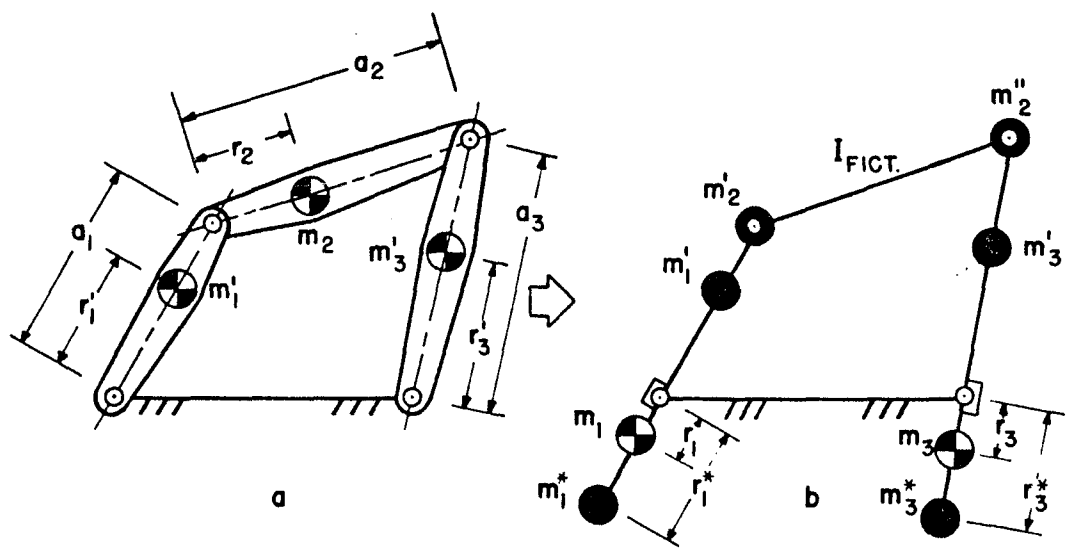

Fig. C1 Dynamic replacement of link masses

As indicated in Fig. C1b, the coupler link mass m_2 is assumed to be replaced by the masses m_2' and m_2'' at points A_1 and A_2 respectively. This replacement is governed by equations (A.17) and (A.18). This operation necessitates the introduction of the fictitious moment of inertia I_{fict} for link 2, according to eq. (A.19):

$$I_{fict} = m_2(k_2^2 + r_2^2 - a_2 r_2). \tag{C.1}$$

In order to place the effective centers of mass of the systems comprising links 1 and 3 at the points A_o and A_3 respectively, one now introduces the counterweights m_1 and m_3. These are located at the distances r_1 and r_3 from the pivots, such that:

$$\left.\begin{aligned} m_1^* r_1^* &= -(m_1' r_1' + m_2' a_1), \\ m_3^* r_3^* &= -(m_3' r_3' + m_2'' a_3). \end{aligned}\right\} \tag{C.2}$$

While, for purposes of finding the counterweights of links 1 and 3, masses m_2' and m_2'' must be accounted for, they no longer are used in the determination of the actual centers of mass of these links. The magnitudes of the actual masses of links 1 and 3 are:

$$\left.\begin{aligned} m_1 &= m_1' + m_1^* , \\ m_3 &= m_3' + m_3^* , \end{aligned}\right\} \tag{C.3}$$

while m_2 remains unchanged. The locations of the actual centers of mass are given by:

$$\left.\begin{aligned} m_1 r_1 &= -\,(m_1' r_1' + m_1^* r_1^*)\ , \\ m_3 r_3 &= -\,(m_3' r_3' + m_3^* r_3^*)\ , \end{aligned}\right\} \tag{C.4}$$

which become, upon substitution of eq. (C.2):

$$\left.\begin{aligned} m_1 r_1 &= m_2' a_1\ , \\ m_3 r_3 &= m_2'' a_3\ . \end{aligned}\right\} \tag{C.5}$$

The actual links 1 and 3 have radii of gyration k_1 and k_3 with respect to the locations of m_1 and m_3.

Since the effective centers of mass of links 1 and 3 are at the pivot points A_o and A_3, all D'Alembert forces vanish, and the shaking moment may be expressed by a reduction of eq. (A.12):

$$M_{M/G} = \sum_{i=1}^{3} M_{D'A_i} = -\sum_{i=1}^{3} I_{e_i} \ddot{\phi}_i\ . \tag{C.6}$$

The effective moments of inertia I_{e_i} of links 1 and 3 are referred to their effective centers of mass, and include the contribution of m_2' and m_2''. The effective moment of inertia of link 2 is furnished by I_{fict} as given by eq. (C.1). Therefore:

$$\left.\begin{aligned} I_{e_1} &= m_1 k_1^2 + m_1 r_1^2 + m_2' a_1^2\ , \\ I_{e_2} &= m_2 (k_2^2 + r_2^2 - a_2 r_2)\ , \\ I_{e_3} &= m_3 k_3^2 + m_3 r_3^2 + m_2'' a_3^2\ . \end{aligned}\right\} \tag{C.7}$$

Upon substitution of eq. (C.5) into eq. (C.7), one obtains:

$$\left.\begin{aligned} I_{e_1} &= m_1(k_1^2 + r_1^2 + a_1 r_1) \ , \\ I_{e_2} &= m_2(k_2^2 + r_2^2 - a_2 r_2) \ , \\ I_{e_3} &= m_3(k_3^2 + r_3^2 + a_3 r_3) \ . \end{aligned}\right\} \qquad (C.8)$$

Finally, substitution of eq. (C.8) into eq. (C.6) leads to the identical form for the shaking moment as eq. (4.34), i.e.

$$M_{M/G} = - m_1(k_1^2 + r_1^2 + a_1 r_1)\ \ddot{\phi}_1 - m_2(k_2^2 + r_2^2 - a_2 r_2)\ \ddot{\phi}_2 - m_3(k_3^2 + r_3^2 + a_3 r_3)\ \ddot{\phi}_3 \ . \qquad (C.9)$$

Thus, the independent check is accomplished.

APPENDIX D

LEAST-SQUARE OPTIMIZATION OF A FUNCTION

The optimization, in the least-square sense, of a function which is comprised of a linear combination of terms is presented in a general form here. The application of this optimization theory to the shaking moment of a force-balanced four-bar linkage is given. A reduced case is treated in Part V.

1. Formulation of Least-Square Optimization

In order to make the root-mean-square error $\mathscr{E}$ of a periodic function M a minimum with respect to another function f, one writes:

$$\mathscr{E} = \sqrt{\frac{1}{2\pi}\int_{o}^{2\pi} \left[M(\phi) - f(\phi)\right]^2 \, d\phi} = \text{minimum.} \tag{D.1}$$

Let us consider only the case in which the function M is to be minimized itself in the least-square sense, i.e.

$$f(\phi) = 0. \tag{D.2}$$

Equation (D.1) becomes:

$$\mathscr{E} = \sqrt{\frac{1}{2\pi}\int_{o}^{2\pi} M^2 \, d\phi} \; . \tag{D.3}$$

Thus, the minimization of the integral:

$$E = \int_{o}^{2\pi} M^2 \, d\phi \tag{D.4}$$

means both that the root-mean-square error of M as well as the area under the M^2 curve are minimized.

The specific form of the function M which is to be optimized is now presented.

2. Optimization of a Function Comprised of a Linear Combination of Terms

Assume that the function M takes the form of a linear combination of n terms:

$$M = \sum_{i=1}^{n} K_i \, \Phi_i(\phi), \tag{D.5}$$

in which the Φ_i are functions of the independent variable ϕ, and the K_i are unspecified coefficients which must be optimized.

In order to optimize the function M in the sense of eq. (D.4), it is necessary to find the appropriate values of the coefficients K_i. This is accomplished by taking the partial derivative of eq. (D.4) with respect to the individual coefficients K_j, one at a time, and setting the result equal to zero, i.e.

$$\frac{\partial E}{\partial K_j} = 2\int_0^{2\pi} M \frac{\partial M}{\partial K_j} \, d\phi = 0, \tag{D.6}$$

or:

$$\int_0^{2\pi} M \frac{\partial M}{\partial K_j} \, d\phi = 0 \qquad (j = 1,2,\ldots,n). \tag{D.7}$$

Since K_j represents any of the n coefficients K_i in eq. (D.5), there will be n equations of the type of eq. (D.7).

Upon substitution of eq. (D.5) into (D.7), one obtains:

$$\int_0^{2\pi} \left(\sum_{i=1}^{n} K_i \, \Phi_i \right) \Phi_j \, d\phi = 0, \tag{D.8}$$

which results in:

$$\sum_{i=1}^{n} K_i \int_0^{2\pi} \Phi_i \Phi_j \, d\phi = 0. \qquad (D.9)$$

Defining the integral portion of eq. (D.9) as:

$$\mathcal{J}_{ij} = \mathcal{J}_{ji} = \int_0^{2\pi} \Phi_i \Phi_j \, d\phi \ , \qquad (D.10)$$

eq. (D.9), and thus the form of the n simultaneous equations, becomes:

$$\sum_{i=1}^{n} K_i \mathcal{J}_{ij} = 0 \qquad (j = 1,2,\ldots,n) \ . \qquad (D.11)$$

It is desirable to determine all the n coefficients K_j simultaneously so that the function M will deviate least from zero in the least-square sense. It will now be shown that there is a limitation on the number of coefficients K_j which may be found simultaneously.

3. Limitations to Simultaneous Optimization of All Coefficients K_j

The homogeneous system of n equations in n unknowns K_j as given by eq. (D.11) may be displayed as:

$$\left.\begin{aligned} K_1\mathcal{J}_{11} + K_2\mathcal{J}_{12} + \ldots + K_n\mathcal{J}_{1n} &= 0, \\ K_1\mathcal{J}_{12} + K_2\mathcal{J}_{22} + \ldots + K_n\mathcal{J}_{2n} &= 0, \\ \ldots \quad \ldots \quad \ldots \quad \ldots & \\ K_1\mathcal{J}_{1n} + K_2\mathcal{J}_{2n} + \ldots + K_n\mathcal{J}_{nn} &= 0. \end{aligned}\right\} \qquad (D.12)$$

[See eq. (D.10)] .

A simultaneous solution to equations (D.12), other than the trivial solution

$$K_1 = K_2 = \ldots = K_n = 0,$$

exists only if the following determinant vanishes:

$$\mathcal{D} = \left|\mathcal{J}_{ij}\right| = \begin{vmatrix} \mathcal{J}_{11} & \mathcal{J}_{12} & \cdots & \mathcal{J}_{1n} \\ \mathcal{J}_{12} & \mathcal{J}_{22} & \cdots & \mathcal{J}_{2n} \\ \cdots & \cdots & & \cdots \\ \mathcal{J}_{1n} & \mathcal{J}_{2n} & \ldots & \mathcal{J}_{nn} \end{vmatrix} . \qquad (D.13)$$

It can be shown that the determinant $\mathcal{D}$ does not vanish by proving that it will be greater than zero at all times.

According to G. H. Hardy, et al.[34], the generalization of the integral version of Cauchy's† Inequality is given by:

Theorem.

$$\begin{vmatrix} \int f^2\,dx & \int fg\,dx & \cdots & \int fh\,dx \\ \int gf\,dx & \int g^2\,dx & \cdots & \int gh\,dx \\ \cdots & \cdots & & \cdots \\ \int hf\,dx & \int hg\,dx & \cdots & \int h^2\,dx \end{vmatrix} > 0, \qquad \text{(D.14)}$$

unless the functions f, g,...,h are linearly dependent, i.e. unless there are constants A,B,...,C, not all zero, such that:

$$Af + Bg + \ldots + Ch \equiv 0.$$

The determinant of eq. (D.13) is of the same form as that of eq. (D.14), i.e.

$$\mathscr{D} = \begin{vmatrix} \int_0^{2\pi} \Phi_1^2\,d\phi & \int_0^{2\pi} \Phi_1\Phi_2\,d\phi & \cdots & \int_0^{2\pi} \Phi_1\Phi_n\,d\phi \\ \int_0^{2\pi} \Phi_1\Phi_2 d\phi & \int_0^{2\pi} \Phi_2^2\,d\phi & \cdots & \int_0^{2\pi} \Phi_2\Phi_n\,d\phi \\ \cdots & \cdots & & \cdots \\ \int_0^{2\pi} \Phi_1\Phi_n d\phi & \int_0^{2\pi} \Phi_2\Phi_n\,d\phi & \cdots & \int_0^{2\pi} \Phi_n^2\,d\phi \end{vmatrix} . \qquad \text{(D.15)}$$

---

† Also attributed to Schwartz and Buniakowsky.

If it can be shown that the functions $\Phi_1, \Phi_2, \ldots, \Phi_n$ are linearly independent, then:

$$\mathscr{D} > 0 \ , \tag{D.16}$$

and only the trivial solution of system (D.12) exists.

While it is therefore not possible to determine the n coefficients K_j simultaneously, it is possible to find the simultaneous optimum values of sets of (n-1) coefficients K_j.

4. Local Optimization of Coefficients

A local optimization of (n-1) coefficients K_j may be obtained by assuming that one of the coefficients of eq. (D.5), say K_p, is specified. With this assumption, the partial derivative $\frac{\partial M}{\partial K_p}$ vanishes and, for this case, eq. (D.7) becomes identically zero.

Thus, equations (D.11) reduce in number to (n-1), and become nonhomogeneous, since K_p is known:

$$\sum_{\substack{i=1 \\ i\neq p}}^{n} K_i \mathcal{I}_{ij} = - K_p \mathcal{I}_{pj} \qquad (D.17)$$

$$(j = 1,2,\ldots,n;\ j \neq p) .$$

The solution to this nonhomogeneous system of (n-1) equations in (n-1) unknowns is unique and can be given by Cramer's Rule.

There will be n sets of the type of eq. (D.17), since the subscript p of K_p can have any value from 1 to n. This means that there will be n local optimum solutions, depending on the choice of K_p.

This optimization procedure will now be illustrated by an example in which n = 3. (For the reduced case of Part V, n = 2.)

5. Application of Least-Square Optimization to Shaking Moment of Force-Balanced Four-Bar Linkage with Constant Input Angular Velocity

Equation (4.32) of Part IV gives the expression for the shaking moment of a force-balanced four-bar linkage. With a constant input angular velocity ($\ddot{\phi}_1 = 0$), the shaking moment becomes:

$$M_{M/G} = K_2\ddot{\phi}_2 + K_3\ddot{\phi}_3 + K_4\ddot{\phi}_4, \tag{D.18}$$

where $\ddot{\phi}_4$, which is unrelated to link 4, represents for convenience:

$$\ddot{\phi}_4 = \dot{\tau}_1\dot{\phi}_1. \tag{D.19}$$

The rest of the parameters of eq. (D.18) remain as defined in eq. (4.33) and earlier. Note that the terms $\ddot{\phi}_i$ are all periodic functions of the input crank angle ϕ_1.

Eq. (D.11) becomes a system of three equations:

$$\left.\begin{aligned} K_2\mathcal{J}_{22} + K_3\mathcal{J}_{23} + K_4\mathcal{J}_{24} &= 0, \\ K_2\mathcal{J}_{23} + K_3\mathcal{J}_{33} + K_4\mathcal{J}_{34} &= 0, \\ K_2\mathcal{J}_{24} + K_3\mathcal{J}_{34} + K_4\mathcal{J}_{44} &= 0. \end{aligned}\right\} \tag{D.20}$$

As has been shown in Section 3 of this Appendix, there cannot be a simultaneous solution to these equations other than the trivial one, and the method shown in Section 4 must be used. The equations must be solved as three partial sets of two, by prescribing each of the coefficients K_p in turn. These nonhomogeneous sets of equations become, according to the form of eq. (D.17):

$$\left.\begin{aligned} K_3\mathcal{J}_{33} + K_4\mathcal{J}_{34} &= -K_2\mathcal{J}_{23}, \\ K_3\mathcal{J}_{34} + K_4\mathcal{J}_{44} &= -K_2\mathcal{J}_{24}, \end{aligned}\right\} \quad (K_2 \text{ given}) \tag{D.21}$$

$$\left.\begin{aligned} K_2\mathcal{J}_{22} + K_4\mathcal{J}_{24} &= -K_3\mathcal{J}_{23}, \\ K_2\mathcal{J}_{24} + K_4\mathcal{J}_{44} &= -K_3\mathcal{J}_{34}, \end{aligned}\right\} \quad (K_3 \text{ given}) \tag{D.22}$$

$$\left.\begin{aligned} K_2\mathcal{J}_{22} + K_3\mathcal{J}_{23} &= -K_4\mathcal{J}_{24}, \\ K_2\mathcal{J}_{23} + K_3\mathcal{J}_{33} &= -K_4\mathcal{J}_{34}. \end{aligned}\right\} \quad (K_4 \text{ given}) \tag{D.23}$$

The solution to each of these simultaneous pairs of equations furnishes the optimum K_i for a given K_j. Introducing the ratios ξ_{ij}:

$$\xi_{ij} = \frac{K_i \big/ \text{ optimum}}{K_j \big/ \text{ given}}, \tag{D.24}$$

the solutions to equations (D.21)-(D.23) may be displayed as:

$$\xi_{32} = C/F, \qquad \xi_{42} = B/F, \tag{D.25}$$

$$\xi_{23} = C/E, \qquad \xi_{43} = A/E, \tag{D.26}$$

$$\xi_{24} = B/D, \qquad \xi_{34} = A/D, \tag{D.27}$$

where:

$$
\left.
\begin{aligned}
A &= \mathcal{J}_{23}\mathcal{J}_{24} - \mathcal{J}_{22}\mathcal{J}_{34}, \\
B &= \mathcal{J}_{23}\mathcal{J}_{34} - \mathcal{J}_{33}\mathcal{J}_{24}, \\
C &= \mathcal{J}_{24}\mathcal{J}_{34} - \mathcal{J}_{44}\mathcal{J}_{23}, \\
D &= \mathcal{J}_{22}\mathcal{J}_{33} - \mathcal{J}_{23}^{2}, \\
E &= \mathcal{J}_{22}\mathcal{J}_{44} - \mathcal{J}_{24}^{2}, \\
F &= \mathcal{J}_{33}\mathcal{J}_{44} - \mathcal{J}_{34}^{2}.
\end{aligned}
\right\} \qquad \text{(D.28)}
$$

APPENDIX E

MOMENT OPTIMIZATION CURVES

The following appendix contains the moment optimization curves whose construction and use is discussed in Part VC. Graphs of the optimum ratios ξ_{ij} form the bases of these curves. Superimposed on them are the actual ratios η_{ij} for the assumed linkage configuration.

The equations needed for plotting the curves as well as the linkage dimensions used are given below.† Figures E1 - E8 represent the moment optimization curves proper, while Figures E9 - E12 illustrate the effect of parameter variations on the preceding curves.

---

†All computations for ξ_{ij} and η_{ij} were performed on the City College IBM 7040 Computer, with programs written in MAD (Michigan Algorithm Decoder).

1. Evaluation of Ideal Ratios ξ_{ij}

The optimum ratios ξ_{23} and ξ_{32} are found from the definitions of equations (5.17) and (5.18):

$$\xi_{23} = \frac{K_2\big|_{optimum}}{K_3\big|_{given}} = -\frac{\int_o^{2\pi} \ddot{\phi}_2 \, \ddot{\phi}_3 \, d\phi_1}{\int_o^{2\pi} \ddot{\phi}_2^2 \, d\phi_1} , \qquad (E.1)$$

$$\xi_{32} = \frac{K_3\big|_{optimum}}{K_2\big|_{given}} = -\frac{\int_o^{2\pi} \ddot{\phi}_2 \, \ddot{\phi}_3 \, d\phi_1}{\int_o^{2\pi} \ddot{\phi}_3^2 \, d\phi_1} . \qquad (E.2)$$

These equations are evaluated by the numerical integration of the angular acceleration values, expressions for which are found in Appendix I.

2. Evaluation of Actual Ratios η_{ij}

The actual ratios η_{23} and η_{32} are defined by eq. (5.20) as:

$$\eta_{32} = \frac{1}{\eta_{23}} = \frac{m_3(k_3^2 + r_3^2 + a_3 r_3)}{m_2(k_2^2 + r_2^2 - a_2 r_2)} . \tag{E.3}$$

In terms of dimensionless parameters, eq. (E.3) is rewritten as:

$$\eta_{32} = \frac{1}{\eta_{23}} = - \frac{P_3}{P_2} , \tag{E.4}$$

in which, according to eq. (G.49) of Appendix G, P_2 and P_3 are only functions of:

$$\left.\begin{aligned} \alpha_i &= \frac{a_i}{a_1} , \qquad \beta_i = \frac{d_i}{a_1} , \qquad \gamma_i = \frac{h_i}{d_i} , \\ \delta_i &= \frac{h_i^*}{h_i} , \qquad \sigma_i = \frac{r_i}{a_i} . \end{aligned}\right\} \tag{E.5}$$

Thus, the values of η_{ij} are calculated for given values of the dimensionless parameters of eq. (E.5).

3. Range of Linkages Chosen

The ratios ξ_{ij} and η_{ij} are computed for four-bar linkages within the Grashof criteria. That is, the sum of the longest and shortest links is less than the sum of the remaining two links, with the input crank being the shortest link.

The ranges of $\alpha_i = \frac{a_i}{a_1}$ for which these curves are plotted are:

(1) $2.0 \leq \frac{a_2}{a_1} \leq 5.0$ at increments of 1.0,

(2) $1.5 \leq \frac{a_3}{a_1} \leq 6.0$ at increments of 0.5,

(3) $1.0 \leq \frac{a_4}{a_1} \leq 7.0$.

4. Linkage Dimensions

The dimensions of the nominal linkage configuration used are expressed by the following parameters for each link i, as defined in eq. (E.5):

$$\beta_i = 0.5 , \qquad \gamma_i = 0.4 , \qquad \delta_i = 2.5 .$$

The coupler center of mass location varies between:

$$\sigma_2 = 0, 0.25, 0.50, 0.75, 1.00.$$

5. Variation of Linkage Parameters

The effect of varying the link cross-section as well as the counterweight density for the nominal linkage configuration is discussed in Part VC. Figures E9 - E12 of this Appendix show bands of variation of the moment optimization curves, for the full range of linkages examined. Based on the extreme values of the parameters of Table 6 (in Part V), these bands are constructed for:

$$\frac{a_2}{a_1} = 2,\ 3,\ 5,$$

and:

$$\sigma_2 = 0,\ 0.5,\ 1.0.$$

6. Additional Observations

From the calculated values of ξ_{23} and ξ_{32}, the following equality† has been observed to hold:

$$\xi_{32}\big|_{abcd} = \xi_{23}\big|_{acbd} . \qquad (E.6)$$

This means that the value of ξ_{32} for a mechanism in which $a_1 = a$, $a_2 = b$, $a_3 = c$, $a_4 = d$, equals the value of ξ_{23} for a different mechanism, where $a_1 = a$, $a_2 = c$, $a_3 = b$, $a_4 = d$. It also follows that, if $a_2 = a_3$ for a linkage, $\xi_{32} = \xi_{23}$.

---

†This equality has not been proven analytically, but has only been observed from the computer output data.

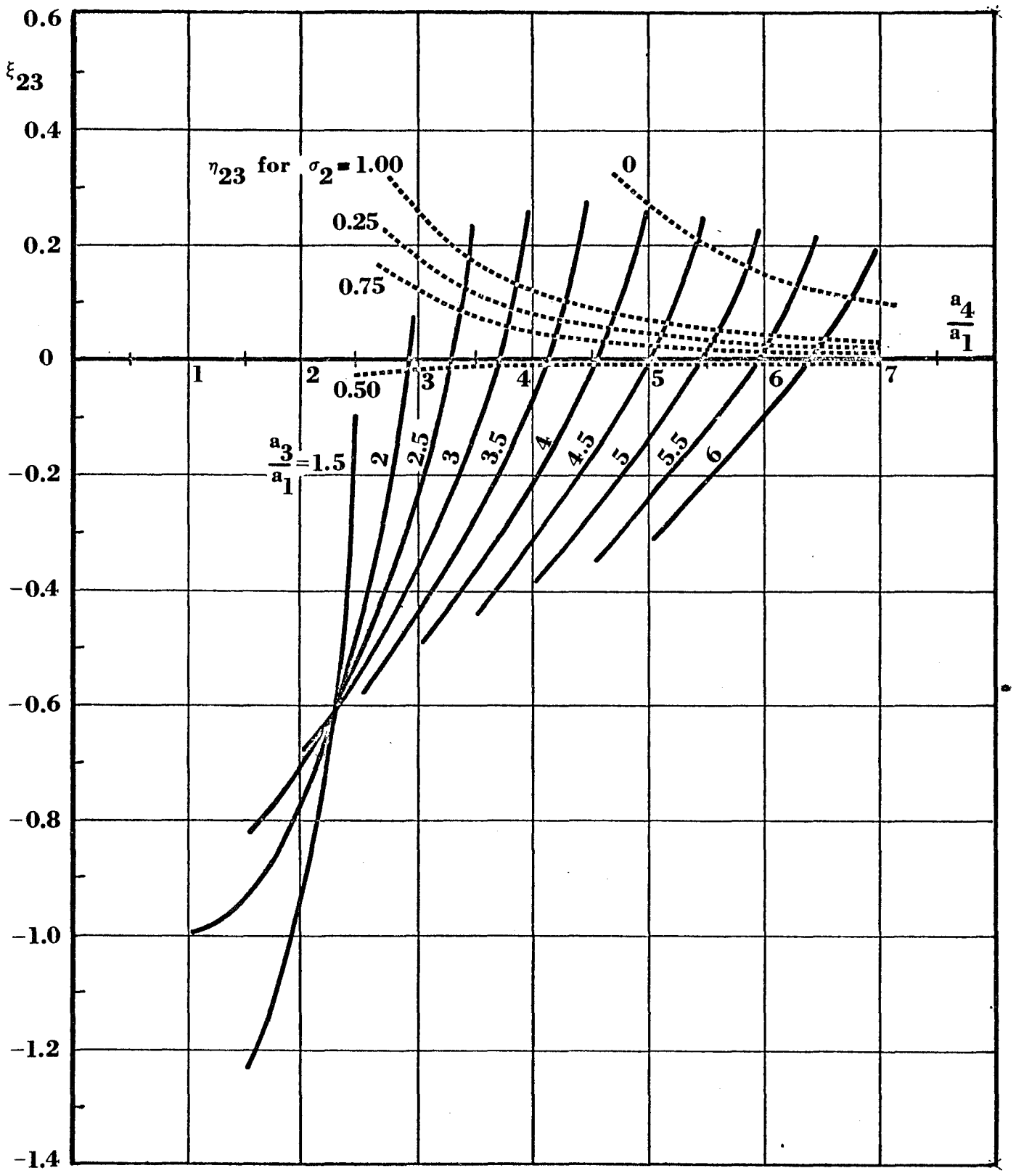

Fig. E1 Moment optimization curves for families $a_2/a_1 = 2$ and ξ_{23}

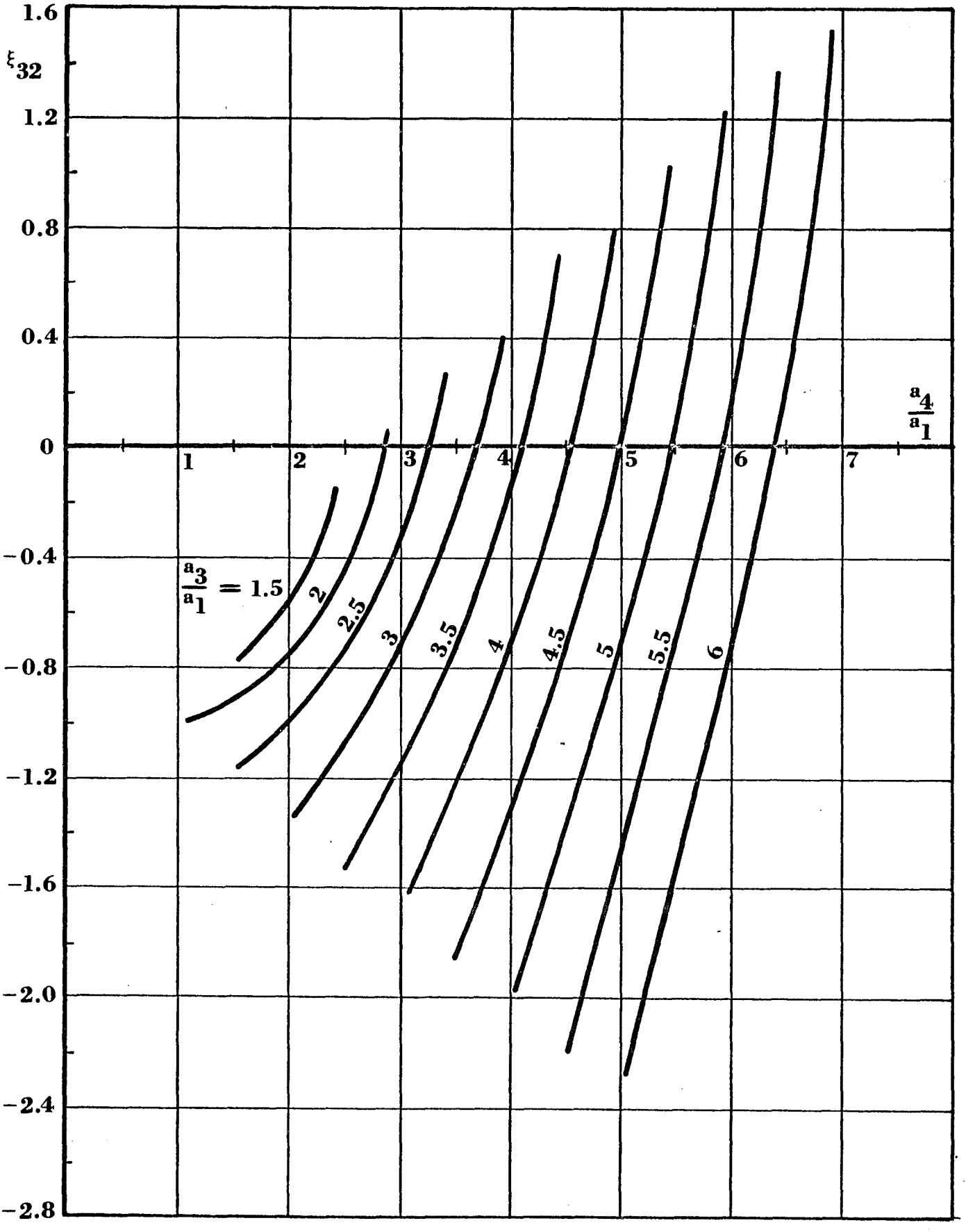

Fig. E2 Moment optimization curves for families $a_2/a_1 = 2$ and ξ_{32}

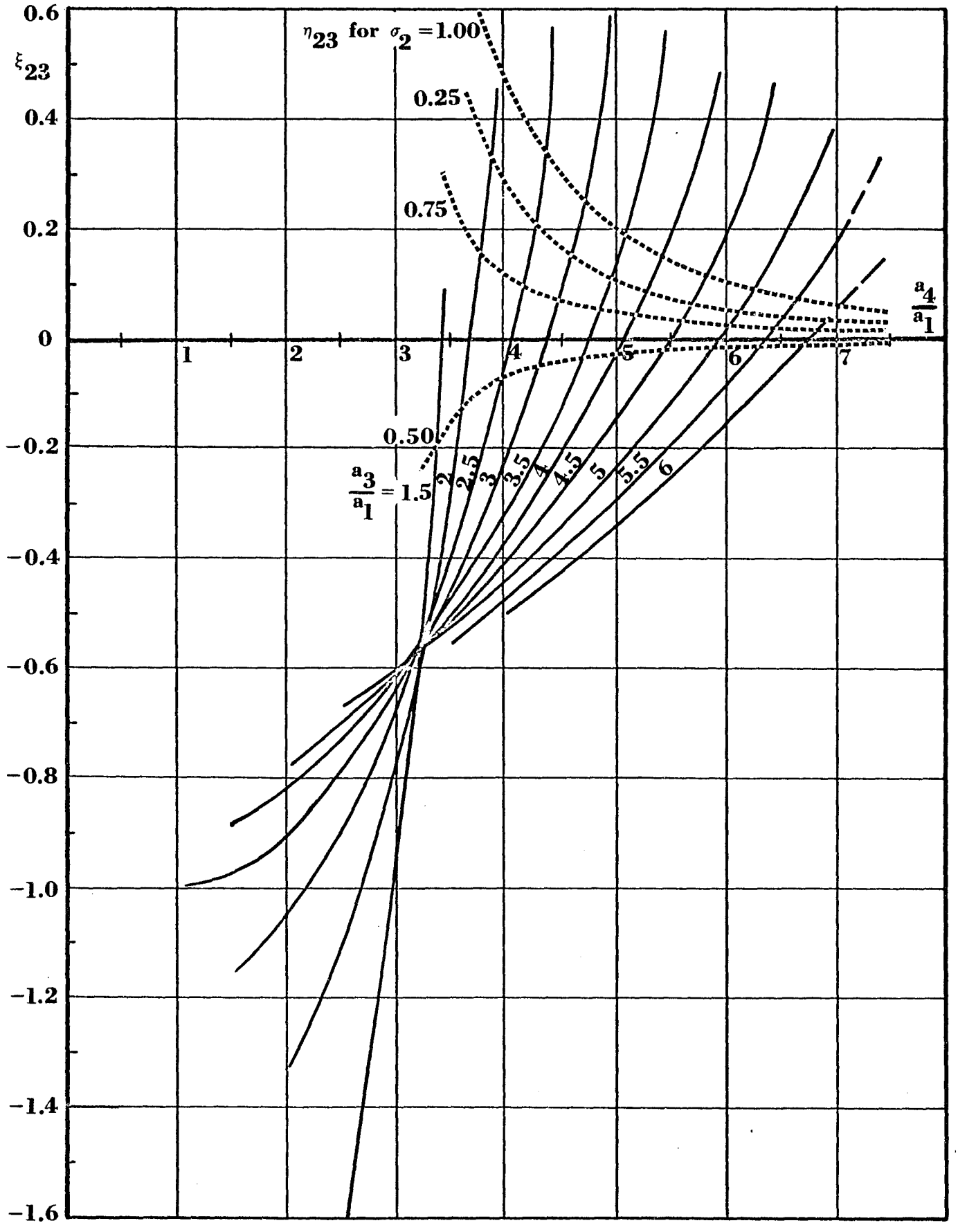

Fig. E3 Moment optimization curves for families $a_2/a_1 = 3$ and ξ_{23}

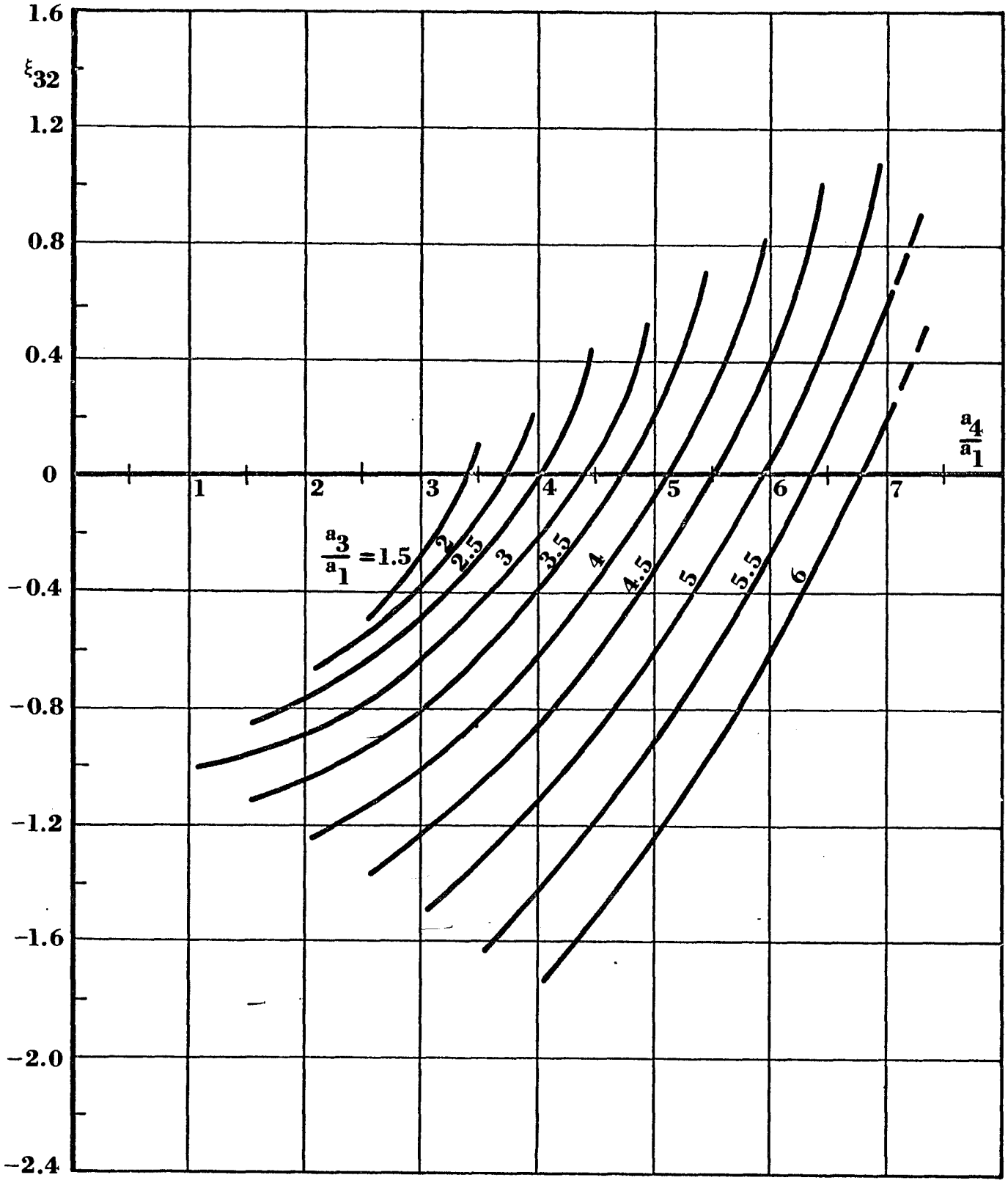

Fig. E4 Moment optimization curves for families $a_2/a_1 = 3$ and ξ_{32}

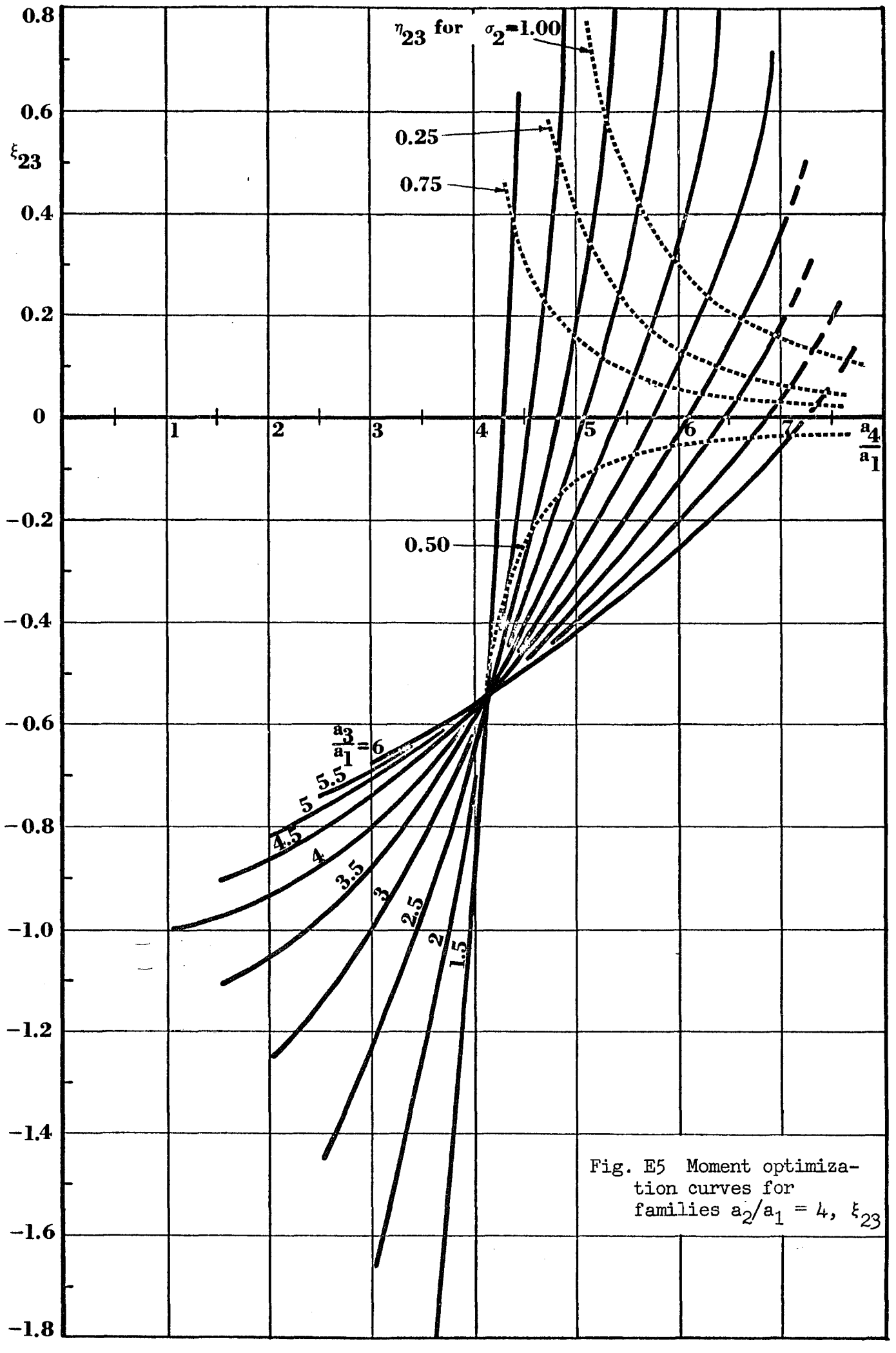

Fig. E5 Moment optimization curves for families $a_2/a_1 = 4$, ξ_{23}

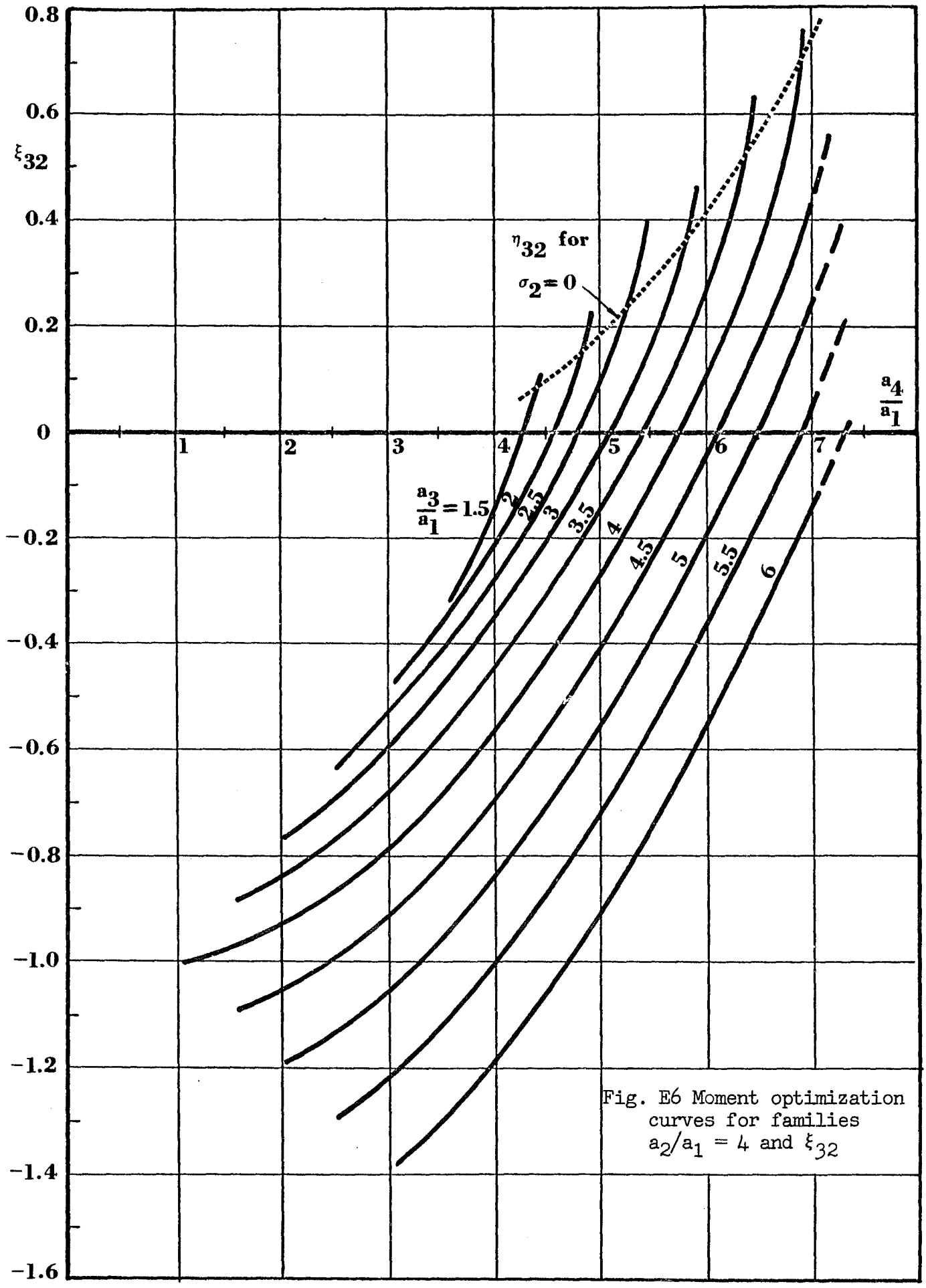

Fig. E6 Moment optimization curves for families $a_2/a_1 = 4$ and ξ_{32}

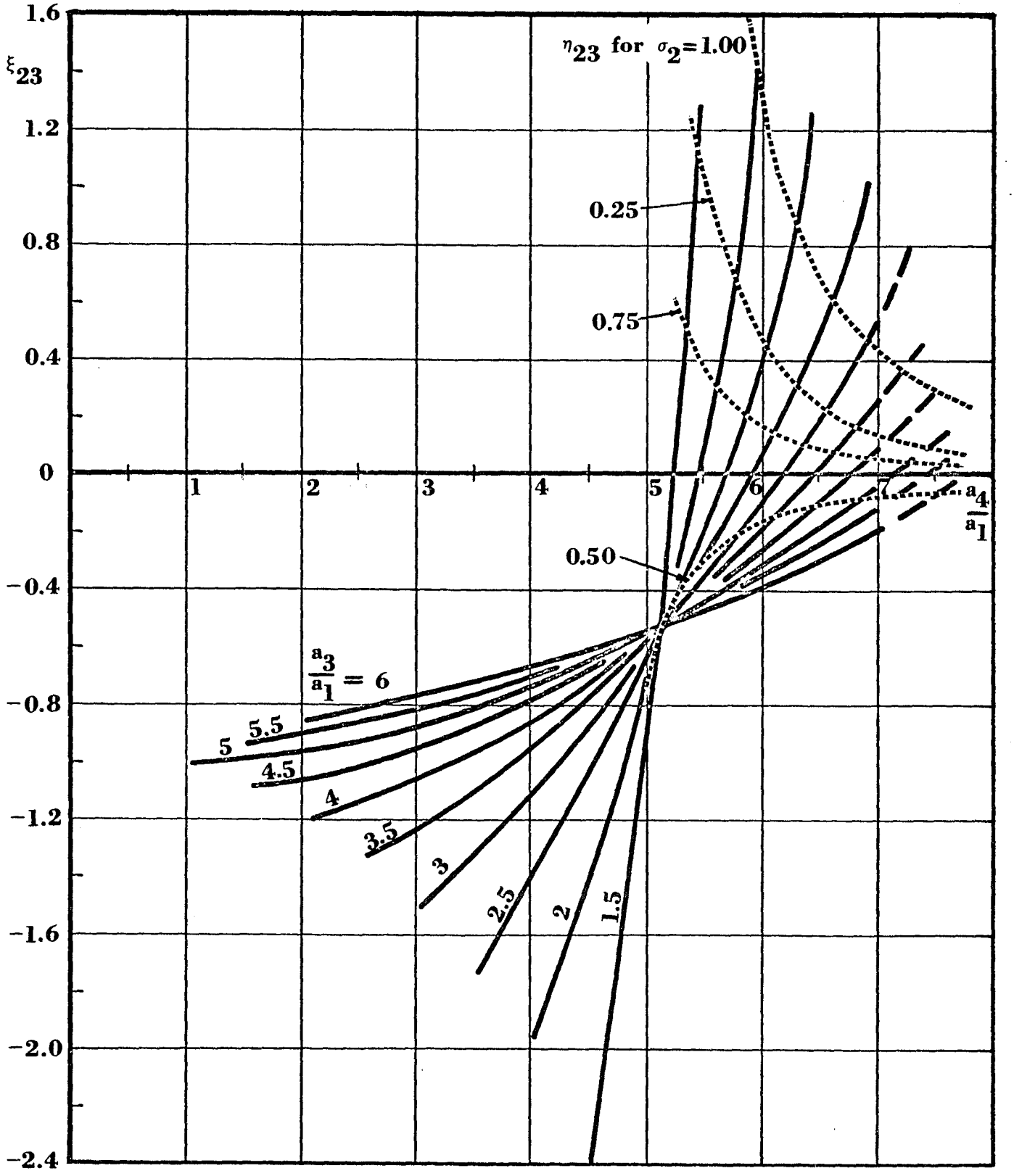

Fig. E7 Moment optimization curves for families $a_2/a_1 = 5$ and ξ_{23}

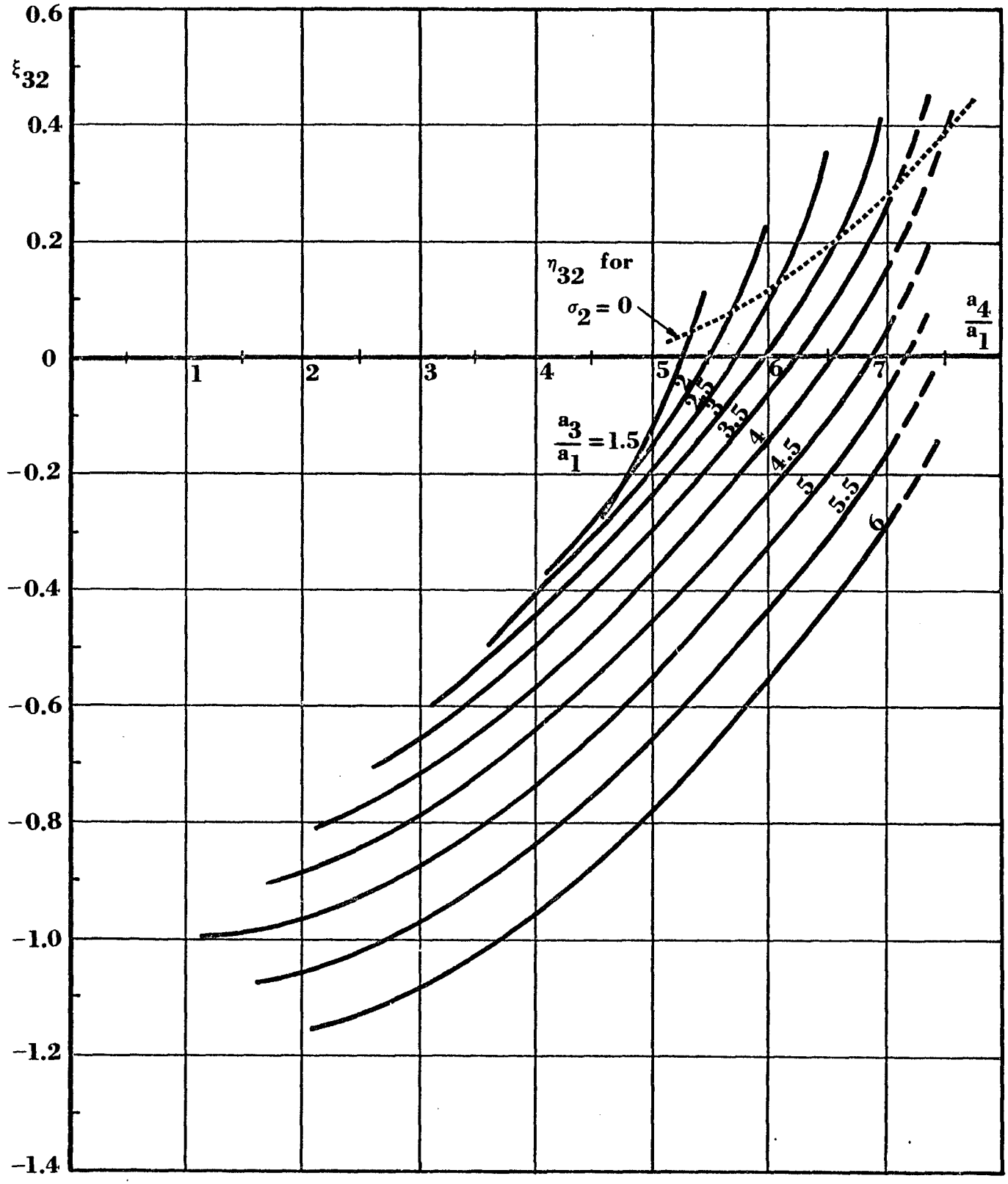

Fig. E8 Moment optimization curves for families $a_2/a_1 = 5$ and ξ_{32}

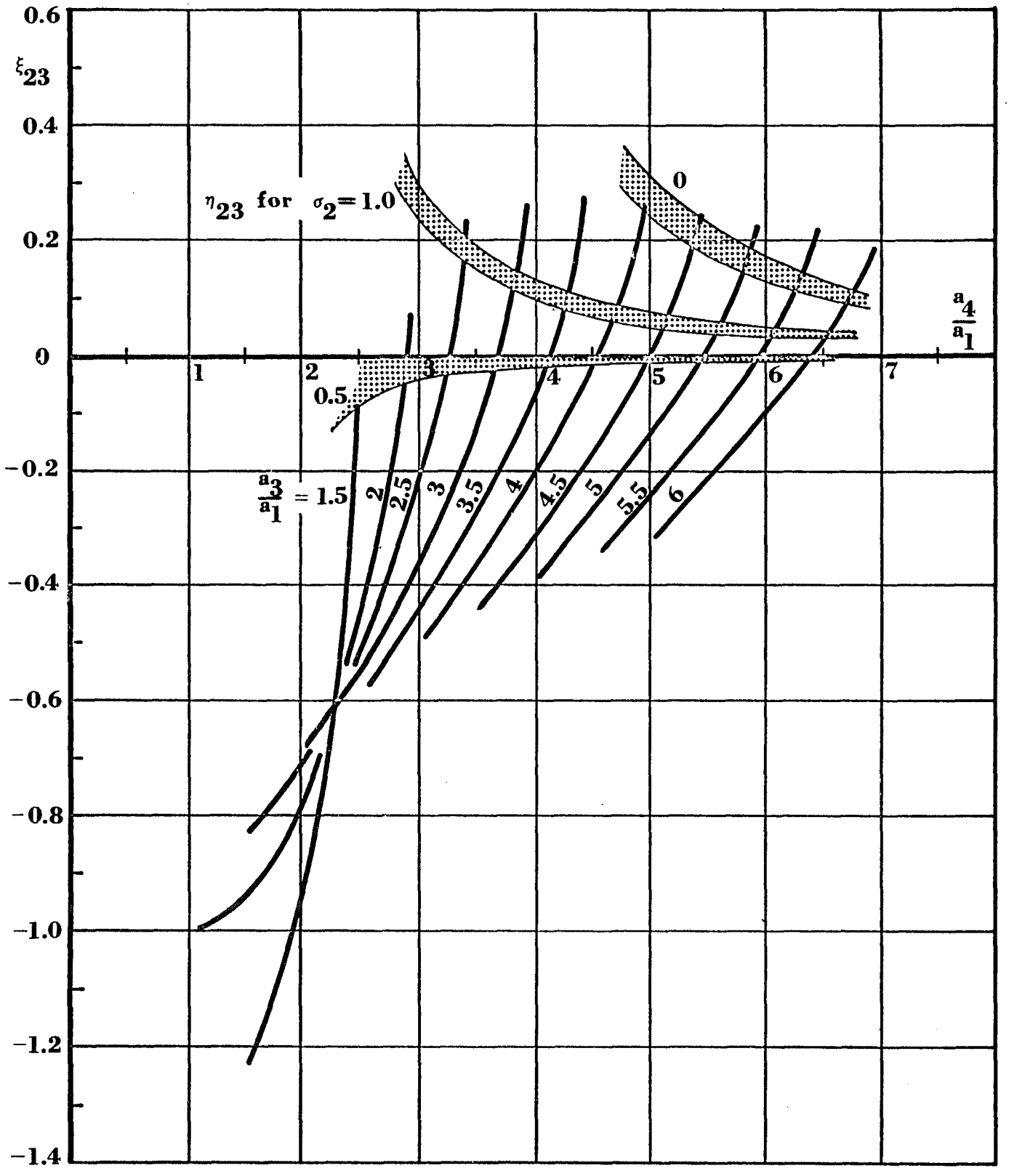

Fig. E9 Moment optimization curves with bands for varying parameters, for families $a_2/a_1 = 2$ and ξ_{23}

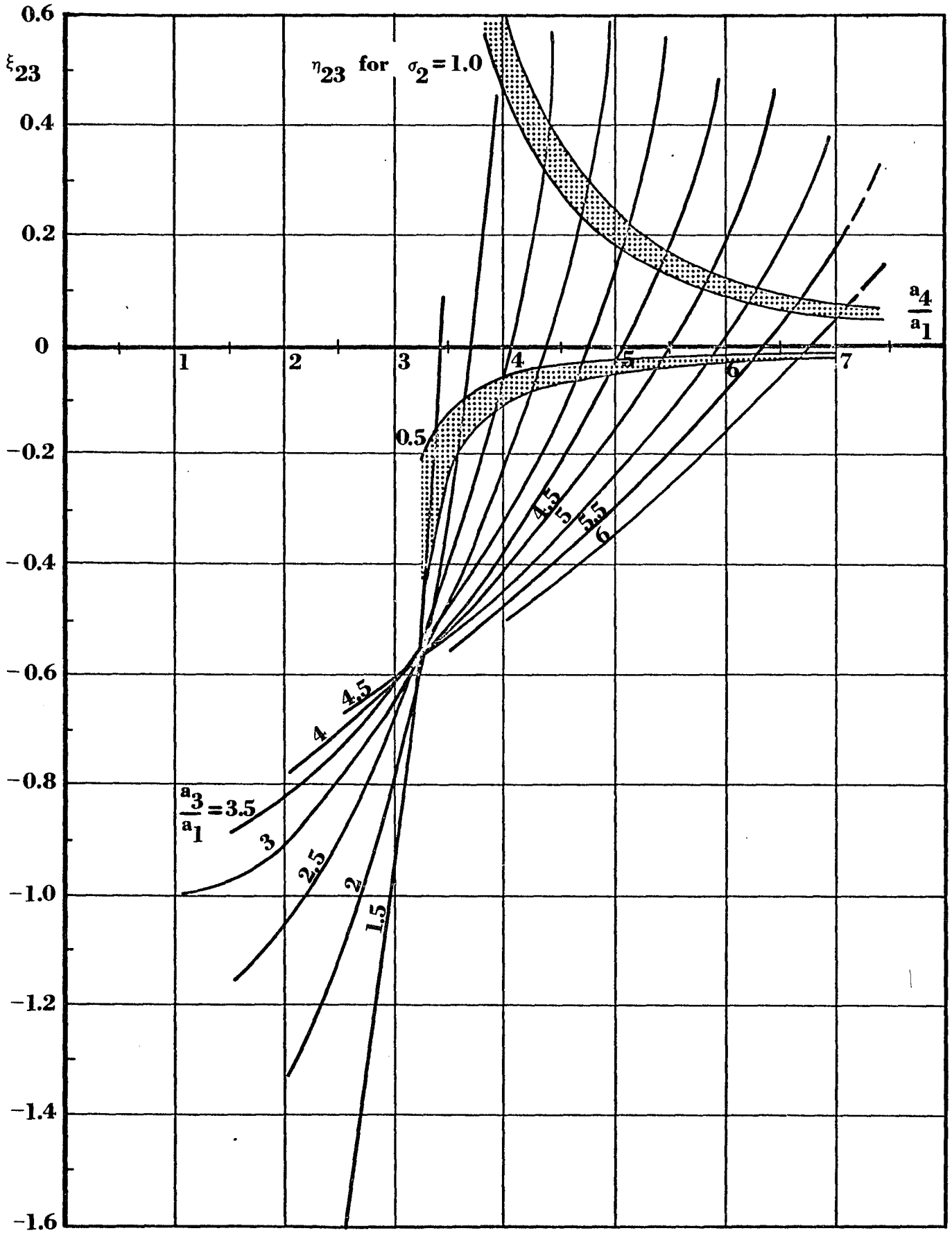

Fig. E10 Moment optimization curves with bands for varying parameters, for families $a_2/a_1 = 3$ and ξ_{23}

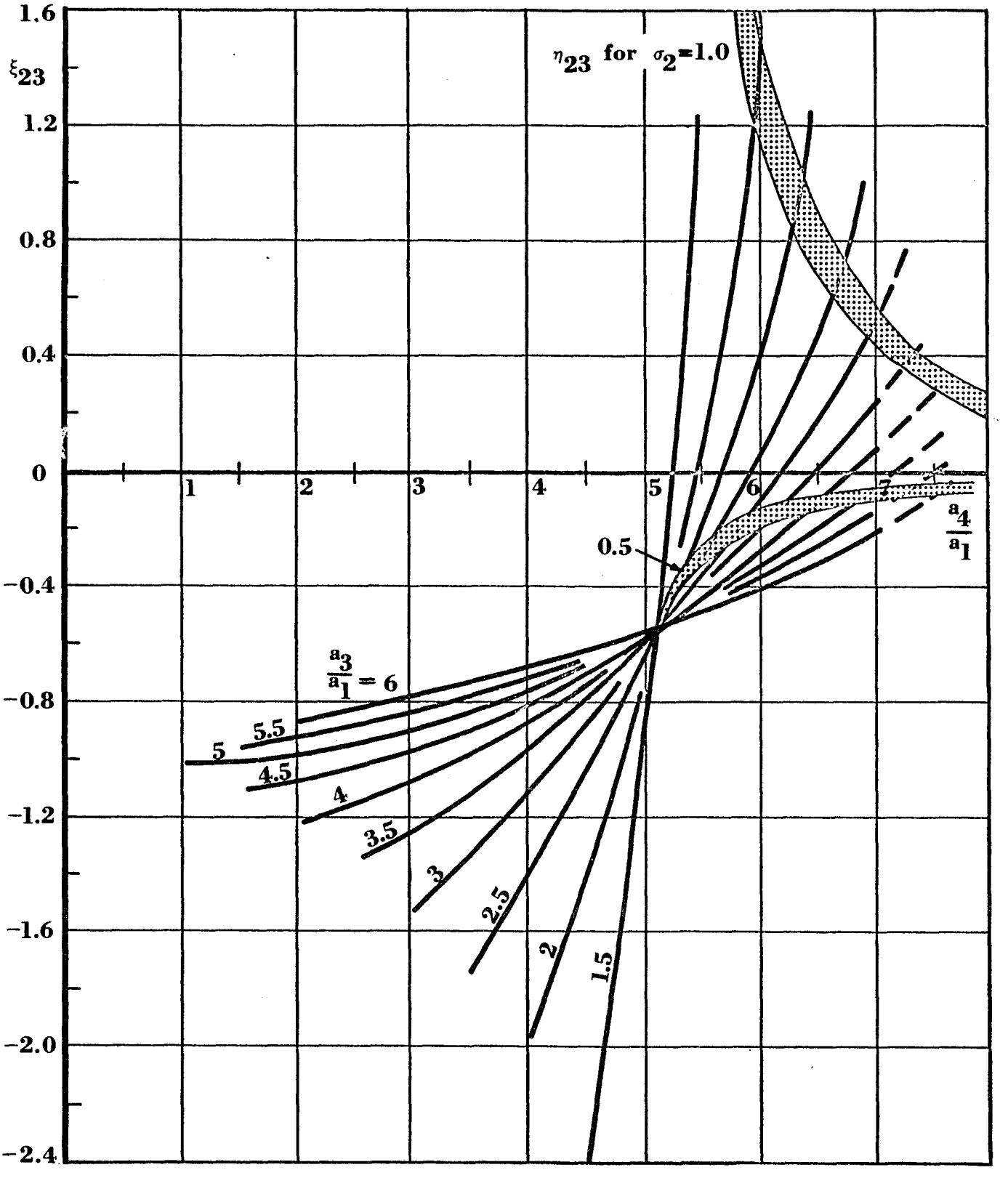

Fig. E11 Moment optimization curves with bands for varying parameters, for families $a_2/a_1 = 5$ and ξ_{23}

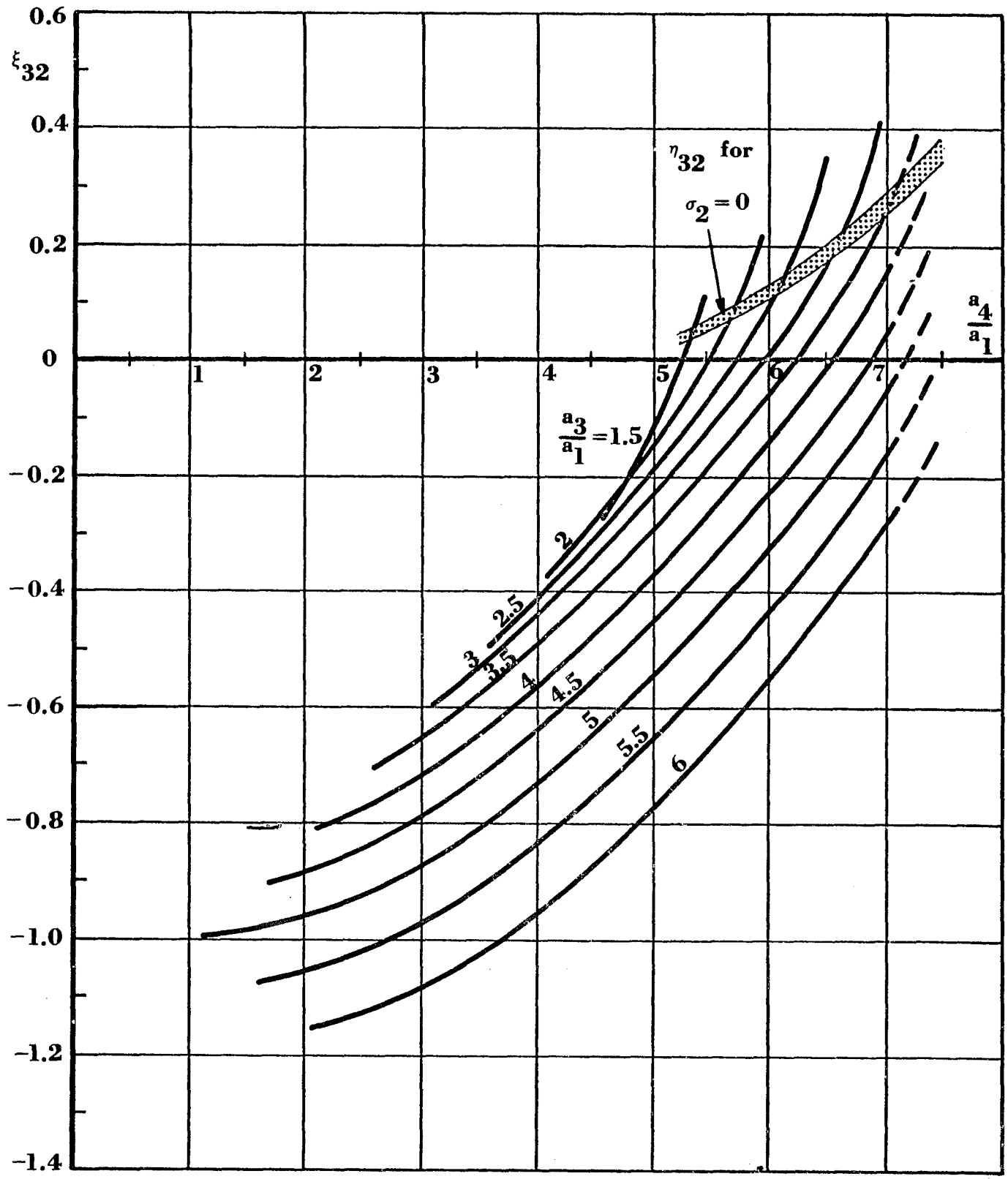

Fig. E12 Moment optimization curves with bands for varying parameters, for families $a_2/a_1 = 5$ and ξ_{32}

APPENDIX F

APPLICABILITY RESTRICTION OF LEAST-SQUARE OPTIMUM

The optimum ratio ξ_{32} (as opposed to ξ_{23}) will be applicable only when it may be equated with the actual ratio η_{32}. For a certain mass distribution, it may be proven that η_{32} is beyond the range of possible matching with any ξ_{32}.

This case refers to the special mass distribution in which:

$$k_2^2 < r_2(a_2 - r_2) \ , \tag{F.1}$$

for $0 < r_2 < a_2$, $\theta_2 = 0$, $\theta_3 = \pi$. Recall that this is the only case in which η_{32} is negative, as seen in Table 5 of Part VC (case II).

Computation shows that the following inequality holds:

$$\xi_{32} > -3\mu^2 \ , \tag{F.2}$$

where:

$$\mu = \frac{a_3}{a_2} \ . \tag{F.3}$$

It will now be proven that:

$$\eta_{32} < -3\mu^2 \ , \tag{F.4}$$

so that it may be concluded that:

$$\eta_{32} \neq \xi_{32} \ . \tag{F.5}$$

Proof.

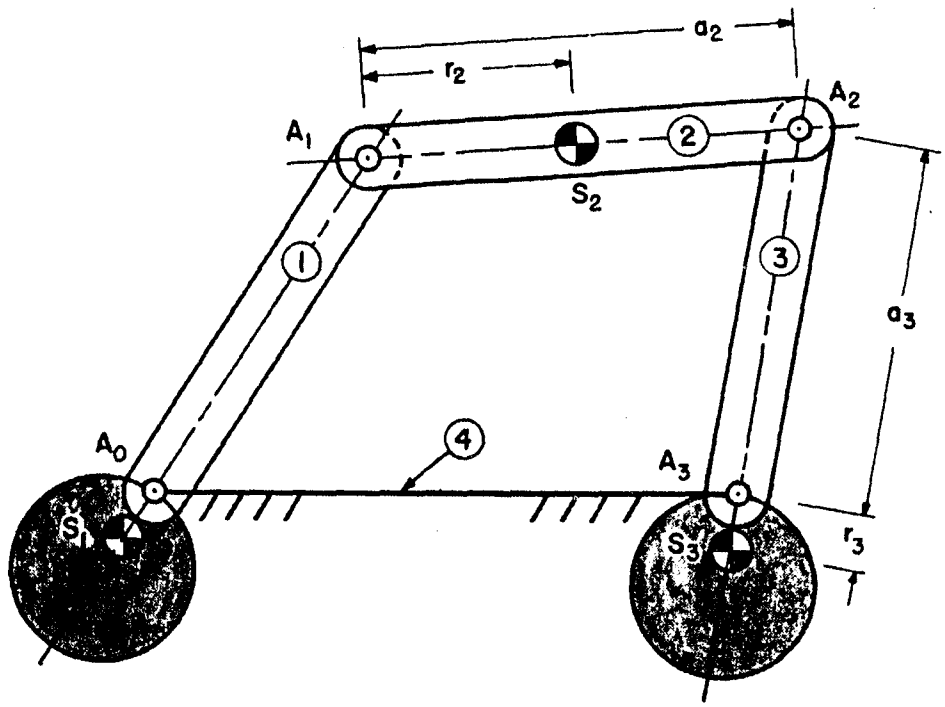

Fig. F1 Balanced four-bar linkage, $\theta_2 = 0$

For the case under consideration, the linkage resembles the mechanism depicted in Fig. F1. From Part V, eq. (5.20) is rearranged as:

$$\eta_{32} = - \frac{m_3(a_3 r_3 + r_3^2 + k_3^2)}{m_2(a_2 r_2 - r_2^2 - k_2^2)} . \qquad (F.6)$$

The value of η_{32} will remain negative as long as the prescribed inequality of eq. (F.1) holds.

If the moments of inertia taken with respect to pivots A_1 and A_3 are given as:

$$\left.\begin{aligned} I_2\big|_{A_1} &= I_2 + m_2 r_2^2 = m_2(k_2^2 + r_2^2) \ , \\ I_3\big|_{A_3} &= I_3 + m_3 r_3^2 = m_3(k_3^2 + r_3^2) \ , \end{aligned}\right\} \qquad (F.7)$$

then eq. (F.6) may be rewritten as:

$$\eta_{32} = -\left(\frac{m_3 r_3 a_3 + I_3\big|_{A_3}}{m_2 r_2 a_2 - I_2\big|_{A_1}}\right) = -Z \ . \qquad (F.8)$$

The absolute value of the term within the parenthesis, Z, increases as $I_2\big|_{A_1}$ increases, within the prescribed limits of the inequality of eq. (F.1).

The value of $I_2\big|_{A_1}$ will be larger for a realistic link than for a link consisting of only a thin uniform rod. If it can be shown that Z has the smallest absolute value for a uniform rod, and that this value increases when a more realistic link is considered, it is proven that:

$$\eta_{32} < -Z \ . \qquad (F.9)$$

Accordingly, choose link 2 to be a uniform thin rod, such that:

$$\left.\begin{aligned} r_2 &= \frac{1}{2} a_2 \ , \\ I_2\big|_{A_1} &= \frac{1}{3} m_2 a_2^2 \ . \end{aligned}\right\} \qquad (F.10)$$

Because of the force balance, eq. (3.13) may also be utilized:

$$m_3 r_3 = m_2 r_2 \frac{a_3}{a_2} . \tag{F.11}$$

Substituting equations (F.10) and (F.11) into eq. (F.8) gives:

$$\eta_{32} = - \left(\frac{\frac{1}{2} m_2 a_3^2 + I_{3|A_3}}{\frac{1}{6} m_2 a_2^2} \right) , \tag{F.12}$$

or:

$$\eta_{32} = - \left(3\mu^2 + \frac{6 I_{3|A_3}}{m_2 a_2^2} \right) , \tag{F.13}$$

in which μ is given by eq. (F.3). Since:

$$\frac{6 I_{3|A_3}}{m_2 a_2^2} > 0 , \tag{F.14}$$

eq. (F.13) proves that:

$$\eta_{32} < - 3\mu^2 , \quad \text{Q.E.D.} \tag{F.15}$$

Fig. F2 illustrates the envelope of all possible values of ξ_{32}, as taken from Figures E2, E4, E6, and E8 of Appendix E. Values of ξ_{32} and $(-3\mu^2)$ are plotted as functions of μ, and it can be seen that these curves do not intersect. Since $\eta_{32} < -3\mu^2$, matching is never possible.

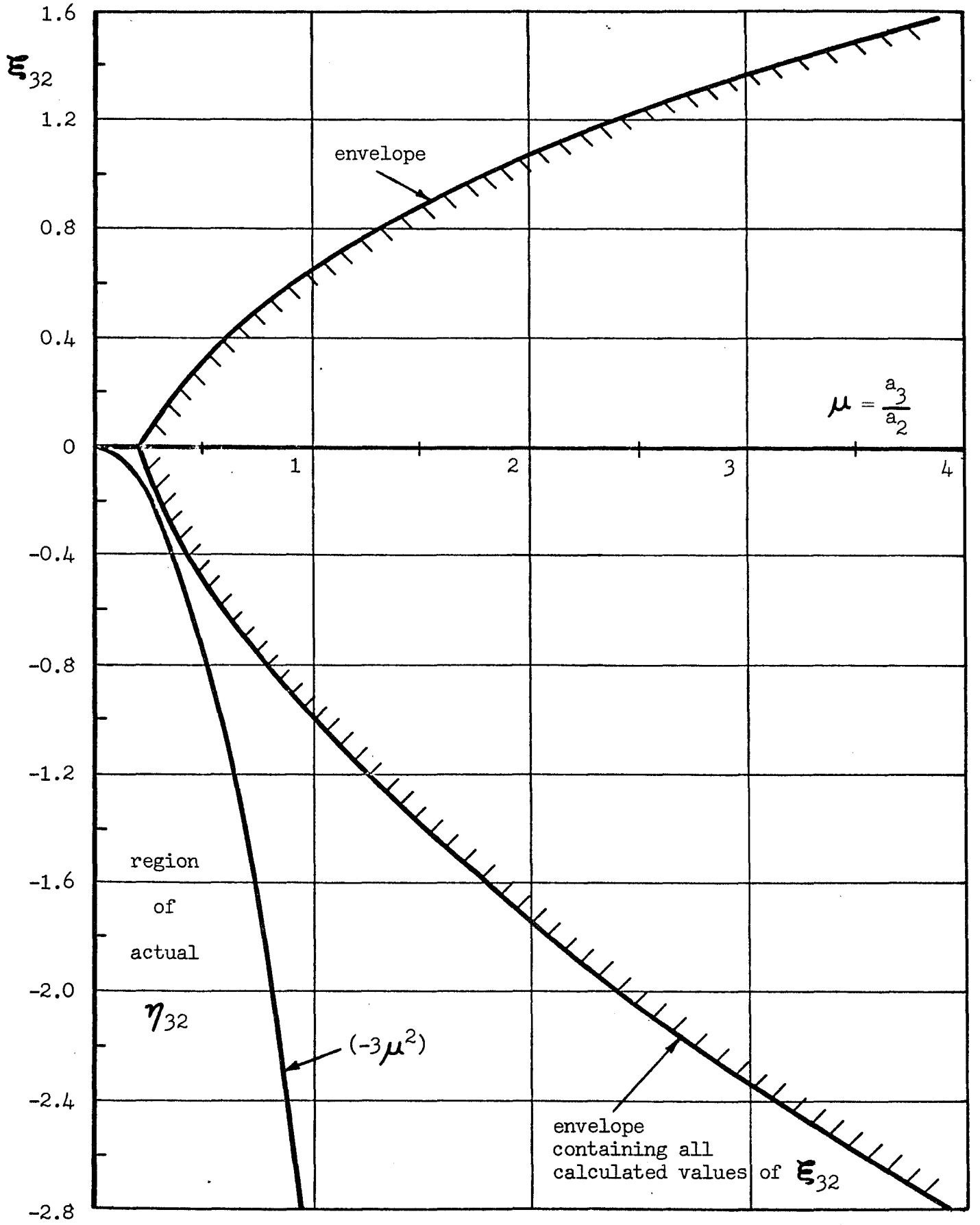

Fig. F2 Graph of ξ_{32} vs. μ

APPENDIX G

MAGNIFICATION PROOFS

This appendix contains proofs that certain expressions are unaffected by magnification (i.e. the variation of physical dimensions in a uniformly proportional manner for the entire linkage). The relations discussed are (1) the optimum ratios ξ_{ij}, and (2) the actual ratios η_{ij}.

1. Optimum Ratios ξ_{ij}

Equations (5.17) and (5.18) of Part V define the optimum ratios ξ_{23} and ξ_{32} as:

$$\xi_{23} = - \frac{\mathcal{I}_{23}}{\mathcal{I}_{22}} , \tag{G.1}$$

$$\xi_{32} = - \frac{\mathcal{I}_{23}}{\mathcal{I}_{33}} , \tag{G.2}$$

where:

$$\mathcal{I}_{ij} = \int_0^{2\pi} \ddot{\phi}_i \, \ddot{\phi}_j \, d\phi_1 . \tag{G.3}$$

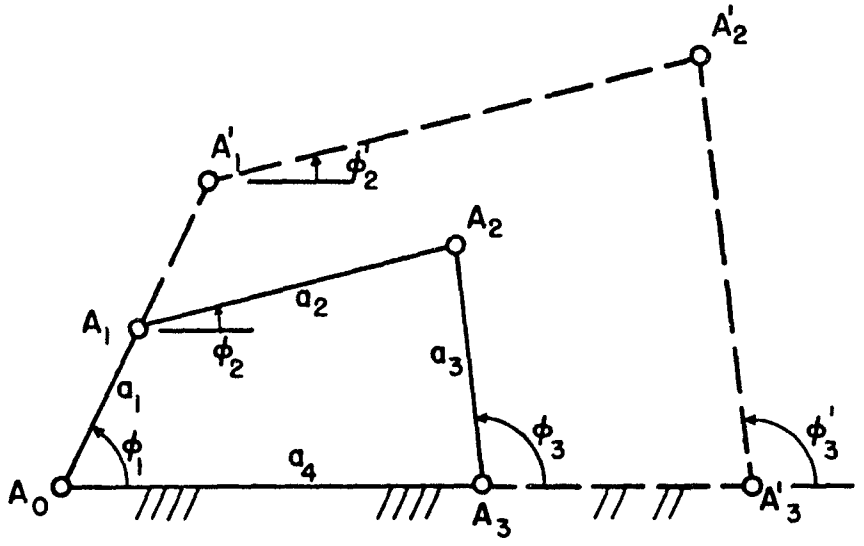

Fig. G1 Original and magnified four-bar linkage

The angular accelerations $\ddot{\phi}_2$ and $\ddot{\phi}_3$ are invariant when the linkage is subjected to a uniformly proportional magnification. Fig. G1 uses geometric means to illustrate this point. The quadrilateral

$A_0A_1A_2A_3$ represents the original four-bar linkage, and $A_0A_1'A_2'A_3'$ is the magnified linkage. Thus:

$$\left.\begin{aligned} A_0A_1 &= a_1 , & A_0A_1' &= ka_1 , \\ A_1A_2 &= a_2 , & A_1'A_2' &= ka_2 , \\ A_2A_3 &= a_3 , & A_2'A_3' &= ka_3 , \\ A_0A_3 &= a_4 , & A_0A_3' &= ka_4 , \end{aligned}\right\} \qquad (G.4)$$

where k is the constant magnification ratio.

All angles ϕ_i' in the magnified linkage will equal the angles ϕ_i in the original linkage for all positions, since the quadrilaterals are similar. Consequently, all derivatives of the corresponding angles will be identical, and $\ddot{\phi}_2$ and $\ddot{\phi}_3$, and hence ξ_{23} and ξ_{32} are independent of magnification.

2. Actual Ratios η_{ij}

Equation (5.20) defines the actual ratios η_{32} and η_{23} as:

$$\eta_{32} = \frac{1}{\eta_{23}} = \frac{K_3}{K_2}, \tag{G.5}$$

where:

$$K_2 = - m_2(k_2^2 + r_2^2 - a_2 r_2), \tag{G.6}$$

$$K_3 = - m_3(k_3^2 + r_3^2 + a_3 r_3). \tag{G.7}$$

In order to determine these ratios, the relationships between link dimensions must be known.

Fig. 12 in Part V illustrates the nominal linkage configuration chosen. In order to prove independence of magnification, more specific dimensional relations must be given. Each original link i has a constant width d_i, except at the bearings, where a circular shape of radius d_i exists (see Fig. G2). Also, a uniform thickness h_i as well as a uniform mass density ρ are chosen. The counterweights are circular, and tangent to the centers of rotation. (See Appendix H for minimum moment of inertia considerations.) They have radii $R_i = r_i^*$, thicknesses h_i^*, and mass density ρ.

In order to show the dimensionless quality of the equations for this linkage, the following ratios are defined:

$$\left.\begin{aligned} \alpha_i &= \frac{a_i}{a_1}, \qquad \beta_i = \frac{d_i}{a_1}, \qquad \gamma_i = \frac{h_i}{d_i}, \\ \delta_i &= \frac{h_i^*}{h_i}, \qquad \sigma_i = \frac{r_i}{a_i}. \end{aligned}\right\} \tag{G.8}$$

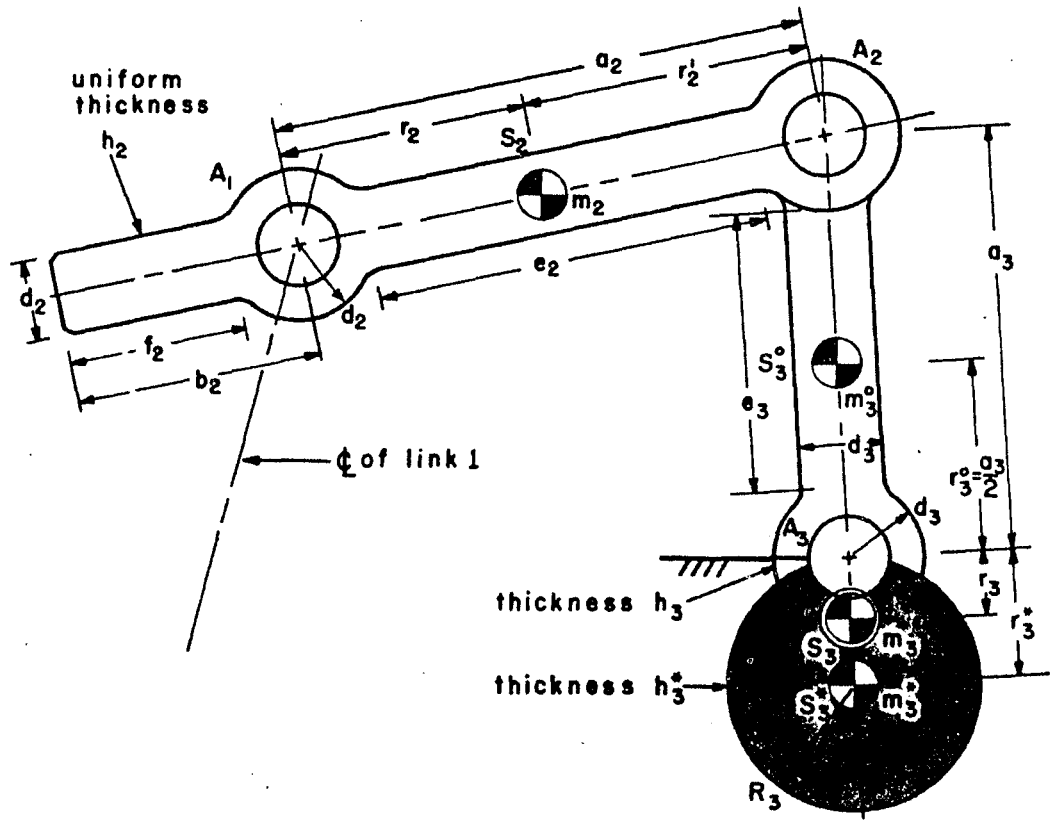

Fig. G2 Parameters of coupler and output links for chosen four-bar linkage configuration

The coefficients K_2 and K_3 of equations (G.6) and (G.7) will now be expressed in terms of these dimensionless ratios. It will be shown that their resulting forms are:

$$\left.\begin{aligned} K_2 &= \rho a_1^5 P_2 \ , \\ K_3 &= -\rho a_1^5 P_3 \ . \end{aligned}\right\} \qquad (G.9)$$

The parameters P_2 and P_3 are comprised only of the ratios of eq. (G.8), thereby making the ratio η_{ij} independent of magnification. This derivation is now shown in detail.

a. Expansion of Coefficient K_2

The parameters of coefficient K_2, i.e. eq. (G.6), are now expressed first in terms of the dimensions of the nominal linkage configuration, and then in terms of the dimensionless ratios defined above.

(1) Equations for Link 2

Referring to Fig. G2, the following relations hold for $0 \leq r_2 \leq \frac{a_2}{2}$:†

$$\left.\begin{aligned} e_2 &= a_2 - 2d_2 \ , \\ f_2 &= b_2 - d_2 \ , \\ r_2' &= a_2 - r_2 \ . \end{aligned}\right\} \qquad \text{(G.10)}$$

The extension length b_2 of the coupler depends on the dimension r_2, which locates the link center of mass. By writing the equation for r_2 in terms of the subcomponents of the link, the length b_2 can be solved for in terms of r_2:

$$b_2 = - r_2 + \sqrt{r_2^2 - 2r_2\left[a_2 + d_2(2\pi-3)\right] - 2a_2d_2(1-\pi) + d_2^2 + a_2^2} \ . \qquad \text{(G.11)}$$

The total link mass becomes:

$$m_2 = m_{R_1} + m_{R_2} + 2m_C \ , \qquad \text{(G.12)}$$

---

†For $\frac{a_2}{2} < r_2 \leq a_2$, the same expressions will be valid if r_2' is substituted for r_2.

in which the m_{R_1} is the mass of the rectangular extension section, m_{R_2} is the mass of the rectangular center section, and m_C is the mass of a circular bearing section, and where:

$$\left.\begin{aligned} m_{R_1} &= \rho f_2\, d_2\, h_2 \,, \\ m_{R_2} &= \rho e_2\, d_2\, h_2 \,, \\ m_C &= \rho \pi d_2^2\, h_2 \,. \end{aligned}\right\} \qquad \text{(G.13)}$$

The link moment of inertia is given by:

$$I_2 = m_2 k_2^2 = I_{R_1} + m_{R_1}\left(\frac{f_2}{2} + d_2 + r_2\right)^2 + I_{R_2} + m_{R_2}\left(\frac{a_2}{2} - r_2\right)^2 + 2\, I_C + m_C\,(r_2^2 + r_2'^2) \,, \qquad \text{(G.14)}$$

where:

$$\left.\begin{aligned} I_{R_1} &= \frac{1}{12}\, m_{R_1}\,(f_2^2 + d_2^2) \,, \\ I_{R_2} &= \frac{1}{12}\, m_{R_2}\,(e_2^2 + d_2^2) \,, \\ I_C &= \frac{1}{2}\, m_C d_2^2 \,. \end{aligned}\right\} \qquad \text{(G.15)}$$

(2) Dimensionless Forms

All of the above equations may now be put in terms of the input link length a_1, the density ρ, and the dimensionless ratios of eq. (G.8). Thus, upon substitution of the parameters of eq. (G.8), equations (G.10) become, with eq. (G.11):

$$\left.\begin{aligned} e_2 &= a_1\,(\alpha_2-2\beta_2)\ , \\ f_2 &= a_1\,T_2\ , \\ r_2' &= a_1\,\alpha_2\,(1-\sigma_2)\ , \end{aligned}\right\} \qquad (G.16)$$

where:

$$T_2 = \sqrt{\alpha_2^2(1-\sigma_2)^2 + (\alpha_2-\beta_2)^2 - \alpha_2^2 + 2\alpha_2\beta_2\left[\pi-\sigma_2(2\pi-3)\right]}$$

$$- \sigma_2\alpha_2 - \beta_2\ . \qquad (G.17)$$

Equations (G.13) become:

$$\left.\begin{aligned} m_{R_1} &= \rho a_1^3\,\beta_2^2\,\gamma_2\,T_2\ , \\ m_{R_2} &= \rho a_1^3\,\beta_2^2\,\gamma_2\,(\alpha_2-2\beta_2)\ , \\ m_C &= \rho a_1^3\,\pi\beta_2^3\,\gamma_2\ , \end{aligned}\right\} \qquad (G.18)$$

such that the total mass becomes:

$$m_2 = \rho a_1^3\,B_2\ , \qquad (G.19)$$

where:

$$B_2 = \beta_2^2\,\gamma_2\left[T_2 + \alpha_2 + 2\beta_2\,(\pi-1)\right]\ . \qquad (G.20)$$

From equations (G.14) and (G.15), the total link moment of inertia may be written in the form:

$$I_2 = \rho a_1^5 C_2 \ , \tag{G.21}$$

where:

$$C_2 = \beta_2^2 \gamma_2 \left\{ \frac{1}{12} T_2 \left[\beta_2^2 + T_2^2 + 3(T_2 + 2\beta_2 + 2\sigma_2\alpha_2)^2 \right] \right.$$

$$+ \frac{1}{12} (\alpha_2 - 2\beta_2) \left[(\alpha_2 - 2\beta_2)^2 + \beta_2^2 + 3\alpha_2^2 (1-2\sigma_2)^2 \right]$$

$$\left. + \pi\beta_2 \left[\beta_2^2 + \alpha_2^2 (2\sigma_2^2 - 2\sigma_2 + 1) \right] \right\} \ . \tag{G.22}$$

Thus, from equations (G.6), (G.19), and (G.21), coefficient K_2 may be written as:

$$K_2 = \rho a_1^5 P_2 \ , \tag{G.23}$$

which corresponds to the form of eq. (G.9), where P_2 is given by:

$$P_2 = \alpha_2^2 \sigma_2 (1-\sigma_2) B_2 - C_2 \ . \tag{G.24}$$

Note that this expression is valid for $0 \leq \sigma_2 \leq \frac{1}{2}$. A similar equation may be derived for $\frac{1}{2} < \sigma_2 \leq 1$ if necessary.

b. Expansion of Coefficient K_3

Following a procedure similar to the foregoing, the parameters of coefficient K_3, i.e. eq. (G.7), are expressed first in terms of nominal linkage dimensions, and then in terms of dimensionless ratios.

Fig. G2 shows that link 3 consists of two parts: an "original" link, and a counterweight.

(1) Original Link

The original link is composed of a rectangular midsection and circular ends, whose masses are:

$$\left.\begin{aligned} m_R &= \rho e_3 \, d_3 \, h_3 \, , \\ m_C &= \rho \pi \, d_3^2 \, h_3 \, , \end{aligned}\right\} \qquad (G.25)$$

where:

$$e_3 = a_3 - 2d_3 \, . \qquad (G.26)$$

The original link mass is then:

$$m_3^o = m_R + 2m_C \, . \qquad (G.27)$$

The moment of inertia of the original link about its center of mass S_3^o is given by:

$$I_3^o = m_3^o k_3^{o2} = \frac{1}{12} m_R (e_3^2 + d_3^2) + m_C (d_3^2 + \frac{a_3^2}{2}) \, . \qquad (G.28)$$

(2) Counterweight

The mass and moment of inertia of the circular counterweight depend upon its radius, which in turn may be derived from the force balancing condition [see eq. (3.13)] :

$$m_3 r_3 = m_2 r_2 \frac{a_3}{a_2} . \tag{G.29}$$

In addition, the influence of the original link must be taken into account, therefore [see Fig. G2 and eq. (3.15a)] :

$$m_3^* r_3^* = m_3 r_3 + m_3^o r_3^o . \tag{G.30}$$

Recall that the product $m_3^* r_3^*$ is a constant known value for a given coupler and original output link, and thus:

$$C_3^* = m_3^* r_3^* . \tag{G.31}$$

Because of the circular shape of the counterweight, its mass is:

$$m_3^* = \rho \pi R_3^2 h_3^* , \tag{G.32}$$

and its moment of inertia is:

$$I_3^* = m_3^* k_3^{*2} = \frac{1}{2} m_3^* R_3^2 . \tag{G.33}$$

In order to solve for the radius of the counterweight R_3, where:

$$r_3^* = R_3 , \tag{G.34}$$

multiply both sides of eq. (G.32) by r_3^*:

$$m_3^* r_3^* = C_3^* = \rho\pi R_3^3 h_3^* \ . \tag{G.35}$$

With C_3^* known and h_3^* chosen, eq. (G.35) can now be solved for R_3:

$$R_3 = \sqrt[3]{\frac{C_3^*}{\rho\pi h_3^*}} \ . \tag{G.36}$$

(3) Combined Original Link and Counterweight

The total link parameters resulting from the original link and the counterweight become:

$$m_3 = m_3^o + m_3^* \ , \tag{G.37}$$

$$I_3 = m_3 k_3^2 = I_3^o + m_3^o(r_3^o + r_3)^2 + I_3^* + m_3^*(r_3^* - r_3)^2, \tag{G.38}$$

where:

$$r_3 = \frac{(m_3 r_3)}{m_3} \ . \tag{G.39}$$

(4) Dimensionless Forms

All of the above equations are now put in terms of the dimensionless ratios. Substituting eq. (G.8) into equations (G.27) and (G.28), with (G.25) and (G.26), the following original link equations result:

$$\left.\begin{aligned} m_3^o &= \rho a_1^3 B_3 , \\ I_3^o &= \rho a_1^5 C_3 , \end{aligned}\right\} \qquad (G.40)$$

where:

$$\left.\begin{aligned} B_3 &= \beta_3^2\gamma_3\left[\alpha_3 + 2(\pi-1)\beta_3\right] , \\ C_3 &= \frac{1}{12}\beta_3^2\gamma_3(\alpha_3-2\beta_3)\left[(\alpha_3-2\beta_3)^2 + \beta_3^2\right] \\ &\quad + \frac{1}{2}\pi\beta_3^3\gamma_3(\alpha_3^2+2\beta_3^2). \end{aligned}\right\} \qquad (G.41)$$

Similarly, for the counterweight, equations (G.32) and (G.33) become, with the help of equations (G.29), (G.30), (G.34)-(G.36), and (G.40):

$$\left.\begin{aligned} m_3^* &= \rho a_1^3 D_3 , \\ I_3^* &= \rho a_1^5 E_3 , \end{aligned}\right\} \qquad (G.42)$$

where:

$$\left.\begin{aligned} D_3 &= \pi\beta_3\gamma_3\delta_3 F_3^2 , \\ E_3 &= \frac{1}{2}\pi\beta_3\gamma_3\delta_3 F_3^4 , \\ F_3 &= \frac{R_3}{a_1} = \sqrt[3]{\frac{\alpha_3}{\pi\beta_3\gamma_3\delta_3}\left(\sigma_2 B_2 + \frac{1}{2}B_3\right)} . \end{aligned}\right\} \qquad (G.43)$$

Combining the results of equations (G.40) and (G.42) according to (G.37) - (G.39), the combined link equations result:

$$m_3 = \rho a_1^3 (B_3 + D_3) , \tag{G.44}$$

$$I_3 = \rho a_1^5 L_3 , \tag{G.45}$$

where:

$$\left.\begin{aligned} L_3 &= C_3 + E_3 + B_3\left(\frac{\alpha_3}{2} + H_3\right)^2 + D_3(F_3 - H_3)^2 , \\ H_3 &= \frac{r_3}{a_1} = \sigma_3\alpha_3 . \end{aligned}\right\} \tag{G.46}$$

Finally, coefficient K_3 becomes, with the help of equations (G.7), (G.44), and (G.45):

$$K_3 = - \rho a_1^5 P_3 , \tag{G.47}$$

which is the same form as eq. (G.9), where P_3 is given by:

$$P_3 = \alpha_3^2\sigma_3 (1+\sigma_3)(B_3+D_3) + L_3 . \tag{G.48}$$

c. Conclusions

The combined form of η_{ij} obtained from equations (G.5), (G.23), (G.24), (G.47), and (G.48) is:

$$\eta_{32} = \frac{1}{\eta_{23}} = -\frac{P_3}{P_2} = -\left[\frac{\alpha_3^2\sigma_3(1+\sigma_3)(B_3+D_3) + L_3}{\alpha_2^2\sigma_2(1-\sigma_2)\,B_2 - C_2}\right], \qquad (G.49)$$

which, since it is composed of only dimensionless parameters, proves that η_{ij} is independent of magnification.

APPENDIX H

OPTIMUM SHAPE OF A COUNTERWEIGHT

Counterweights appear in many shapes, such as the sector on automobile crankshafts (see Figures 3 and 6), and the segment on locomotive driving wheels. The concept of the circular shape, however, has only been discussed in the literature relatively recently.

Yu. V. Epshtein and L. I. Shteinvol'f [20] as well as F. R. Hertrich [35] show that circular counterweights have minimum inertia. As illustrated in Fig. H1, these counterweights must be tangent to their centers of rotation. In order to achieve the minimum moments of inertia possible, these cylindrical shapes should be as long as the particular design allows (perpendicular to the plane of the linkage).

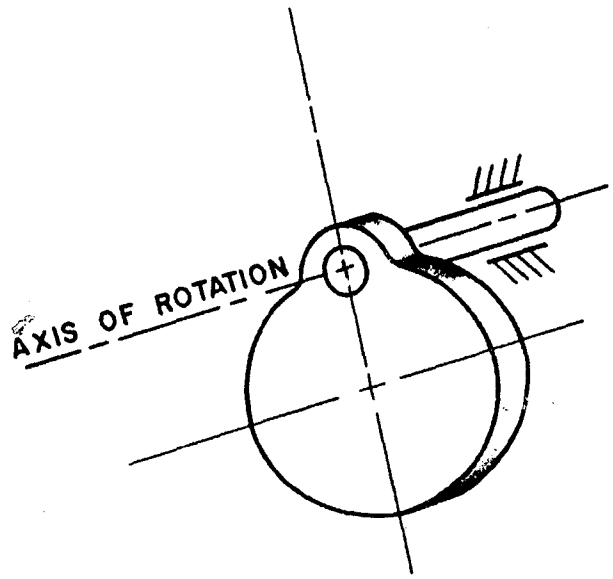

Fig. H1 Circular counterweight

APPENDIX I

COLLECTION OF KINEMATIC EQUATIONS

This appendix contains a collection of kinematic equations for the four-bar linkage of Fig. I1, which were found to be most convenient for various computer programs. Derivations have been omitted, since most equations represent minor deviations from those in the existing literature.

Linear and angular displacements, velocities, and accelerations are given for the center of mass S_i of each moving link i or the link itself. These equations are shown for the case in which the ground link angle $\theta_4 = 0$ (see Fig. I1).

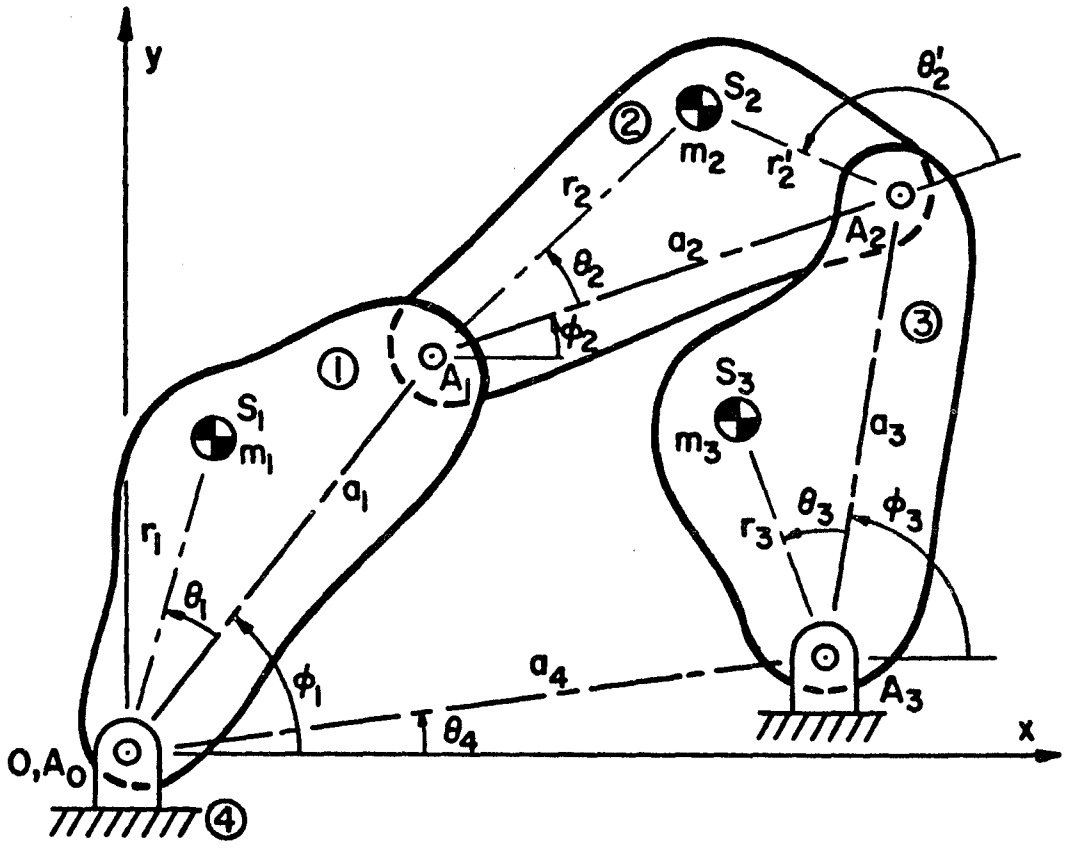

Fig. I1 Four-bar linkage nomenclature

1. Definitions

$$\lambda = \frac{a_1}{a_2}, \qquad \mu = \frac{a_3}{a_2}, \qquad \nu = \frac{a_4}{a_2}, \tag{I.1}$$

$$\tau_1 = \mu \sin (\phi_1 - \phi_3) + \nu \sin \phi_1 , \tag{I.2}$$

$$\tau_3 = \lambda \sin (\phi_1 - \phi_3) + \nu \sin \phi_3 . \tag{I.3}$$

2. Link Angles

a. Output Link

$$\phi_3 = 2 \tan^{-1} \left(\frac{A \pm \sqrt{A^2 + B^2 - C^2}}{B + C} \right), \tag{I.4}$$

where: $A = \sin \phi_1$,

$$\left.\begin{aligned} B &= \cos \phi_1 - \frac{\nu}{\lambda} , \\ C &= \frac{\lambda^2 + \mu^2 + \nu^2 - 1}{2\mu\lambda} - \frac{\nu}{\mu} \cos \phi_1 . \end{aligned}\right\} \tag{I.5}$$

b. Coupler Link

$$\phi_2 = \tan^{-1} \left(\frac{\lambda \sin \phi_1 - \mu \sin \phi_3}{\lambda \cos \phi_1 - \mu \cos \phi_3 - \nu} \right) . \tag{I.6}$$

3. Link Angular Velocities

a. Output Link

$$\dot{\phi}_3 = \frac{\lambda \tau_1}{\mu \tau_3} \dot{\phi}_1 \ . \tag{I.7}$$

b. Coupler Link

$$\dot{\phi}_2 = \frac{\lambda}{\tau_3} \sin(\phi_1 - \phi_3) \dot{\phi}_1 \ . \tag{I.8}$$

c. Combined Form

$$\dot{\phi}_3 = \left[1 + \frac{\nu}{\mu} \frac{\sin \phi_1}{\sin(\phi_1 - \phi_3)}\right] \dot{\phi}_2 \ . \tag{I.9}$$

4. Link Angular Accelerations

a. Output Link

$$\ddot{\phi}_3 = \left(\frac{\dot{\phi}_3}{\dot{\phi}_1}\right) \ddot{\phi}_1 + \frac{\lambda}{\tau_3} \cos(\phi_1 - \phi_3)(\dot{\phi}_1 - \dot{\phi}_3)^2$$

$$+ \frac{\nu}{\mu \tau_3} (\lambda \cos \phi_1 \dot{\phi}_1^2 - \mu \cos \phi_3 \dot{\phi}_3^2) \ . \tag{I.10}$$

b. Coupler Link

$$\ddot{\phi}_2 = \left(\frac{\dot{\phi}_2}{\dot{\phi}_1}\right) \ddot{\phi}_1 + \frac{\nu \lambda}{\tau_3^2} \left[\cos(\phi_1 - \phi_3) \sin \phi_3 \dot{\phi}_1 - \sin \phi_1 \dot{\phi}_3\right] \dot{\phi}_1 \ . \tag{I.11}$$

c. Combined Form

Differentiation of eq. (I.9) results in:

$$\ddot{\phi}_3 = \ddot{\phi}_2 + \frac{\nu}{\mu} \frac{d}{dt} \left[\frac{\sin \phi_1}{\sin(\phi_1 - \phi_3)} \dot{\phi}_2\right] \ . \tag{I.12}$$

This equation, which illustrates the fact that $\ddot{\phi}_3$ is not a linear function of $\ddot{\phi}_2$, is referred to in Part VB.

5. Displacements of Link Centers of Mass

a. Input Link

$$\left.\begin{aligned} x_1 &= r_1 \cos(\theta_1 + \phi_1), \\ y_1 &= r_1 \sin(\theta_1 + \phi_1). \end{aligned}\right\} \qquad (I.13)$$

b. Coupler Link

$$\left.\begin{aligned} x_2 &= a_1 \cos\phi_1 + r_2 \cos(\theta_2 + \phi_2), \\ y_2 &= a_1 \sin\phi_1 + r_2 \sin(\theta_2 + \phi_2). \end{aligned}\right\} \qquad (I.14)$$

c. Output Link

$$\left.\begin{aligned} x_3 &= r_3 \cos(\theta_3 + \phi_3) + a_4 , \\ y_3 &= r_3 \sin(\theta_3 + \phi_3). \end{aligned}\right\} \qquad (I.15)$$

6. Velocities of Link Centers of Mass

a. Input Link

$$\left.\begin{aligned} \dot{x}_1 &= - r_1 \sin(\theta_1 + \phi_1)\,\dot{\phi}_1 , \\ \dot{y}_1 &= r_1 \cos(\theta_1 + \phi_1)\,\dot{\phi}_1 . \end{aligned}\right\} \qquad (I.16)$$

b. Coupler Link

$$\left.\begin{aligned} \dot{x}_2 &= - a_1 \sin\phi_1\,\dot{\phi}_1 - r_2 \sin(\theta_2 + \phi_2)\,\dot{\phi}_2 , \\ \dot{y}_2 &= a_1 \cos\phi_1\,\dot{\phi}_1 + r_2 \cos(\theta_2 + \phi_2)\,\dot{\phi}_2 . \end{aligned}\right\} \qquad (I.17)$$

c. Output Link

$$\left.\begin{aligned} \dot{x}_3 &= - r_3 \sin(\theta_3 + \phi_3)\,\dot{\phi}_3 , \\ \dot{y}_3 &= r_3 \cos(\theta_3 + \phi_3)\,\dot{\phi}_3 . \end{aligned}\right\} \qquad (I.18)$$

7. Accelerations of Link Centers of Mass

a. Input Link

$$\left.\begin{aligned} \ddot{x}_1 &= - r_1 \left[\sin (\theta_1 + \phi_1)\, \ddot{\phi}_1 + \cos (\theta_1 + \phi_1)\, \dot{\phi}_1^{\,2} \right], \\ \ddot{y}_1 &= r_1 \left[\cos (\theta_1 + \phi_1)\, \ddot{\phi}_1 - \sin (\theta_1 + \phi_1)\, \dot{\phi}_1^{\,2} \right]. \end{aligned}\right\} \qquad (I.19)$$

b. Coupler Link

$$\left.\begin{aligned} \ddot{x}_2 &= - a_1 \left(\sin \phi_1\, \ddot{\phi}_1 + \cos \phi_1\, \dot{\phi}_1^{\,2}\right) \\ &\quad - r_2 \left[\sin (\theta_2 + \phi_2)\, \ddot{\phi}_2 + \cos (\theta_2 + \phi_2)\, \dot{\phi}_2^{\,2} \right], \\ \ddot{y}_2 &= a_1 \left(\cos \phi_1\, \ddot{\phi}_1 - \sin \phi_1\, \dot{\phi}_1^{\,2}\right) \\ &\quad + r_2 \left[\cos (\theta_2 + \phi_2)\, \ddot{\phi}_2 - \sin (\theta_2 + \phi_2)\, \dot{\phi}_2^{\,2} \right]. \end{aligned}\right\} \qquad (I.20)$$

c. Output Link

$$\left.\begin{aligned} \ddot{x}_3 &= - r_3 \left[\sin (\theta_3 + \phi_3)\, \ddot{\phi}_3 + \cos (\theta_3 + \phi_3)\, \dot{\phi}_3^{\,2} \right], \\ \ddot{y}_3 &= r_3 \left[\cos (\theta_3 + \phi_3)\, \ddot{\phi}_3 - \sin (\theta_3 + \phi_3)\, \dot{\phi}_3^{\,2} \right]. \end{aligned}\right\} \qquad (I.21)$$

VIII. REFERENCES

1. V. Ya. Anilovich, "Some Problems in Analytical Kinematics and Dynamics of Plane Multi-Link Mechanisms" (Russian), Trudy Inst. Mash., Sem. po Teor. Mash. i Mekh., vol. 22, no. 87, 1961, pp. 5-20.

2. I. I. Artobolevskii, "Basic Questions of the Dynamics of the Slider-Crank Mechanisms of Agricultural Machines," in Theory, Construction and Production of Agricultural Machines (Russian), ed. by V. P. Goryachkin, vol. I, Sel'khozgiz, Moscow, 1935, 534 pp. (pp. 232-270).

3. I. I. Artobolevskii, Theory of Mechanisms and Machines (Russian), Gos. Izdat. Tekh.-Teoret. Lit., Moscow, 2nd Ed., 1951.

4. I. I. Artobolevskii, V. A. Zinov'yev, & B. V. Edel'shtein, Collected Problems on the Theory of Mechanisms and Machines (Russian), Gos. Izdat. Tekh.-Teoret. Lit., Moscow, 3rd Ed., 1955.

5. G. G. Baranov, A Course in the Theory of Mechanisms and Machines (Russian), Mashinostroenie, Moscow, 4th Ed., 1967.

6. A. P. Bessonov, Basic Dynamics of Mechanisms with Variable Link Masses (Russian), Izdat. "Nauka," Moscow, 1967.

7. C. B. Biezeno & R. Grammel, Engineering Dynamics, vol. IV, Internal Combustion Engines, D. Van Nostrand Co., Princeton, N. J., 1954.

8. S. A. Cherkudinov & N. V. Speranskii, "The Calculation of a Spring Balancing Mechanism" (Russian), Trudy Inst. Mash., Sem. po Teor. Mash. i Mekh., vol. 21, no. 81-82, 1960, pp. 4-11.

9. P. Cormac, A Treatise on Engine Balance Using Exponentials, E. P. Dutton & Co., N. Y., 1923.

10. F. R. E. Crossley, Dynamics in Machines, Ronald Press, N. Y., 1954.

11. F. E. Crossley, "The Balancing of High-Speed Oscillating Feed Mechanisms," ASME Paper 64-MECH-28, Mechanisms Conf., Oct. 19-21, 1964.

12. W. E. Dalby, The Balancing of Engines, Arnold, London, 4th Ed., 1929.

13. T. H. Davies, "The Kinematics and Design of Linkages, Balancing Mechanisms and Machines," Machine Design Engineering, March 1968, pp. 40-51.

14. Ya. S. Davydov, Balancing of Mechanisms (Russian), Izdat. "Rechnoi Transport," Moscow, 1963, 24 pp.

15. J. Denavit & S. Hasson, "On the Harmonic Analysis of the Four-Bar Linkage," Proceedings: Int'l. Conf. for Teachers of Mechanisms (Yale Univ.), F. R. E. Crossley, Ed., Shoe String Press, 1961, pp. 169-185.

16. B. Dizioglu, Getriebelehre, Band 3, Dynamik, F. Vieweg & Sohn, Braunschweig, 1966, 199 pp.

17. V. V. Dobrovol'skii, "On the Motion of the Center of Mass of a Four-Bar Linkage" (Russian), Izv. Akad. Nauk SSSR, Otd. Tekh. Nauk, no. 4, 1941, pp. 107-108.

18. Yu. V. Epshtein, "The Works of Ya. L. Geronimus on the Theory of Machines and Mechanisms" (Russian), Trudy Inst. Mash., Sem. po Teor. Mash. i Mekh., vol. 20, no. 77, 1959, pp. 27-38.

19. Yu. V. Epshtein & E. P. Rapota, "On the Efficiency of Methods for the Best External Balancing of Masses of an Engine" (Russian), Trudy Inst. Mash., Sem. po Teor. Mash. i Mekh., vol. 23, no. 91, 1962, pp. 45-53.

20. Yu. V. Epshtein & L. I. Shteinvol'f, "The Optimum Shape for Rotating Counterweights" (Russian), Trudy Inst. Mash., Sem. po Teor. Mash. i Mekh., vol. 15, no. 57, 1955, pp. 47-60.

21. O. Fischer, "Über die reduzierten Systeme und die Hauptpunkte der Glieder eines Gelenkmechanismus," Zeit. für Math. und Phys., vol. 47, 1902, pp. 429-466.

22. F. Freudenstein, "Harmonic Analysis of Crank-and-Rocker Mechanisms with Application," Trans. ASME, J. Applied Mechanics, vol. 81, Series E, 1959, pp. 673-675.

23. P. N. Gartshtein, "The Best Self-Balancing of the Masses of a Multi-Link Machine" (Russian), Trudy Inst. Mash., Sem. po Teor. Mash. i Mekh., vol. 19, no. 75, 1959, pp. 4-15.

24. Ya. L. Geronimus, "On the Balancing of the Forces of Inertia of a Single Cylinder Engine" (Russian), Vestnik Mashinostr., no. 7-8, 1946, pp. 25-30.

25. Ya. L. Geronimus, "On the Calculation of the Counterweights of a Crankshaft, Provided for the Unloading of the Support Bearings" (Russian), Trudy Sem. po Teor. Mash. i Mekh., vol. II, no. 8, 1947, pp. 164-174.

26. Ya. L. Geronimus, "On the Application of the Methods of the Best Approximation of Functions to the Balancing of Mechanisms" (Russian), Trudy Sem. po Teor. Mash. i Mekh., vol. IV, no. 14, 1947, pp. 64-67.

27. Ya. L. Geronimus, On the Application of Chebyshev's Methods to the Problem of the Balancing of Mechanisms (Russian), OGIZ, Gostekhizdat, Moscow-Leningrad,-1948, 148 pp.

28. Ya. L. Geronimus, "An Approximate Method of Calculating a Counterweight for the Balancing of Vertical Inertia Forces" (Russian), Trudy Sem. po Teor. Mash. i Mekh., vol. 11, no. 41, 1951, pp. 61-66.

29. Ya. L. Geronimus, The Dynamic Synthesis of Mechanisms According to Chebyshev (Russian), Izdatel'stvo Khar'kovskogo Universiteta, Kharkov, 1958, 136 pp.

30. V. P. Goryachkin, "The Forces of Inertia and Their Balancing," in Collected Works (Russian), vol. I, Izd. "Kolos," Moscow, 1965, 720 pp. (1914, pp. 283-418).

31. K. Hain, "Der Federausgleich von Lasten," Grundlagen der Landtechnik, no. 2, 1952.

32. C. W. Ham, E. J. Crane, & W. L. Rogers, Mechanics of Machinery, McGraw-Hill Book Co., New York, 4th Ed., 1958.

33. C.-Y. Han, "Balancing of High Speed Machinery," Trans. ASME, J. Eng. for Industry, vol. 89, Series B, Feb. 1967, pp. 111-118.

34. G. H. Hardy, J. E. Littlewood, & G. Pólya, Inequalities, University Press, Cambridge, Great Britain, 1952.

35. F. R. Hertrich, "How to Balance High-Speed Mechanisms with Minimum Inertia Counterweights," Machine Design, vol. 35, no. 6, March 14, 1963, pp. 160-164.

36. H. Hilpert, "Gewichtsausgleich an feinmechanischen Geräten," Feingerätetechnik, vol. 14, no. 2, 1965, pp. 61-66.

37. W. E. Johnson, "A Method of Balancing Reciprocating Machines," Trans. ASME, J. Applied Mechanics, vol. 57, Sept. 1935, pp. A81-86, (discussion) vol. 58, March 1936, pp. A34-35.

38. V. A. Kamenskii, "On the Question of the Balancing of Plane Linkages" (Russian), Trudy Moskovskogo Inst. Inzh. Zhel.-dor. Transporta, no. 150, 1962, pp. 29-49.

39. V. A. Kamenskii, Statico-Dynamic Balancing of Linkages; Textbook for a Course of Lectures (Russian), Mosk. Inst. Inzh. Zhel.-dor. Transporta, Moscow, 1964, 72 pp.

40. V. A. Kamenskii, "On the Problem of the Number of Counterweights in the Balancing of Plane Linkages," in Balancing of Machines and Instruments (Russian), ed. by V. A. Shchepetil'nikov, Mashinostroenie, Moscow, 1965, 571 pp. (pp. 435-445).

41. A. Kobayashi, "Analytical Study of Crank Effort in Reciprocating Engines," Ryojun College Eng.-Memoirs, vol. IV, no. 3, Aug. 1931, pp. 127-183.

42. N. I. Kolchin, Mechanics of Machines (Russian), vol. V, Mashgiz, Moscow-Leningrad, 1957, 320 pp.

43. A. I. Komissarov & N. I. Krapivin, "Balancing of the Crankgear Mechanisms of Sewing Machine Needles" (Russian), Izv. Vyssh. Ucheb. Zaved.-Tekhnol. Legkoi Promysh., no. 1, 1965, pp. 154-162.

44. J. Kožesník, Dynamics of Machines, SNTL, Prague, and E. P. Noordhoff, Groningen, 1962.

45. R. Kreutzinger, "Über die Bewegung des Schwerpunktes beim Kurbelgetriebe," Getriebetechnik, vol. 10, no. 9, Sept. 1942, pp. 397-398.

46. R. Kreutzinger, "Kurbeltriebe mit vorgegebener Schwerpunktsbewegung," Werkstattstechn./Betrieb, vol. 11, no. 7, Oct. 1943, pp. 386-388.

47. S. M. Kutsenko, "The Application of Chebyshev's Method of the Best Approximation of Functions to the Calculation of the Counterbalances of a Steam Locomotive" (Russian), Trudy Sem. po Teor. Mash. i Mekh., vol. 11, no. 41, 1951, pp. 5-15.

48. F. W. Lanchester, "Engine Balancing," Horseless Age, vol. 33, nos. 12-16, Mar. 25, Apr. 1, 8, 15, 22, 1914, pp. 494-498, 536-538, 571-572, 608-610, 644-646.

49. L. B. Levenson, Kinematik und Dynamik der Getriebe, Verlag Technik, Berlin, 1952 (Transl. from Russian).

50. N. I. Manolescu & D. Maros, Teoria Mecanismelor şi a Maşinilor, Editura Tehnică, Bucureşti, 1958, 476 pp.

51. R. L. Maxwell, Kinematics and Dynamics of Machinery, Prentice-Hall, Englewood Cliffs, N.J., 1960.

52. E. Mewes, "Unbalanced Inertia Forces in Slider Crank Mechanisms of Large Eccentricity," Trans. ASME, J. Appl. Mech., vol. 80, June 1958, pp. 225-232.

53. W. Meye.. zur Capellen, Harmonische Analyse bei Kurbelgetrieben, Forschungsberichte des Landes Nordrhein-Westfalen, West-Deutscher Verlag, Cologne, part I, no. 676, 1959; part II, no. 803, 1960.

54. W. Meyer zur Capellen, "Biegungs- und Lagerschwingungen in Kurbeltrieben," Antriebstechnik, vol. II, no. 3, 1963, pp. 81-85.

55. W. Meyer zur Capellen, "Die Bewegung periodischer Getriebe unter Einfluss von Kraft- und Massenwirkungen," Industrie-Anzeiger, vol. 86, nos. 9 & 17, 1964, pp. 135-140 & 283-289.

56. W. Meyer zur Capellen, "Dynamische Ausgleichprobleme bei ebenen und spharischen Kurbeltrieben," Trans.-Internat'l Conf. on Mechanisms and Machines, Varna, Bulgaria, vol. I, 1965, pp. 3-22.

57. K. Ogawa & H. Funabashi, "On the Balancing of the Fluctuating Input Torques Caused by Inertia Forces in the Crank-and-Rocker Mechanisms," ASME Paper 68-MECH-18, Mechanisms Conf., Oct. 6-9, 1968.

58. L. N. Reshetov, "Toward the Question of the Balancing of the Forces of Inertia of Plane Mechanisms" (Russian), Izv. Vyssh. Ucheb. Zaved. - Mashinostroenie, no. 11, 1964, pp. 5-13.

59. R. E. Root, Dynamics of Engine and Shaft, John Wiley & Sons, New York, 1932.

60. M. V. Semenov, "The Synthesis of Partly Balanced Plane Mechanisms" (Russian), Trudy Sem. po Teor. Mash. i Mekh., vol. 8, no. 29, 1941, pp. 74-90.

61. M. V. Semenov, "The Balancing of Spatial Mechanisms" (Russian), Trudy Sem. po Teor. Mash. i Mekh., vol. 8, no. 32, 1950, pp. 31-42.

62. M. V. Semenov, "A Grapho-Analytic Method for the Design of Plane Linkages" (Russian), Trudy Sem. po Teor. Mash. i Mekh., vol. 9, no. 34, 1950, pp. 5-28.

63. M. V. Semenov, "Balancing the k^{th} Harmonic with the Help of a Planetary Mechanism" (Russian), Trudy Sem. po Teor. Mash. i Mekh., vol. 13, no. 49, 1953, pp. 69-78.

64. V. A. Shchepetil'nikov, "The Determination of the Mass Centers of Mechanisms in Connection with the Problem of Mechanism Balancing" (Russian), Trudy Moskovskogo Inst. Inzh. Zhel.-dor. Transporta, no. 92/11, 1957, pp. 211-233.

65. V. A. Shchepetil'nikov, "Balancing of the Crankgear" (Russian), Trudy Moskovskogo Inst. Inzh. Zhel.-dor. Transporta, no. 195, 1964, pp. 5-19.

66. V. A. Shchepetil'nikov, "New Principles for the Approximate Balancing of the Slider-Crank Mechanism," in Balancing of Machines and Instruments (Russian), ed. by V. A. Shchepetil'nikov, Mashinostroenie, Moscow, 1965, 571 pp. (pp. 399-411).

67. L. S. Sheino, "The Balancing of Four-Bar Mechanisms," Vestnik Mashinostroeniya and Russian Eng. Journal, vol. 46, no. 6, 1966, pp. 30-33.

68. A. A. Sherwood, "The Dynamics of the Harmonic Space Slider-Crank Mechanism," J. Mechanisms, vol. I, 1966, pp. 203-208.

69. A. A. Sherwood, "The Optimum Distribution of Mass in the Coupler of a Plane Four-Bar Linkage," J. Mechanisms, vol. I, 1966, pp. 229-234.

70. M. R. Smith & L. Maunder, "Inertia Forces in a Four-Bar Linkage," J. Mech. Eng. Science, vol. 9, no. 3, 1967, pp. 218-225.

71. G. J. Talbourdet & P. R. Shepler, "Mathematical Solution of 4-Bar Linkages, Part IV - Balancing of Linkages," Machine Design, vol. 13, July 1941, pp. 73-77.

72. D. L. Thornton, Mechanics Applied to Vibrations and Balancing, Chapman & Hall, London, 2nd Ed., 1951.

73. S. Timoshenko & D. H. Young, Advanced Dynamics, McGraw-Hill Book Co., New York, 1948.

74. L. Toft & A. T. J. Kersey, Theory of Machines, Sir Isaac Pitman & Sons, London, 6th Ed., 1949.

75. VDI/AWF-Fachgruppe Getriebetechnik, "Ebene Kurbelgetriebe: Allgemeine Massenkraftberechnung auf zeichnerisch-rechnerische Weise," VDI-Richtlinien 2144, Feb. 1964.

76. W. Wunderlich, "Über die Schwerpunktsbahn des Dreistab- und Schubkurbelgetriebes," Buletinul Institutului Politehnic, Din Iasi, Serie Noua, Tomul X (XIV), Fasc. 1-2, 1964, pp. 285-291.

77. A. T. Yang, "Harmonic Analysis of Spherical Four-Bar Mechanisms," Trans. ASME, J. Applied Mechanics, vol. 84, Series E, 1962, pp. 683-688.

78. V. A. Yudin, The Balancing of Machines and Their Stability (Russian), Izd. Voenno-Inzh. Akad. Krasnoi Armii, Moscow, 1941, 124 pp.

IX. SUPPLEMENTARY BIBLIOGRAPHY

S1. V. Ya. Anilovich, "Fundamentals of the Dynamics of Shock-Absorber Screens" (Russian), Trudy Inst. Mash., Sem. po Teor. Mash. i Mekh., vol. 19, no. 74, 1959, pp. 5-13.

S2. I. I. Artobolevskii, "Balancing the Inertia Forces of Plane Mechanisms" (Russian), Izv. TsNIITMASh, no. 10, 1935, pp. 5-26.

S3. I. I. Artobolevskii, Methods of Balancing the Inertia Forces in Working Machines with Complex Kinematic Schemes (Russian), Akad. Nauk SSSR, Otd. Tekh. Nauk, 1938, 47 pp.

S4. I. I. Artobolevskii, "Successes of Soviet Theory of Mechanisms and Machines" (Russian), Trudy Sem. po Teor. Mash. i Mekh., vol. 4, no. 16, 1948, pp. 5-46.

S5. I. I. Artobolevskii, B. V. Edel'shtein, & S. I. Artobolevskii, "Methods of Inertia Calculation for Mechanisms of Agricultural Machines," in Theory, Construction and Production of Agricultural Machines (Russian), ed. by V. P. Goryachkin, vol. 1, Sel'khozgiz, Moscow, 1935, 534 pp. (pp. 343-448).

S6. J. S. Beggs, Advanced Mechanism, Macmillan Co., New York, 1966.

S7. D. M. Berkovich, Inertia Forces in Engineering and Their Balancing (Russian), Mashgiz, Moscow, 1963, 102 pp.

S8. R. Beyer, Kinematisch-getriebedynamisches Praktikum, Springer Verlag, Berlin/Gottingen/Heidelberg, 1960.

S9. P. L. Chebyshev, Selected Works (Russian), Izdat. Akad. Nauk SSSR, Moscow, 1955, 926 pp. (Theory of Mechanisms: pp. 609-839, 888-923).

S10. R. Clink, "Balancing of High-Speed Four-Stroke Engines," Inst. Mech. Eng. - Proc. (Automobile Div.), no. 2, 1958-59, pp. 73-86, (discussion) 87-110.

S11. F. M. Cousins, Analytical Design of High Speed Internal Combustion Engines, Pitman Publ. Corp., N. Y., 1941.

S12. M. D. Creech, "Dynamic Analysis of Slider-Crank Mechanisms," Prod. Eng., vol. 33, Oct. 29, 1962, pp. 58-65.

S13. G. Delanghe, "Certaines propriétés générales d'équillibrage des machines à piston, d'après la methode des vecteurs tournants symétriques," Acad. des Sciences - CR, vol. 206, no. 22, May 30, 1938, pp. 1617-1618.

S14. V. I. Doronin, "New Method for Determining the Balancing Force" (Russian), Izv. Vyssh. Ucheb. Zaved.-Mashinostroenie, no. 4, 1964, pp. 5-10.

S15. E. Doucet, "Équilibrage dynamique des moteurs en ligne," Tech. Automobile et Arienne, vol. 37, nos. 230-232, Apr. 1946, pp. 30-31; June, pp. 35-37; Aug., pp. 55-56.

S16. R. Eksergian, Dynamical Analysis of Machines, Lancaster Press, Lancaster, Pa., 1931.

S17. Yu. V. Epshtein & L. I. Shteinvol'f, "On the Optimum Shape for Rotating Counterweights" (Russian), Trudy Sem. po Teor. Mash. i Mekh., vol. 15, no. 57, 1955, pp. 47-60.

S18. R. Galin, "Balance a Swashplate Mechanism Used in an Automotive Air Conditioning System Compressor," Problem 35, Solutions to Typical Problems in Engineering, Set No. 2, General Motors Corp., 1964.

S19. T. T. Gappoev, "Balancing the Inertia Loads of a Plane Mechanism" (Russian), Izv. Vyssh. Ucheb. Zaved.-Mashinostroenie, no. 8, 1967, pp. 5-8.

S20. T. T. Gappoev, "On the Question of the Balancing of the Internal Combustion Engine" (Russian), Izv. Vyssh. Ucheb. Zaved.-Mashinostroenie, no. 9, 1967, pp. 126-130.

S21. K. Hain, "Gelenkarme Bandgetriebe für den Kraftausgleich durch Federn," Grundlagen der Landtechnik, no. 4, 1953.

S22. K. Hain, "Zum federausgleich der Schlepper Anbaugeräte," Die Landtechnik, no. 1, 1951.

S23. J. B. Hartman, Dynamics of Machinery, McGraw-Hill Book Co., N.Y., 1956.

S24. J. Hirschhorn, Kinematics and Dynamics of Plane Mechanisms, McGraw-Hill Book Co., New York, 1962.

S25. A. R. Holowenko, Dynamics of Machinery, John Wiley & Sons, N.Y., 1955.

S26. A. W. Judge, Automobile and Aircraft Engines, Sir Isaac Pitman & Sons, London, 3rd Ed., 1936.

S27. H. H. Mabie & F. W. Ocvirk, Mechanisms and Dynamics of Machinery, John Wiley & Sons, N.Y., 2nd Ed., 1963.

S28. W. E. Marshall & P. Waldron, "Inertia Torques in Four-Bar Mechanisms," J. Mech. Eng. Science, vol. 9, no. 4, Oct. 1967, pp. 309-317.

S29. E. Mewes, "Massenausgleich an ebenen Kurbelgetrieben," Zeit. für angewandte Math. und Mech., vol. 35, no. 9/10, 1955, pp. 349-350.

S30. E. Mewes, "Massenkräfte in Landmaschinen und ihr Ausgleich," Grundlagen der Landtechnik, no. 6, 1955, pp. 116-133.

S31. E. Mewes, "Massenkräfte in Landmaschinen," VDI - Zeit., vol. 98, no. 34, 1956, pp. 1889-1890.

S32. E. Mewes, "Die Massenkräfte, Lagerkräfte und Kurbelwellendrehmomente beim Lauf eines Schüttlers," Landtechnische Forschung, no. 6, 1958, pp. 145-150.

S33. E. N. Nikolaev, "A Graphical Method for Determining the Resultant Inertia Force Vector of a Mechanism" (Russian), Trudy Sem. po Teor. Mash. i Mekh., vol. 10, no. 40, 1951, pp. 98-101.

S34. E. V. Nikolaevskii, "Balancing Mechanisms with Rocking Disks" (Russian), Izv. Vyssh. Ucheb. Zaved. - Mashinostroenie, no. 1, 1965, pp. 12-20.

S35. E. V. Nikolaevskii, "Dynamic Balancing of Cardan Transmissions" (Russian), Izv. Vyssh. Ucheb. Zaved. - Mashinostroenie, no. 6, 1965, pp. 40-47.

S36. R. M. Phelan, Dynamics of Machinery, McGraw-Hill Book Co., N.Y., 1967.

S37. C. C. Pounder, The Balancing of Engines, The Draughtsman Publ. Co., London, 1930.

S38. E. P. Rapota & V. E. Shapovalov, "On One Problem of the Best Uniform Balancing of the Masses of a Machine" (Russian), Teoriya Mekh. i Mash. (Khar'kov), no. 2, 1966, pp. 65-70.

S39. V. A. Shchepetil'nikov, ed., Balancing of Machines and Instruments (Russian), Mashinostroenie, Moscow, 1965, 571 pp.

S40. J. E. Shigley, Dynamic Analysis of Machines, McGraw-Hill Book Co., N.Y., 1961.

S41. L. I. Shteinvol'f, Dynamic Calculations of Machines and Mechanisms (Russian), Mashgiz, Moscow, 1961, 340 pp.

S42. B. Szoke, "Verschiedene Methoden des Massenausgleiches an Kurbelgetrieben," Acta Technica (Budapest), vol. 45, no. 3-4, 1964, pp. 315-326.

S43. M. Tolle, Die Regelung der Kraftmaschinen, J. Springer, Berlin, 1909.

S44. W. K. Wilson, The Balancing of Oil Engines, C. Griffin & Co., London, 1929.

X. AUTOBIOGRAPHICAL STATEMENT

Richard Stanley Berkof was born on March 2, 1941 in Brooklyn, New York. He attended Queens Public Schools Nos. 3 and 157, Stephen A. Halsey Junior High School, and Forest Hills High School, graduating from the latter with an academic diploma in June 1957.

He attended Queens College for two years, and then the City College of New York, from which he received a Bachelor of Mechanical Engineering degree in January 1962. He graduated in June 1963 from Columbia University with the degree of Master of Science in Mechanical Engineering.

Subsequently, he joined Gibbs and Cox, Inc. as a Design Engineer, where he worked on various naval analysis problems.

In September 1964, he entered the doctoral program at the City University of New York. From 1965 to 1967, while continuing his studies, he was a Lecturer in the Mechanical Engineering Department of the City College of New York, teaching Stress Analysis, Vector Mechanics and Mechanical Systems, and Thermodynamics.

As he entered upon the final phases of doctoral work in September 1968, he joined the American Can Company, Princeton Laboratory, as a Research Associate.

On April 24, 1969, he successfully defended his dissertation, thus completing the requirements for the degree of Doctor of Philosophy.

In 1968 he published two papers on the balancing of linkages together with Dr. Gerard G. Lowen.

He presently resides in Princeton, New Jersey, with his wife and his son.